Title
Molecular Architecture of the Centriole Proteome

Author
Keller, Lani C.

Publication Date
2009

Peer reviewed|Thesis/dissertation

Molecular Architecture of the Centriole Proteome

by

Lani C. Keller

DISSERTATION

Submitted in partial satisfaction of the requirements for the degree of

DOCTOR OF PHILOSOPHY

in

CELL BIOLOGY

in the

GRADUATE DIVISION

of the

UNIVERSITY OF CALIFORNIA, SAN FRANCISCO

Acknowledgements

The one thing about graduate school that people often fail to mention is that it is hard, really, really hard. There is no way that I could have made it through without the support of the following people. Some contributed scientifically, others supported me with love and helped me laugh when it was desperately needed, and then there was Wallace…

I first saw Wallace in Seattle while he was interviewing for a job and wiping his dusty chalk-filled hands on the back of his professional black pants. It was a whirlwind of science, theories, crazy analogies, and chalk. I knew immediately that I wanted to work for him. Wallace is a scientific inspiration to everyone around him. He finds even the most mundane scientific topics fascinating and has this amazing ability to make *you* interested. As a scientist, Wallace is bold, creative, and always full of at least one hundred ideas that he can spew at you about any particular scientific question. He let me explore my ambitions and never prevented me from teaching, traveling or heading off for a summer on the east coast. I appreciate his philosophy on science and his unwavering confidence in me. I cannot even begin to write everything that he has taught me but needless to say that I will miss him and his crazy meat-loving antics.

Wallace is also the common thread keeping many of us together in the place that we have called home for more years than we care to admit. I do not have the time or pages to write everything that I feel about the people in the

Marshall Lab but I will say a few things. I sat back-to-back with fabulous Japanese postdocs my whole graduate career and I would not have it any other way. Shige taught me that if you up all night, you cannot function the next day and you *will* fall asleep on your computer. Hiro is one of the most kind, patient, friendly lab mates that a person could ask for. If I designed the perfect colleague it would be in the form of a Hiro, possibly wearing a fabulous fake mustache. William Basil Ludington has always brought a bit of much needed calmness to the lab along with a bunch of crazy organisms and plants which in turn brought an ant infestation to the entire third floor. I was always grateful that he ended up in our lab. Susanne, my morning partner in crime, was always there to chat before the lab got crazy with activity. She was there when I really needed to see a smiling face. Kim Wemmer is my staple of all staples. I'm not sure what I'm going to do without her in my lab. She gave me her tea and her time, both of which I am incredibly grateful for. The person in the lab with whom I am most appreciative is Elisa. I truly believe that I would not have made it through certain times in graduate school without her. All in all, there were some tough times and some fabulous times but I never once regretted my decision to join the Marshall Lab. We were and continue to be one big dysfunctional family.

In addition to my lab, I have to thank Ron Vale and the people in his lab. Ron has supported me throughout graduate school and has written me approximately thirty letters of recommendation (seriously). He welcomed me into his lab, and although I joined the Marshall lab, there was always a spot for me in the Vale lab. They still welcome me, even after many years of borrowing

reagents, using microscopes, and asking question after question. I also had the privilege of going to Woods Hole with Ron for a much needed summer of science-reinvigoration. Ron is one of my stable scientific rocks!

Every Tuesday for over three years of my life I dined on cheap sushi, drank cheap beer, and had the best conversations of my life. It never mattered what we talked about, it was just important that we got together and forgot about all the stresses of life. I am indebted to “The sushi crew” for all of eternity. Mary, one of the founding members of “The sushi crew” is the kind of friend that everyone talks about meeting in graduate school, the kind of friend that is with you for life. She is the kind of friend that remembers your most embarrassing moments and actually documents them, the kind of friend that you want to live the dream with. Thank goodness that there are many more years to come.

Family. Everyone has a family, but very few people have a family like the Keller’s. Seriously. We laugh together, we have family calendars made each year (that we all really look forward to), we talk weekly, we get together whenever we can, we are there for each other every step of the way. They have encouraged me to pursue my dreams without ever putting pressure on me. They also taught me how to live life to the fullest while not treading upon other people along the way. I am thankful for every day that I get to spend with them.

During my first (and most hellish) year of graduate school, I met the most influential person in my graduate student life. He was waiting for me after my bioreg exam six months after I started at UCSF and he was there six years later, after my thesis talk. I owe Topher Carroll more than I know how to put down with

words. He has always, and continues to be, there for me, as a scientist, a best friend, and a woof.

Acknowledgments of Published Material

Chapter two of this dissertation is a reprint of material as it appears in "Isolation and proteomic analysis of *Chlamydomonas* centrioles." Lani C. Keller and Wallace F. Marshall, *Methods in Molecular Biology*. 2008. **432**: 289-300. Chapter three of this dissertation is a reprint of material as it appears in "Proteomic analysis of isolated *Chlamydomonas* centrioles reveals orthologs of ciliary-disease genes." Lani C. Keller, Edwin P. Romijn, Ivan Zamora, John R. Yates III, and Wallace F. Marshall. *Current Biology*. 2005. June 21; **15**(12): 1090-1098. Chapter four of this dissertation is a reprint of material as it appears in "Molecular architecture of the centriole proteome: the conserved WD40 domain protein POC1 is required for centriole duplication and length control." Lani C. Keller, Stefan Geimer, Edwin P. Romijn, John R. Yates III, Ivan Zamora, and Wallace F. Marshall. *Molecular Biology of the Cell*. 2009. February 20; **4**: 1150-1166.

Molecular Architecture of the Centriole Proteome

Lani C. Keller

Abstract

Centrioles were first described over a century ago as small, geometrically precise cellular entities composed of nine triplet microtubule blades arranged in a pinwheel-like array. The structure of the centriole is complex and highly precise, with centriole geometry and dimensions being tightly controlled, but the molecular mechanisms governing centriole assembly, length control, and maturation into basal bodies remain mysterious. The biological significance of centrioles is demonstrated by the fact that they are necessary for recruitment of pericentriolar material (PCM) to form a complete centrosome and that they act as basal bodies, during the formation of cilia and flagella. The remarkable centriole duplication cycle in which new daughter centrioles form at an intriguing right angle to the pre-existing mother centriole, along with unique ability of centrioles to act as basal bodies to initiate ciliogenesis have perplexed researchers for decades.

Much of the aura of mystery that surrounds centrioles stems from the fact that the protein composition of centrioles is largely unknown. To gain molecular insights into the function and assembly of centrioles, I set out to identify a parts list for the centriole through direct proteomic analysis of isolated centrioles. Prior to this study there were only eleven known core centriole proteins. I developed a purification protocol allowing for the isolation of virtually “naked” centrioles, with

little to no obscuring PCM, from the green alga, *Chlamydomonas*. Proteomic analysis of these isolated centrioles provided the first opportunity to reveal the specific parts of the centriole and constitutes the centriole proteome. This investigation into centriole composition has helped elucidate the function and properties of this unique organelle, which has remained mysterious for more than a century.

Remarkably, this proteomic analysis of centrioles has provided not only a full and complete parts list for the centriole but has also demonstrated that human disease proteins are highly represented in the centriole proteome suggesting that multiple human disease gene products encode protein components of the centriole. In fact, known human disease genes encode over seventeen percent of the cross-validated *Chlamydomonas* centriole proteins. In particular, two classes of ciliary disease genes are highly represented among the centriole proteome: cystic kidney disease syndrome genes and cone-rod dystrophy syndrome genes. One possibility is that the human disease genes found in the centriole proteome encode for structurally conserved core centriole proteins that are necessary for establishing or maintaining the integrity of the complex triplet microtubules structure. Another possibility is that these proteins are involved in ciliogenesis-related functions. This research has laid a foundation for future studies of this enigmatic organelle.

Our published centriole proteome identified proteins predicted to compose the centriole, although we had no concrete evidence that these proteins were actually centriolar. To validate their *in vivo* localization to centrioles I created

GFP-fusion proteins for candidate centriole proteins and have localized over sixty percent of all the proteins that we feel are core centriole components based our bioinformatics approach. To begin to learn how the centriole proteome is put together, I investigated POC1, one of the most abundant proteins from our centriole proteome, which is conserved in all organisms with triplet microtubules. I found that POC1 is a proximal and very early marker of centriole duplication and has a unique localization on intact mature centrioles, being found to colocalize with attachment points of multiple distinct fiber systems that contact the centriole. This is the first protein to date that localizes to both early duplicating centrioles and to places of centriole fiber attachment, indicating that POC1 may be involved in multiple distinct aspects of centriole biology. Furthermore, POC1 is involved in the early stages of centriole duplication and also plays a role in the enigmatic process of centriole length control.

Together this research signifies a cohesive body of work starting with the isolation and purification of *Chlamydomonas* centrioles leading to the first published centriole proteome and continuing with the detailed characterization of one particular protein involved in both centriole duplication and length control.

Table of Contents

List of Tables

Chapter Two

Chapter Three

Chapter Four

List of Figures

Chapter Two

Chapter Three

Chapter Four

Chapter Five

Chapter 1

Introduction

Centrioles have fascinated and perplexed researchers even since their discovery in 1887, as permanent cellular organelles with the unique ability for self-replication. This centrally localized organelle is found throughout evolution, in organisms ranging from protists to humans, and has clearly been instrumental in the evolution of the modern eukaryotic cell (Chapman et al., 2000). In the 19th century two scientists separately recognized and documented that centrioles and basal bodies have the same underlying structure. This remarkable discovery, known as the Henneguy-Lenhossek theory, proves the evolutionary importance of centrioles and hints at their importance during multiple stages of a cell's life. Despite over one hundred years of research surrounding this enigmatic organelle, the precise function of centrioles along with how the centriole's complex architecture is erected once and only once every cell cycle remain mysterious.

Centrioles: The Most Handsome Organelle

Advances in microscopy over time have led to a nearly complete picture of the centriole at the level of its sophisticated ultrastructure. Each centriole is comprised of nine triplet microtubules arranged in a pin-wheel like array. These tiny geometrically precise organelles are approximately 500nm in length and have a nine-fold symmetry clearly observed by peering through either of the 200nm diameter ends (Beisson and Wright, 2003). Either end of the centriole may be conceived as "business end" depending of the specific function that one is examining. The distal end, with its many connecting fibers, holds the plus ends

of the triplet microtubules, anchors cytoplasmic microtubules, and interacts with the plasma membrane during the assembly of cilia and flagella (Vladar and Stearns, 2007). The proximal end of the centriole consists of a cartwheel, characterized by nine spokes radiating from a central axis, that is responsible for establishing the initial nine-fold symmetry (Hiraki et al., 2007). Additionally, the proximal end is where newly forming centrioles assemble each cell cycle at an intriguing right angle to the preexisting centriole. Structural studies have provided a plethora of information about centriole structure and have even allowed scientists to gain insights into the distinct steps of the centriole duplication cycle (Kochanski and Borisy, 1990). However, structural studies on centrioles have severe limitations and have failed to provide much insight into the precise function and self-assembly process of centrioles.

The Centriole Duplication Cycle

The centriole duplication cycle presents an interesting biological problem. That is, the cell must construct one of the its most sophisticated architectural designs in a highly reproducible manner at a specified time each and every cell cycle with no numerical mistakes. There must be tight control of centriole number because any abnormalities may lead directly to cancer progression (Marshall, 2001; Sluder and Hichcliffe, 1999). Centrioles, much like DNA, have an innate reproductive capacity. However, unlike DNA, centrioles duplicate conservatively, without the division or disassembly of the preexisting centriole. This duplication process is tightly coupled to DNA synthesis and is regulated via a complex

signaling mechanism which produces a strict number control system whereby the number of centrioles and the ploidy of the cell is regulated throughout the cell cycle (Sorokin, 1968). Following cytokinesis, a normal diploid cell inherits two centrioles in an orthogonal configuration, that differ in age by one cell cycle. The older, more mature centriole is termed the mother centriole, while the younger one is called the daughter centriole. In early G1 phase of the cell cycle, these centrioles lose their orthogonal relationship in a step termed ‘disorientation.’ The resultant single centrioles gain the capacity to replicate, and newly forming daughter procentrioles begin to assemble adjacent to and at right angles with, the preexisting centrioles during the S phase of the cell cycle. At this time the cell has two new daughter procentrioles and the previous mother centriole becomes a grandmother, while the previous daughter centriole becomes a mother centriole. The newly formed procentrioles subsequently elongate to full-length centrioles in the G2 phase of the cell cycle. Thus within one cell cycle, the centriole duplication cycle must involve not only the production of two procentrioles, but also the maturation of the original immature centriole, resulting in two pairs of centrioles, one for each daughter cell (Lange and Gull, 1995).

Why Use Green Algae to Study Centrioles?

Centriole duplication is controlled by a number of known molecular cues, however until recently the structural components of centrioles remained unknown, making it virtually impossible to fully understand centriole assembly. Much like how early biologist relied on dissections to uncover the mysteries of

how organisms were built, proteomic approaches can now reveal the entire protein composition of specific structures and organelles. To further delve into the centriole assembly process we have turned to the unicellular biflagellate green alga, *Chlamydomonas reinhardtii*, because it has a number of unique advantages for biochemical and proteomic analyses. *Chlamydomonas* centrioles exist in a more primitive form than mammalian centrioles in that they have virtually no surrounding pericentriolar matrix. These “naked” centrioles are ideal for isolation and subsequent proteomic analysis because of the absence of this obscuring material. *Chlamydomonas* is also inherently suited for biochemical analysis because it can be cheaply and easily grown in large quantities. Additionally, *Chlamydomonas* is favorable in comparison to other model organisms because, unlike *Drosophila* and *C.elegans* which have centrioles that are structurally highly divergent from human centrioles, this green alga has triplet microtubules nearly identical to our centrioles (Dutcher, 2003). Despite being separated by more than 109 years of evolution, *Chlamydomonas* and human centrioles are amazingly similar in structure and function (Silflow and Lefebvre, 2001). Additionally, in contrast to other systems, most *Chlamydomonas* centriole genes also have clear mammalian homologs, allowing us to use any obtained proteomic data to enhance our understanding of centriole biology in humans.

Determining a Parts List for the Centriole

To fully understand the centriole assembly process it is necessary to first breakdown the ultrastructural complexity of the centriole into all of its

components. In order to do this I developed a procedure for the isolation and purification of *Chlamydomonas* centrioles, which is discussed in Chapter Two (Keller and Marshall, 2008). Taking advantage of the fact that *Chlamydomonas* shed their flagella under specific conditions, I was able to isolate the centrioles away from the flagella. A specifically designed mass-spectrometry method was then utilized to identify the entire molecular composition of centrioles. This proteomic analysis of centrioles allowed for the identification of centriole proteins involved in all aspects of centriole biology and is shown in Chapter Three (Keller et al., 2005). In particular, we focused on proteins implicated in the early steps of centriole assembly and on proteins involved in centriole's subsequent maturation into basal bodies capable of nucleating cilia formation.

The Centriole Proteome and Beyond

The centriole proteome has laid the foundation for future studies of the centriole by laying out all of the parts that are necessary to assembly the complex triplet microtubule structure of a centriole. Additionally, this parts list for revealed orthologs of many human ciliary-disease genes emphasizing the importance of centriole for normal human tissue homeostasis. Cells lacking functional centrioles are often viable but have the potential to cause disease. Many of these human diseases can be attributed to defects in centrioles in their basal body form and their associated cilium as discussed in Chapters Three and Four. In addition, to discovering centriole proteins important in human health, the centriole proteome has revealed individual proteins recruited to centrioles during

the assembly process. One of these highly abundant centriole proteins, discussed in Chapter Four, is absolutely required for centriole duplication and is intimately involved in the centriole length control process.

It is now understood that centrioles present an important link to human disease, however the long-standing question of the precise role of centrioles during cell division remains. Taking advantage of *Chlamydomonas* mutations with either abnormal centriole structure or abnormal numbers of centrioles finally allows for an in depth examination of this question. I provide evidence that centrioles play a role in biasing spindle morphology towards a bipolar arrangement and in promoting completion of cytokinesis. These data, discussed in Chapter Five, suggest Theodor Boveri's theory that abnormal centriole numbers may place a causal role in development of cancer by contributing to chromosome instability does have some validity.

The Future of the Centriole

While giving a seminar, someone once asked if scientists would be able to reconstitute the centriole *in vitro* within my lifetime. Hopefully, with the help of this work we are one step closer to this colossal feat.

References

Beisson J and Wright M. (2003). Basal body/centriole assembly and continuity. Current Opinion in Cell Biology, **15**: 96-104.

Chapman MJ, Dolan MF, and Margulis L. (2000). Centrioles and kinetosomes: form, function, and evolution. The Quarterly Review of Biology, **75**(4): 409-429.

Dutcher SK. (2003). Elucidation of basal body and centriole functions in *Chlamydomonas reinhardtii*. Traffic, **4**: 443-451.

Hiraki M, Nakazawa Y, Kamiya R, and Hirono M. (2007). Bld10p constitutes the cartwheel-spoke tip and stabilizes the 9-fold symmetry of the centriole. Current Biology, **17**(20): 1778-1783.

Keller LC, Romijn EP, Zamora I, Yates J 3rd, and Marshall WF. (2005). Proteomic analysis of isolated *Chlamydomonas* centrioles reveals orthologs of ciliary-disease genes. Current Biology, **15**(21): 1090-1098.

Keller LC and Marshall WF. (2008). Isolation and proteomic analysis of *Chlamydomonas* centrioles. Methods in Molecular Biology**, 432**: 289-300.

Keller LC, Geimer S, Romijn E, Yates J 3rd, Zamora I, and Marshall WF. (2009). Molecular architecture of the centriole proteome: the conserved WD40 domain protein POC1 is required for centriole duplication and length control. Molecular Biology of the Cell, **20**(4): 1150-1166.

Kochanski RS, and Borisy GG. (1990). Mode of centriole duplication and distribution. The Journal of Cell Biology, **110**: 1599-1605.

Lange BMH and Gull K. (1995). A molecular marker for centriole maturation in

the mammalian cell cycle. The Journal of Cell Biology, **130**(4): 919-927.

Marshall WF. (2001). Centrioles take center stage. Current Biology, **11**: R487-R496.

Silflow CD and Lefebvre PA. (2001). Assembly and motility of eukaryotic cilia and flagella. Lessons from *Chlamydomonas reinhardtii*,. Plant Physiology, **127**(4): 1500-1507.

Sluder G, and Hinchcliffe EH. (1999). Control of centrosome reproduction: the right number at the right time. Biology of the Cell, **91**: 413-427.

Sorokin SP. (1968). Reconstructions of centriole formation and ciliogenesis in mammalian lungs. Journal of Cell Science, **3**(2): 207-230.

Vladar EK and Stearns T. (2007). Molecular characterization of centriole assembly in ciliated epithelial cells. The Journal of Cell Biology, **178**: 31-42.

Chapter 2

Isolation and Proteomic Analysis of *Chlamydomonas* Centrioles

Abstract

Centrioles are barrel-shaped cytoskeletal organelles composed of nine triplet microtubules blades arranged in a pinwheel-shaped array. Centrioles are required for recruitment of pericentriolar material during centrosome formation and they act as basal bodies, which are necessary for the outgrowth of cilia and flagella. Despite being described over a hundred years ago, centrioles are still among the most enigmatic organelles in all of cell biology. To gain molecular insights into the function and assembly of centrioles we sought to determine the composition of the centriole proteome. Here, we describe a method that allows for the isolation of virtually "naked" centrioles, with little to no obscuring pericentriolar material, from the green alga, *Chlamydomonas*. Proteomic analysis of this material provided evidence that multiple human disease gene products encode protein components of the centriole, including genes involved in Meckel Syndrome and Oral-Facial-Digital Syndrome. Isolated centrioles can be used in combination with a wide variety of biochemical assays in addition to being utilized as a source for proteomic analysis.

Key Words

centrioles; basal bodies; *Chlamydomonas*; proteomics; MudPIT; nephronophthisis; Meckel Syndrome; Oral-Facial-Digital Syndrome; primary cilia; PACRG

Introduction

The centriole (1), which is at the heart of the centrosome, is composed of nine triplet microtubule blades arranged in a pinwheel-like array. The biological significance of centrioles is demonstrated by the fact that they are required for recruitment of pericentriolar material during centrosome formation and that they act as basal bodies, which are necessary for the outgrowth of cilia and flagella. Other roles for centrioles in cytokinesis and cell-cycle regulation have been proposed but remain controversial. The remarkable centriole duplication cycle in which new daughter centrioles form at an intriguing right angle to the pre-existing mother centriole, along with the precise function of centrioles have perplexed researchers for decades.

In order to fully understand large macromolecular structures, such as the centriole, it is essential to identify the protein composition in its entirety. We therefore determined the first published centriole proteome, using material isolated from the green alga *Chlamydomonas reinhardtii* (2). *Chlamydomonas* has become a prominent model organism to study centrioles for several reasons: *Chlamydomonas* has genetics very similar to yeast, but unlike yeast, has centrioles similar to animal cells. Many molecular and genomic techniques are now routine in *Chlamydomonas* including RNA-interference (RNAi), GFP-tagging, and microarrary analysis. Furthermore, *Chlamydomonas*, unlike other genetic model organisms including *Drosophila* and *C.elegans*, has centrioles with triplet microtubules that are virtually identical to mammalian centrioles in both

structure and duplication cycle. Unlike mammalian centrioles, which are surrounded by a complex mesh-work of pericentriolar material (PCM) containing over 300 proteins, *Chlamydomonas* has virtually “naked” centrioles allowing for convenient large-scale biochemical isolation and direct analysis in the absence of the obscuring PCM (3). These features make *Chlamydomonas* an ideal model organism to study the composition of centrioles via proteomics.

Previously, comparative-genomic analyses were used to unveil genes conserved in species with cilia and flagella (4). In addition, proteomic analyses were reported on enriched preparations of centrosomes, but that analysis was unable to distinguish the bona fide centriolar proteins from the surrounding PCM (5). The exploitation of *Chlamydomonas* allows direct proteomic analysis of isolated centrioles which lack PCM, presenting a huge advantage over mammalian systems (2). Our method, adapted from an earlier procedure developed in the Rosenbaum lab (6), utilizes large-scale isolation of centrioles from *Chlamydomonas* cells. Briefly, *Chlamydomonas* cells are deflagellated and lysed in detergent before enriching for centrioles through multiple rounds of velocity sedimentation and a final round of equilibrium centrifugation. The isolated centrioles are then examined proteomically using MudPIT (Multidimensional Protein Identification Technology), a mass-spectrometry-based method in which complex mixtures of proteins can be analyzed without prior electrophoretic separation (7).

2. Materials

2.1 Cell Culture

1. *Chlamydomonas* (cell-wall-less strain), Chlamydomonas Genetics Center Duke University. Web site for the center: http://www.chlamy.org.

2. 100X Tris: dissolve 24.2 g of Tris in 100 mL of distilled H_2O (dH_2O).

3. 100X TAP (tris-acetate-phosphate) Salts: dissolve 18.75 g of NH_4Cl, 5 g of $MgSO_4.7H_2O$, 2.5 g of $CaCl_2.2H_2O$ in 500 mL of dH_2O.

4. Phosphate Solution: dissolve 21.6 g of K_2HPO_4, 10.8 g of KH_2PO_4 in 200 mL of dH_2O.

5. Hunter Trace Elements (see below).

6. Cell culture carboy, 2 gallon (for large-scale isolation), Nalgene #2551.

7. Two-liter glass bottle (for small-scale isolation), Fisher.

8. Foam corks.

9. Boring tool.

10. Stir plate large enough for carboy, with large-size magnetic stir bar.

11. Fish tank pump with regulation valve (see **Note 1**).

12. Rubber latex tubing.

13. Glass filter unit (Bellco) plugged with cotton.

2.2 Deflagellation and Cell Lysis

1. Deflagellation buffer: 0.5 M acetic acid.

2. Recovery buffer: 0.5 M KOH.

3. TE: 10 mM Tris adjusted to pH 8.0 with HCl, 1 mM EDTA.

4. 25% (w/v) sucrose in TE.

5. Nonidet P-40 (NP-40): (see **Note 2**).

6. Protease inhibitors (final concentrations): 2 μg/mL aprotinin, 1 μg/mL pepstatin, 1 μg/mL leupeptin, 1 mM phenlymethylsulfonyl fluoride (PMSF), 10 μg/mL soybean trypsin inhibitor (STBI).

2.3 Centriole enrichment

1. TE: 10 mM Tris adjusted to pH 8.0 with HCl, 1 mM EDTA.

2. 25% (w/v) sucrose in TE.

3. 40% (w/v) sucrose in TE.

4. 50% (w/v) sucrose in TE.

5. 60% (w/v) sucrose in TE.

6. 70% (w/v) sucrose in TE.

7. 80% (w/v) sucrose in TE.

8. 40% (w/v) Nycodenz in TE.

9. 2 M NaCl.

10. Dounce Homogenizer (40 mL).

11. Light microscope.

12. Coverslips (circle and square).

13. 12-well dish.

14. Swinging bucket rotor.

15. Plate spinner.

16. High-speed centrifuge that can reach 14000 g.

2.4 Monitoring and evaluating centriole enrichment

2.4.1 Immuno-fluorescence

1. Anti-acetylated tubulin antibody (Sigma, #T6693, clone 6-11B-1).
2. Anti-mouse secondary antibody (Jackson ImmunoResearch Laboratories #115-095-003).
3. Poly-lysine solution (Sigma).
4. PBST: PBS (Phosphate Buffered Saline) + 0.1% (w/v) Tween-20.
5. Normal goat serum.
6. Vectashield (Vector #H-1000).

2.4.2 Western Blot

1. 0.45-μm nitrocellulose (Biorad #162-0115).
2. Peroxidase-conjugated donkey anti-mouse IgG (Jackson ImmunoResearch Laboratories #115-035-003).
3. Chemiluminescence detection reagents (Amersham Biosciences #RPN2132).

3. Methods

The use of a flagellated cell type (*Chlamydomonas*) as a source of centrioles creates a potential pitfall in that flagella share many proteins in common with centrioles, and are of a similar radius and density. This makes it difficult to separate flagella from centrioles if both are present in the starting lysate. For this reason, it is critical to carefully remove the flagella prior to cell lysis. Fortunately, the natural biology of *Chlamydomonas* provides a simple solution. *Chlamydomonas* cells exposed to a transient decrease in pH will spontaneously

shed their flagella, which can then be easily separated from the cell bodies since the cell bodies are much larger than the flagella. In order for this strategy to work it is critical to verify, by microscopy, that virtually all cells have undergone flagellar loss, prior to beginning cell lysis. It is also important to keep the cells in the cold after deflagellation, to prevent flagellar regrowth.

The major contaminant in all biochemical preparations from *Chlamydomonas* cell bodies is the chloroplast. Because the chloroplast contains naturally pigmented chlorophyll, it is possible to visually assess the degree of chloroplast contamination at each stage simply by observing the green color.

3.1 Preparation of media

1. In order to make 1 liter of TAP media, add 10 mL of 100X Tris, 10 mL of 100X TAP Salts, 1 mL of Phosphate Solution, 1 mL Hunter Trace Elements and 1 mL of Glacial acetic acid to a bottle and add water to 1 liter.

2. To make 1 liter of Hutner Trace Elements, dissolve each compound in the volume of dH_2O indicated in Table 1. Mix all solutions together in a large flask, except for the EDTA stock solution. Bring this mixture to a boil before adding the EDTA. This mixture should be green in color. After everything has dissolved, cool to 70°C and maintain this temperature while adjusting the pH to 6.7 with approximately 85 mL of hot KOH (20%, w/v). The pH-meter should first be standardized with buffer of the same temperature. Bring this mixture to a final volume of 1 liter. Put a cotton plug in the flask and let stand for 1-2 weeks at room temperature, swirling it once per day. The initially clear-green solution

should turn purple eventually and have a rust-brown precipitate settled at the bottom of the flask. The precipitate is filtered through two layers of Whatman #1 filter paper two times. This clear-purple solution can be kept at 4°C for years (8).

3.2 Cell culture

1. A small pea-sized amount of a cell-wall-less strain of *Chlamydomonas* is inoculated into a 200 mL flask containing 100 mL of TAP media with a foam cork that has a hole bored through it. Allow this culture to grow until reaching a dark green color by bubbling air through a disposable pipet, sticking through the foam cork, hooked up to a standard fishtank air pump. A dark green color (demonstrated in Figure 1) indicates an approximate cell density of 10^7 cells/mL. For best results, bubble at a constant but slow rate so as not to lyse the cells (a sterile stir bar can also be used to keep the cells from settling).

2. Prepare the 8-liter culture carboy of TAP media. Autoclave TAP media in container with foam cork that has a glass pipet through it attached to a glass filter unit filled with cotton and latex rubber tubing (see Figure 2 for photograph of apparatus). Sterilization of entire apparatus plus tubing significantly decreases the chance of contamination. Once the 100 mL culture is dark green, pour this into the 8-liter carboy and allow growth with aeration and stirring until obtaining a dark green color. For proteomic analysis it is recommended to start with at least 32 liters of *Chlamydomonas* culture (see **Note 3**).

3.3 Deflagellation and cell lysis

1. Concentrate *Chlamydomonas* from 32 L of culture by low speed centrifugation (400 g for 3 min without brake). Aspirate media off cell pellet. Add TAP media to each of the cell pellets and combine them until a final volume of 400 mL is reached. Let the cells bubble and stir for 90 min. Check that cells are alive and motile by looking with a compound microscope.

2. After 90 min of aeration, concentrate the cells again by centrifugation at 400 g for 3 min without brake. Aspirate the supernatant and resuspend in 100 mL of TAP media.

3. Put the 100 mL on ice and reduce the pH to 4.5-4.7 with 0.5 M acetic acid for 1 min while stirring and monitoring with a pH-meter. Then add 0.5 M KOH to return the pH to 7.0. At this point check that deflagellation was successful by looking at the cells on a compound microscope.

4. After deflagellation, overlay the cells onto ice-cold 25% sucrose in TAP media. Spin cells on sucrose cushion for 30 min at 1200 g. This spin should pellet the cells through the sucrose while keeping the flagella above the sucrose cushion. Aspirate and discard the supernatant.

5. Resuspend cell pellet in 150 mL of ice-cold TAP. Centrifuge 20 min at 1200 g at 4°C. Aspirate supernatant and resuspend the pellet in 25 mL of ice-cold TE.

6. Add NP-40 to 10% of the volume (in this case add 2.5 mL). Also add the protease inhibitors. Let this stir for 5 min on ice and then take this sample and put it in a 40 mL Dounce homogenizer. Dounce 15 strokes and then put the sample back on ice for stirring for an additional 10 min.

7. Check cell lysis by phase contrast microscopy. It is absolutely essential that all cells are completely lysed (see **Note 4**).

8. Layer the 25 mL of lysate onto 25 mL of 25% sucrose in TE cushion. This can be done in disposable 50 mL conical tubes. Centrifuge the lysate/cushion at 1500 g for 15 min at 4°C in a hanging bucket rotor. Then collect the entire green supernatant (that which did not go into the cushion). This sample will still contain lots of vesicles and starch granules visible by microscopy. Layer this supernatant onto a second 25 mL cushion of 25% sucrose in TE and centrifuge at 1500 g in hanging bucket rotor for 15 min at 4°C. Collect the entire supernatant. At this point the sample can be frozen in liquid nitrogen until future use. Keep at –80°C.

3.4 Enrichment of centrioles by sedimentation

1. Layer the 25 mL of lysate onto 10 mL of 50% sucrose in TE overlayed with 10 mL of 40% sucrose in TE in a 50 mL polycarbonate tube. Spin at 14000 g in hanging bucket rotor for 1 h. Collect the entire 40% sucrose fraction. Layer this 40% sucrose fraction onto a step gradient in a polycarbonate tube consisting of (from the bottom) 5 mL of 80%, 5 mL of 70%, 5 mL of 60%, and 5ml of 50% sucrose in TE. Centrifuge this sample at 14000 g in hanging bucket rotor for 3 h. After centrifugation collect 2 mL fractions starting from the top and freeze in liquid nitrogen. Save each of these fractions at –80°C for Western blot analysis and immunofluorescence.

2. During analysis of the fractions from the 80-50% sucrose in TE spin (see sections 3.5 and 3.6), prepare a Nycodenz gradient. Make 40% Nycodenz in TE and freeze-thaw the solution in a polycarbonate tube three times. This freeze-thaw method creates a continuous density gradient of Nycodenz.

3. Take the two fractions having the highest enrichment of centrioles (as determined by Western blot and/or immunofluorescence) from the 80-50% sucrose, spin down them down, combine them, and wash them in a single wash containing 2% NP-40 and 500 mM NaCl for 10 min to remove any peripherally associated proteins. Add the mixture of the two fractions to the top of the pre-made Nycodenz gradient and centrifuge for 18 h at 14000 g in hanging bucket rotor to reach equilibrium. At this point there should be a visible band where the fractions migrated during the spin. Take 1 mL fractions from the top of the tube and proceed with determination of centriole enrichment by both Western blot and immunofluorescence.

3.5 Tracking Centriole Enrichment by Immunofluorescence

1. It is important to be able to track where the centrioles are during the course of the isolation in order to select the fractions from each step that contain the majority of centrioles. Using antibodies directed against centriolar proteins one can determine which of the fractions collected throughout the preparation are enriched for centrioles. We have used commercially available acetylated tubulin antibodies for this procedure.

2. Add 200 μL of polylysine to coverslips and let sit for 5 min. Rinse the coverslips in dH_2O and let air-dry. To speed procedure up, excess of dH_2O can be aspired. Pipet approximately 20 μL of sample onto poly-lysine-coated coverslip and let sit 10 min in order to adhere (see below for method to increase the number of centrioles per coverslip). After the 10 min, rinse coverslips in PBST once quickly followed by a one-min and a five-min incubation in PBST. Block coverslips with Normal goat serum diluted 1:10 in PBST for 15 min. After blocking, wash coverslips with PBST for 5 min.

3. In order to stain coverslips with acetylated tubulin, dilute antibody 1:500 in PBST and put 100 μL drops on a piece of Parafilm. Then take coverslips and invert them onto the 100 μL drops of diluted antibody. Let coverslips sit for 20 min. After antibody staining, wash the coverslips twice with PBST for 10 min each. During these washes dilute anti-mouse secondary antibody 1:1000 in PBST and make 100 μL drops on Parafilm again. After washing invert the coverslips onto the secondary antibody. Let coverslips incubate in secondary antibody for 15 min. Wash coverslips with PBST twice for 15 min each and mount coverslips with a small drop of Vectashield. For the best visualization, aspirate excess Vectashield around coverslip and nail polish edges.

4. To increase the number of centrioles per coverslip, a spin-down method can be used. This method involves a 12-well dish and 18-mm circle coverslips. Circle coverslips are first washed with water and soap and then rinsed well with dH_2O. Coverslips are then poly-lysine-coated by adding 200 μL of polylysine for 10 min. Rinse coverslips with H_2O and let air-dry. Put the coverslips

into the bottom of the 12-well dish (poly-lysine-coated side up). Dilute sample 1 mL:4 mL in TE and add 4.8 mL of this mixture into each well of the 12-well dish. Spin this sample (make sure there is another 12-well plate for balancing) in a centrifuge with plate holders at 750 g for 10 min with NO brake. Stain coverslips as stated above.

3.6 Evaluating enrichment by Western blotting

1. The immunofluorescence method described above provides a rapid way to assess the progress of the isolation. Once the procedure is completed, progressive enrichment can be evaluated throughout the procedure by analyzing frozen samples on Western blots using centriole-specific antibodies. Samples with equal amounts of protein (determined by Bradford assay) are run on a 10% acrylamide SDS-PAGE gel under normal conditions. The gels are then transferred onto 0.45-μm nitrocellulose.

2. Western blot analysis is then performed by using a mouse monoclonal anti-acetylated tubulin IgG at a dilution of 1:1000 and a peroxidase-conjugated donkey anti-mouse IgG at a dilution of 1:10000. Detection by chemiluminescence can be performed using commercially available reagents.

3. We also analyzed our final preparation using two-dimensional gel electrophoresis, in order to estimate the complexity of the mixture. Starting with 32 L of *Chlamydomonas* cells, we ended up with a 200 μL sample that contained approximately 100 μg of total protein. Two-dimensional gel electrophoresis was then performed on this final sample by Kendrick Labs (Madison, WI) with

ampholines spanning pH values of 3.5-10 (Amersham Pharmacia Biotech, Piscataway, NJ). The second dimension was run in a 10% acrylamide gel (0.75-mm thick) for 4 h at 12.5 mA. This analysis indicated at least 50-100 proteins were present by silver stain.

3.7 Proteomic Analysis by MudPIT Mass Spectrometry

1. LC-LC-MS/MS (two-dimensional liquid chromatography followed by tandem mass spectrometry) was carried out by MudPIT analysis in the Yates laboratory, Scripps Research Institute (see **Note 5**). Each LC-LC-MS/MS analysis was done with a starting material of approximately 100 μg of protein. Fourteen salt steps were performed to ensure all of the peptide fractions went through the two-dimensional liquid chromatography step. Peptides were then eluted into the mass spectrometer using a linear gradient of 5-60% RP-B (0.5% acetic acid, 80% acetonitrile) over 60 min at 50 μL/min.

The collection of resulting MS^2 spectra was searched against the *Chlamydomonas reinhardtii* predicted protein database (JGI Assembly October 2003, release 2.0) using the SEQUEST algorithm (9).

2. In order to compensate for high levels of chloroplast contamination throughout the final Nycodenz gradient (as judged by uniform green color in all fractions), we analyzed not only the peak centriole fraction but also two additional fractions above and below the peak in the gradient. Proteins identified in these fractions were subtracted from the protein list identified in the peak fraction. This resulted in a final list of 194 proteins. This subtracted list still contained a

substantial number of known chloroplast proteins, suggesting that more extensive analysis of the control fractions could be beneficial.

3. The final list of proteins contained 8 out of 11 previously known *Chlamydomonas* centriole proteins. In addition, 45 new proteins were identified whose localization in the centriole was supported by bioinformatic cross-validation, including presence in the human centrosome proteome (5), conservation of the genes in species that contain centrioles but not those missing centrioles (4), or upregulation of the genes during flagellar regeneration (10), a property shared by many genes encoding basal-body-localized proteins. Among the new genes were the *Chlamydomonas* homologs of four mammalian ciliary disease genes: oral-facial-digital syndrome type I, nephronophthisis NPHP-4, Meckel syndrome MKS1, and the Parkin Co-Regulated gene PACRG. These results suggest that mutations in these genes cause ciliary disease due to defects in centrioles/basal bodies that nucleate cilia, and indicate further proteomic analysis of centrioles may identify additional ciliary disease genes.

4. Notes

1. Any fish tank pump with adjustable air-flow rate will be adequate. We used Air-Tech #VAT-5.5.

2. It is essential that name-brand Nonidet P-40 be used. Other supposedly equivalent detergents fail to completely lyse *Chlamydomonas* cell walls.

3. Smaller-scale centriole isolations may be carried out to examine centriole ultrastructure. We recommend a no less than 2-liter starting volume be used for

this purpose. Proceed as suggested above but scale down appropriately. Western blots and immunofluorescence may be done on fractions to determine approximate enrichment. These fractions can then be processed for electron microscopy to investigate ultrastructure. Centrioles from mutant strains of *Chlamydomonas* can be processed in this fashion to examine ultrastructural defects in centrioles. Remember that this procedure is designed for cell-wall-less strains so mutant lines may have to be crossed into a cell-wall-less background. It is often cumbersome to deal with large volumes so we recommend doing a maximum of 8-liters of centriole preparations at one time if larger samples are necessary.

4. If cells visualized by phase contrast microscopy are not completely lysed allow sample to stir on ice for an additional 5 min and re-check.

5. We strongly encourage proteomics to be done in collaboration with established experts in the field.

Acknowledgments

The authors thank Edwin Romijn and John R. Yates III for a highly productive collaboration and for many helpful discussions. This work was supported by NSF grant MCB0416310, NIH grant R01 GM077004-01A1, the Searle Scholars Program, a Hellman Family Award for Early Career Faculty, and a UCSF REAC award.

References

1. Marshall, W.F. (2001) Centrioles take center stage. *Curr. Biol.* 11,R487 R496.

2. Keller, L.C., Romijn, E.P., Zamora, I. Yates, J.R., and Marshall, W.F. (2005) Proteomic analysis of isolated Chlamydomonas centrioles reveals orthologs of ciliary disease genes. Curr. Biol. 15,1090-8.

3. Doxsey, S., Zimmerman, W., and Mikule, K. (2005). Centrosome control of the cell cycle. *Trends in Cell Biology* 15(6):303-311.

4. Li, J.B., Gerdes, J.M, Haycraft, C.J., Fan, Y., Teslovich, T.M., May-Simera, H., LI, H., Blaque, O.E., Li, L, Leitch, C.C., Lewis, R.A., Green, J.S., Parfrey, P.S., Leroux, M.R., Davidson, W.S., Beales, P.L., Guay-Woodford, L.M., Yoder, B.K., Stormo, G.D., Katsanis, N., and Dutcher, S.K. (2004). Comparative genomics identifies a flagellar and basal body proteome that includes the BBS5 human disease gene. *Cell* 117,541-52.

5. Andersen, J.S., Wilkinson, C.J., Mayor, T., Mortensen, P., Nigg, E., and Mann, M. (2003). Proteomic characterization of the human centrosome by protein correlation profiling. *Nature* 426,570-574.

6. Snell WJ, Dentler WL, Haimo LT, Binder LI, Rosenbaum JL. (1974). Assembly of chick brain tubulin onto isolated basal bodies of *Chlamydomonas reinhardtii*. *Science 185*,357-360.

7. Washburn, M.P., Wolters, D., and Yates, J.R. 3rd (2001). Large-scale anslysis of the yeast proteome by multidimensional protein identification technology. *Nature Biotechnology* 19, 242-247.

8. Harris, E.H. The *Chlamydomonas* Sourcebook: A comprehensive guide to biology and laboratory use. Academic Press Inc., 1989. p. 578-579.

9. Eng, J., McCormack, A., and Yates, J.R. (1994). An approach to correlate tandem mass-spectral data of peptides with amino-acid sequences in a protein database. J. Am. Soc. Mass Spectrometry *5,*976-989.

10. Stolc, V., Samanta, M.P., Tongprasit, W., and Marshall, W.F. (2005). Genome-wide trancriptional analysis of flagellar regeneration in *Chlamydomonas reinhardtii* identifies orthologs of ciliary disease genes. Proc. Natl. Acad. Sci. U.S.A. 102,3703-7.

Table 1. Hutner's Trace Elements

	Grams salt	Milliliters of dH_2O
EDTA, disodium salt	50	250
$ZnSO_4.7H_2O$	22	100
H_3BO_3	11.4	200
$MnCl_2.6H_2O$	5.06	50
$CuSO_4.5H_2O$	1.57	50
$((NH4)_6Mo_7)_{24}.4H_2O$	1.10	50
$FeSO_4.7H_2O$	4.99	50

Figure Legends

Figure 1. Photograph of 100 mL culture of *Chlamydomonas* illustrating the correct density of culture for procedure.

Figure 1. Photograph of 100 mL culture of Chlamydomonas illustrating the correct density of culture for procedure

Figure 2. Photograph of 8-liter carboy apparatus showing configuration of foam plug, rubber hose, and glass filter holding unit. This should be assembled, filled with TAP media, a stir-bar added, and then entire apparatus autoclaved.

Figure 2. Photograph of 8-liter carboy apparatus showing configuration of foam plue, rubber hose, and glass filter holding unit. This should be assembled, filled with TAP media, a stir-bar added, and then entire apparatus autoclaved.

Chapter 3

Proteomic Analysis of Isolated *Chlamydomonas* Centrioles Reveals Orthologs of Ciliary Disease Genes

Abstract

Background: The centriole is one of the most enigmatic organelles in the cell. Centrioles are cylindrical microtubule-based barrels found in the core of the centrosome. Centrioles also act as basal bodies during interphase to nucleate the assembly of cilia and flagella. There are currently only a handful of known centriole proteins.

Results: Mass spectrometry-based MudPIT (Multidimensional Protein Identification Technology) was used to identify the protein composition of basal bodies (centrioles) isolated from the green alga *Chlamydomonas reinhardtii*. This analysis detected the majority of known centriole proteins including centrin, epsilon tubulin, and the cartwheel protein BLD10p. By combining proteomic data with information about gene expression and comparative genomics, we identified 45 cross-validated centriole candidate proteins in two classes. The first class of proteins (BUG1-BUG27) are encoded by genes whose expression correlates with flagellar assembly and which therefore may play a role in ciliogenesis-related functions of basal bodies. The second class (POC1-POC18) are implicated by comparative genomics and proteomics studies to be conserved components of the centriole. We confirmed centriolar localization for the human homologs of four candidate proteins. Three of the cross-validated centriole candidate proteins are encoded by orthologs of genes implicated in mammalian ciliary function and disease (OFD1, NPHP-4, and PACRG), suggesting that Oral-Facial-Digital Syndrome and Nephronophthisis may involve a dysfunction of centrioles and/or basal bodies.

Conclusion: By analyzing isolated *Chlamydomonas* basal bodies, we have been able to obtain the first reported proteomic analysis of the centriole.

Introduction

Centrioles are composed of nine triplet microtubules arranged into a 250 nm diameter cylinder [1]. The function of centrioles, and the mechanism of their duplication, remain unclear. Much of the aura of mystery that surrounds centrioles stems from the fact that the protein composition of centrioles is largely unknown.

During interphase, centrioles act as basal bodies, templating the formation of cilia and flagella. The importance of cilia for many developmental and physiological processes [2,3] has generated great recent interest in the function of ciliary basal bodies. Several human diseases that appear to involve ciliary defects, for example Bardet-Biedl syndrome, are now known to result from defects in basal body-localized proteins [4-6]. Given that multiple ciliary disease genes encode basal body associated proteins, one potentially powerful approach for identifying additional basal body-localized ciliary disease genes is to determine the protein composition of centrioles that have matured into basal bodies.

Direct proteomic analysis of centrioles has not previously been reported. In a clever and innovative strategy to define cilia and centriole-related genes, comparative genomic analyses were previously used to determine genes conserved in species that have cilia and flagella [4,7]. Several of these conserved genes are known to localize to centrioles or basal bodies, consistent with the fact that any organism which forms cilia must also contain centrioles. However, despite the fact that one of these datasets was named the flagellar and

basal body proteome (FABP), in fact these analyses were entirely genomics-based and did not directly address the protein composition of centrioles per se. Comparative genomics analyses are unable to detect centriolar proteins, such as centrin or tubulin, which are conserved in species lacking cilia. A direct proteomic analysis of centrioles would therefore be expected to provide complementary information about centriole composition.

A proteomic analysis of whole centrosomes isolated from vertebrate cells has been published [8]. However, it is critical to distinguish between centrioles and centrosomes, which are much larger structures composed of centrioles embedded within a large quantity of amorphous pericentriolar material (PCM) which is responsible for nucleation of microtubules. In metazoans, centrioles are small compared to the large size of the entire centrosome, and one would expect that the proteins comprising the centriole would be swamped out by the large quantity of PCM proteins if entire centrosomes were analyzed by proteomics. In fact, while the published centrosome proteome identified many proteins of the pericentriolar matrix, only a few known centriole proteins were identified in that study; for example epsilon tubulin was not found. In contrast, *Chlamydomonas* basal bodies represent essentially naked centrioles, without any appreciable PCM. Therefore, a proteomic analysis of *Chlamydomonas* basal bodies should allow identification of bona fide centriole proteins with higher sensitivity than previous studies. Moreover, since eukaryotic basal bodies template flagellar assembly during interphase and also act as centrioles in mitosis (as first recognized in the 19th century by Henneguy and von Lenhossék), analysis of

isolated *Chlamydomonas* basal bodies should reveal both proteins found within the mitotic centriole as well as basal body-specific proteins involved in ciliary assembly.

We thus set out to identify centriolar proteins by purifying and isolating basal bodies (i.e. centrioles) from *Chlamydomonas*. Our proteomic analysis of these isolated basal bodies provides the first opportunity to reveal the specific parts list of the centriole. This will help elucidate the function and properties of this unique organelle, which has remained mysterious for over a century.

Results

Isolation of *Chlamydomonas* basal bodies

We developed a procedure for isolating *Chlamydomonas* basal bodies based on a previously published protocol [9], as detailed in Supplementary Protocol S1. *Chlamydomonas* cells first were deflagellated and then lysed in detergent. Basal bodies were then enriched from this lysate using two rounds of velocity sedimentation in sucrose step gradients [9], followed by equilibrium centrifugation in a continuous gradient of Nycodenz.

As illustrated in Figure 1, this procedure was effective in enriching basal bodies from the crude lysate. Overall enrichment was estimated using immunofluorescence analysis of fractions spun down onto coverslips. We estimate the overall enrichment of basal bodies relative to total protein to be on the order of 6000-fold (Table S1). Enrichment of centrioles in the peak fraction was confirmed by Western blot analysis using antibodies against acetylated tubulin, a tubulin isoform that is highly enriched in centrioles (Figure 1C). Examination of the isolated basal body preparation by immunofluorescence and negative stain electron microscopy (Figure 1D) showed a large number of paired centriole structures, indicating that the ultrastructure was maintained during the preparation. It is also apparent from the negative stain images that the isolated basal bodies are not surrounded by any significant quantity of pericentriolar material. Two-dimensional gel electrophoresis analysis indicates that the

preparations contained at least 100 proteins (Figure 1E), consistent with previous estimates [10].

No contamination by flagella or microtubules was observed in our immunofluorescence analysis (Figure 1D). We noted that the final peak basal body fraction, along with most other fractions in the gradient, was slightly green in color, suggesting chloroplast contamination. This was expected a priori, given that the majority of the *Chlamydomonas* cell volume is occupied by the chloroplast. However, the green color (chloroplast) was spread over the entire length of the gradient and was not visibly enriched in the peak basal body fraction. This wide distribution of chloroplast contrasts to the basal bodies themselves, which were highly enriched in just a few adjacent fractions (Figure 1A).

Proteomic analysis of isolated basal bodies

We analyzed the protein composition of the peak basal body fraction from the Nycodenz gradient using MudPIT (Multidimensional Protein Identification Technology), a mass-spectrometry based method in which complex mixtures of proteins can be analyzed without prior electrophoretic separation [11]. Mass spectrometry data was used to match individual peptides to predicted gene models in the *Chlamydomonas* genome sequence. In addition to analyzing the composition of the peak centriole fraction, we also analyzed two neighboring fractions from the final Nycodenz gradient in order to determine which proteins are unique to the peak fraction and which represent contamination with

organelles or structures that fortuitously migrated near the basal body peak. Proteins detected in the peak fraction that were also present in either of the neighboring control fractions were removed from the peak fraction protein list, a subtractive proteomic strategy that has proven effective in other studies of complex organelle isolations [12]. The gene models corresponding to detected peptides in the peak fraction (following subtraction) and the two neighboring control fractions are given in Supplemental Tables S2 and S3. In table S2, which represents the peak fraction, we also list two indicators of protein quantity, the number of peptides identified per protein, and the spectral count divided by the predicted protein mass. The latter number is a more accurate predictor of protein quantity in the mixture [13].

We confirmed the degree of centriole enrichment by determining the percentage of known protein components of various cellular sub-structures or pathways identified in each fraction that was analyzed. As illustrated in Figure 2, the peak basal body fraction is highly enriched in centriole proteins as judged by the fact that 73% (8 out of 11) of known *Chlamydomonas* centriole proteins were detected in the peak fraction. Neither of the neighboring control fractions displayed this enrichment in their protein lists. As predicted from the green color observed during the purification procedure, all three fractions contained a substantial proportion of the known chloroplast proteins tabulated in our validation data set. However, compared to the two control fractions, the peak basal body fraction actually had a smaller fraction of known chloroplast proteins. Mitochondria were also detected as a significant contaminating organelle in the

peak fraction by this bioinformatics-based classification approach. Proteins involved in translation, membrane trafficking, fatty acid synthesis, glycolysis, and the actin cytoskeleton were only minor contributors to all three samples. We therefore conclude, based on Figure 2, that the peak fraction is specifically enriched for basal body/centriole proteins, and that the two other organelles that were present in the peak fraction, chloroplast and mitochondria, were less enriched in the peak than in the neighboring control fraction 1. Consistent with the fact that flagellar axonemes were not observed in immunofluorescence analysis of the peak fraction (Figure 1D), we did not detect any flagellar dyneins or radial spoke proteins in either the peak centriole fraction or either of the two control fractions.

The following known *Chlamydomonas* centriole proteins were found in the peak basal body fraction (Supplemental Table S2) but not in the control fractions (Supplemental Table S3): tektin [14], Rib43a, [15], DIP13 [16], SF-assemblin [17], centrin/VFL2p [18], epsilon-tubulin/BLD2p [19], Bap95 [20], and BLD10p [21]. Both alpha- and beta-tubulin were present in large quantities in the peak fraction although these were not scored as centriole-specific in Figure 2 because they are present throughout the cell in addition to their presence in centrioles.

In addition to the protofilament ribbon (pf-ribbon) components tektin and Rib43a, which have previously been shown to be components of microtubule doublets and triplets found in flagella and in centrioles/basal bodies, we also recovered a third known pf-ribbon protein Rib72, plus a Rib72-related protein. Because Rib72 presumably co-incorporates into the same axonemal sub-

structures as tektin and Rib43a, both of which are also present in centrioles, it is likely that Rib72 and Rib72-like are also centriolar, hence their recovery in this analysis further confirms the detection of bona fide centriole proteins. In addition to centrin (VFL2p), we also identified two additional centrin homologs related to centrin-2 and centrin-3, which are centriole-associated in animal cells. Another protein identified in the peak fraction was a *Chlamydomonas* homolog of the centrin-binding protein SFI1 [22].

Cross-validation of candidate centriole proteins

The enrichment of known centriole proteins in the proteomic data from the peak basal body fraction leaves us with the task of determining which of the remaining proteins are likely candidate centriole proteins as opposed to contaminants. As a first step towards this classification, we cross-validated our centriole proteome candidate list by comparing it to lists of proteins derived from previously published comparative genomics studies of genes conserved in species that have centrioles [4,7] as well as to proteomic analyses of human centrosomes [8] and cilia [23,24]. We also compared our protein list to the products of genes identified in a recent genome-wide transcriptional analysis of gene expression during flagellar regeneration in *Chlamydomonas* [25]. Previous studies have indicated that several proteins which localize to basal bodies are encoded by genes that are transcriptionally upregulated during flagellar regeneration in *Chlamydomonas*. Such upregulation was first shown for genes that encode flagellar proteins, but some encode basal body proteins. Genes

previously shown to be upregulated and that encode basal body proteins include BBS5 (Bardet-Biedl syndrome), which encodes a protein localized to ciliary basal bodies in humans [4], and DIP13 [16], which was identified in our proteomic analysis of the peak basal body fraction.

A protein was considered to be cross-validated as a candidate centriole protein if it was detected in our proteomic analysis of isolated basal bodies and was also scored positive for one or more of the following criteria: (a) conserved among species with centrioles (i.e. present in the comparative genomic analyses of Li et al [4] or Avidor-Reiss et al [7]), (b) present in centrosome or cilia proteome datasets of Andersen [8] or Ostrowski [23], or localized to centrioles/centrosomes based on published studies, or (c) encoded by a gene upregulated during flagellar assembly as judged by genome-wide microarray analysis [25] supplemented by quantitative RT-PCR re-checking of genes initially scored as non-upregulated by the published microarray analysis (Supplementary Table S4).

Figure 3A shows the overall composition of the peak basal body fraction, with proteins classified based on their annotations in the *Chlamydomonas* genome and taking into account the cross-validation criteria outlined above. Proteins for which convincing homology is lacking and for which no cross-validation data are available were considered "unknown." As illustrated in Figure 3A, known centriole proteins (indicated in red) and cross-validated centriole candidates (indicated in shades of blue) constitute roughly one third of the total list of proteins identified in the analysis of the isolated basal bodies. As indicated in

Figure 3B, many of the cross-validated centriole candidate proteins were validated by more than one criterion. The cross-validation criteria did not classify any of the known chloroplast or mitochondrial contaminants as candidate centriole proteins, as judged by lack of overlap in the Venn diagram, confirming the effectiveness of this bioinformatic validation strategy.

Identifying centriole proteins potentially involved in ciliogenesis

As discussed above, gene upregulation during flagellar regeneration indicates a possible role for proteins in the assembly or function of cilia and flagella. Of 59 proteins known to localize within flagella (listed in Table S5), only three, tektin, Rib43a, and Rib72, were also found in the centriole proteome data. These three are components of pf-ribbons structures which are shared between centriole microtubule triplets and flagellar microtubule doublets, and thus they are expected in both structures. Because none of the strictly flagellar proteins were found in the centriole proteome, it is likely that the preparation is entirely free of flagellar contamination and hence any proteins in the proteome encoded by genes upregulated during flagellar regeneration should be associated with basal bodies as opposed to simply being flagellar components.

Comparison of the centriole proteome data obtained from the peak basal body fraction to patterns of gene expression during flagellar assembly as judged by our recently published microarray data ([25] and by quantitative PCR (supplementary table S4) revealed eight known *Chlamydomonas* proteins (TUA1, TUB1, Tektin, DIP13, Rib43a, Rib72, HSP90A, and CCT3) known to be involved

with flagellar structure or assembly, all of which, with the exception of Rib72, have also been previously shown to localize to basal bodies. We also identified 27 new proteins which we have named the BUG proteins (Basal body proteins with Upregulated Genes), which were identified in our centriole/basal body proteome and which are encoded by genes that are upregulated during flagellar assembly (Table 1). As reflected in the name BUG, these proteins are identified by two criteria, one involving proteomics and one involving gene expression. Involvement of these proteins with basal bodies or flagella in *Chlamydomonas* has not previously been reported.

Identification of a conserved set of candidate centriole proteins

Based on cross-validation using comparative genomics data [4,7] as well as published proteomic analyses of human centrosomes and cilia, we have identified a further set of 18 strong candidate centriole proteins. We named the set of proteins cross-validated by conservation but which are not encoded by genes upregulated during flagellar regeneration the POC proteins (Proteome of Centriole), and they are listed in Table 2. The POC proteins are likely to be involved in aspects of centriole structure or functions that are unrelated to ciliogenesis or ciliary function, and therefore are considered potential candidates for core structural components of the centriole itself.

Centriolar localization of four cross-validated centriole candidate proteins

To test the efficacy of our protein identification strategy, we examined localization of a random subset of candidate proteins (Figure 4). Tektin served as a positive control. We constructed C-terminal GFP fusion proteins for the following candidate proteins and examined their localization upon transient transfection in HeLa cells: tektin, BUG14, BUG21, POC1, and POC12. Co-staining with gamma-tubulin, to mark the centrosome, revealed that each of the proteins examined localizes to a pair of dots representing the centrioles (Figure 4, insets). These data indicate that at least four of the newly identified centriolar candidate proteins found in this study do in fact localize to centrioles, confirming the accuracy of our approach.

Discussion

The Centriole Proteome

The analysis presented here is, to our knowledge, the first proteomic analysis to focus directly on the composition of isolated centrioles. Previous studies addressed centriole composition indirectly, either by examining conservation of genes among species which contain centrioles [4,7] or else by proteomic analysis of entire centrosomes [8] whose composition is dominated by pericentriolar material. We developed an isolation procedure to enrich basal bodies from *Chlamydomonas reinhardtii* and determined their protein composition using MudPIT [11]. We find that of the 195 proteins identified in our final enriched preparation, roughly one third (61/195) are either known centriole proteins or are centriole-related as judged by bioinformatics cross-validation using comparative genomics data, centrosome and cilia proteome data, and gene regulation during flagellar assembly. Another third of the proteins are obvious contaminants from chloroplast and mitochondria. A large fraction of the proteins identified by MudPIT (46/195) are novel or hypothetical proteins.

IFT, BBS, and PCM proteins not present in centriole proteome

Although proteins involved in intraflagellar transport (IFT) colocalize in the vicinity of basal bodies in *Chlamydomonas*, our analysis failed to detect any of the known IFT proteins [26]. This is consistent with the fact that isolated basal bodies do not give a positive signal when stained with antibodies against IFT

proteins or FLA10 kinesin (data not shown). Similarly, we did not detect any Bardet-Biedl Syndrome (BBS) proteins in our proteomic analysis of isolated basal bodies. BBS genes are implicated in a ciliary disease syndrome, and at least some of the eight known BBS proteins localize around the basal bodies of ciliated cells [4,5,27]. Despite the apparent co-localization of IFT and BBS proteins to the vicinity of basal bodies in ciliated cells, our results suggest that basal body localization of these proteins may only occur transiently during the course of their dynamic movements in and out of the cilium.

Another class of proteins not found in our centriole proteome data are components of the pericentriolar matrix (PCM). Neither gamma-tubulin, nor the three identified *Chlamydomonas* homologs of gamma-tubulin ring complex proteins, were found in the list of centriole proteome proteins. This confirms our expectation that *Chlamydomonas* interphase basal bodies are relatively free of PCM.

RNAi phenotypes of BUG and POC orthologs in C. elegans and Drosophila

In order to begin identifying candidate centriole proteins that might be important for centriole function, we compared our list of cross-validated candidates to published databases of genome-wide RNAi and insertional mutagenesis results in *C. elegans* and *Drosophila* [28-33]. The results of this analysis are annotated within Supplementary Table S2. Many candidates gave phenotypes suggesting a role in cell viability, but two candidates in particular appear to play specific roles in cell division. RNAi of the C. elegans homolog

(CE16015) of the DnaJ domain protein BUG7 caused a weak spindle phenotype during early embryogenesis [31], suggesting a role in spindle organization, while RNAi of the Drosophila homolog (CG15081) of POC17 is reported to cause formation of binucleate cells in S2 cells, [29] suggesting a cytokinesis defect. These published results confirm our expectation that at least some of the cross-validated centriole candidate proteins defined in this study are likely to have roles in cell division. An important future direction will be to determine the function of the BUG and POC genes in *Chlamydomonas* using RNAi methods.

Ciliary disease-related proteins in the centriole

Among the list of cross-validated centriole proteins obtained in this analysis (Tables 1 and 2), we identified the *Chlamydomonas* orthologs of two human ciliary disease genes, OFD1/BUG11 and NPHP-4/POC10. The OFD1 gene is mutated in human patients with Oral-Facial-Digital syndrome type I, a developmental disease that causes cystic kidney disease and malformations of mouth, face and digits [34]. The OFD1 protein localizes to the vicinity of centrosomes and basal bodies in human ciliated cells [35]. Prior studies of OFD1 localization could not, however, rule out the possibility that OFD1, like the IFT proteins, might localize around the basal bodies without actually being an integral part of the basal body structure. However, the fact that our analysis identified the OFD1 ortholog BUG11 in isolated *Chlamydomonas* basal bodies suggests that OFD1 is an integral component of the basal body. The NPHP-4 gene is mutated in human patients with Nephronophthisis, a disease

characterized by kidney cyst development at the corticomedullary border of the kidneys [36,37]. Similarly to OFD1, the NPHP-4 protein (also called nephrocystin-1 or nephroretinin) has recently been shown to localize in the vicinity of the basal body in human cells [38]. Our recovery of an NPHP4 ortholog in the isolated basal body proteome implies it is a component of the basal body itself and isn't simply localized around the basal body like the IFT proteins. Our data thus support the possibility that both Oral-Facial-Digital syndrome and Nephronophthisis may result from a dysfunction of basal bodies or centrioles which leads indirectly to a defect in ciliary function.

We also identified the *Chlamydomonas* ortholog of Parkin co-regulated gene (PACRG/BUG21. PACRG mutant mice show male infertility consistent with a defect in sperm flagella [39]. The fact that our analysis has revealed two bona fide human ciliary disease genes as well as an additional gene involved in flagellar formation in mice suggests that the centriole/basal body proteome presented here may be a rich source of candidate ciliary disease genes.

Conclusions

In this study, we successfully enriched centrioles from *Chlamydomonas reinhardtii* and utilized this material to generate the first reported centriole proteome. We identified 73% of the known centriole-associated proteins in *Chlamydomonas* in our analysis, as well as *Chlamydomonas* homologs of centriole or centrosome-associated proteins from other species.

Bioinformatic cross-validation established two sets of candidate centriole proteins: the Basal body proteins with Upregulated Genes (BUGs) and the Proteome Of Centriole proteins (POCs). The BUG proteins are likely to be directly involved in ciliogenesis, as suggested by the fact that they are encoded by genes upregulated during flagellar regeneration [25]. The POC proteins are likely to be core structural constituents of the centriole as suggested by their conservation in species with centrioles and/or by their presence in the human centrosome proteome. It is likely that a large fraction of these cross-validated candidates will encode bona fide centriolar proteins, as judged by our localization experiments in which the human orthologs of two BUG and two POC proteins were found to localize to centrioles in HeLa cells.

Within these two unique subsets of cross-validated centriole proteins, our analysis revealed several genes involved in ciliary diseases in humans and ciliary dysfunction in model systems. The identification of these disease genes, including OFD1, NPHP-4, and PACRG, suggests that these diseases are likely to be caused by defects in centriole structure or defects in ciliogenesis-related functions taking place at the basal body. The fact that our proteomic analysis of the centriole has been performed in *Chlamydomonas reinhardtii*, one of the leading genetic model systems for studies of centrioles and basal bodies due to its rapid yeast-like haploid genetics and canonical centriole ultrastructure, opens the door to an integrative approach in which classical genetics can be combined with proteomic approaches to centriole biology.

Experimental Procedures

The basal body isolation procedure and the methods used for analysis of protein composition by MudPIT is described in Supplemental Protocol S1.

Quantitative PCR

To measure gene expression during flagellar assembly, total RNA was isolated from *Chlamydomonas* cells prior to (t=0) and 30 minutes after deflagellation as previously described [25] and reverse transcribed using SuperScript II (Invitrogen, Carlsbad, Ca) following random priming (Invitrogen, Carlsbad, Ca) using 10mg of total RNA per reaction. cDNA (1/20 of the total RT reaction) was used for quantitative PCR using iTaq SYBR Green Supermix following the manufacturers conditions (BioRad, Hercules, Ca) and analyzed using a DNA Engine Opticon system (MJ Research). Primers used in this reaction were designed using the Primer 3 program (Whitehead Institute). C_T were obtained with the help of Opticon software (MJ Research). Products were analyzed by agarose gel electrophoresis to confirm production of correctly sized product.

HeLa Cell Transfection and Immunofluorescence

Mammalian cDNAs from the human ORF collection in the form of Gateway™ entry vectors were purchased from Open Biosystems [44]. The following cDNAs were used with accession numbers and corresponding Chlamydomonas ID

number listed {CV024189- tektin (ID 168881), CV024222- PACRG/BUG21 (ID 162703), CV024270- WD repeat protein POC1 (ID 162499), CV028399- hypothetical protein POC12 (ID 169453), and CV022993- hypothetical protein BUG14 (ID 168135- BUG14)}. Each cDNA was sequenced to verify correct ORF with M13 (-20) forward and M13 reverse primers provided by IDT® before putting them into the C-terminal GFP tagged pcDNA-DEST47 Gateway® Vector according to manufacturers protocol.

HeLa cells (a gift from Mark von Zastrow, UCSF) were grown on coverslips in 12-well plates and transfected with Lipofectamine™ 2000 according to manufacturers guidelines. Cells were fixed the following day with –20° methanol for 5-15min. and permeabilized with 0.2% Triton-X in TBS for 10min. Cells were then stained with anti gamma-tubulin antibodies (GTU-88, Sigma) 1:100 in TBS and TRITC-conjugated AffiniPure Goat Anti-Mouse IgG (115-025-003, Jackson Laboratories) 1:1000 in TBS. Cells were then stained with DAPI for 10min and mounted with Vectashield.

DeltaVision deconvolution microscopy was used to make quick projections of deconvolved images.

Acknowledgments

First and foremost, we thank Joel Rosenbaum for constantly encouraging us to pursue the composition of centrioles. The isolation procedure was first developed while WFM. was a postdoctoral fellow in the Rosenbaum lab, and we are grateful to Joel for his support, insight, and guidance. We also thank Dennis Diener and Doug Cole for invaluable advice and help during the early stages of this work; James Hislop for assistance with HeLa cell localization; Hiten Madhani, Eric Griffis, Marc von Zastrow, Heather Deacon, and Lotte Pedersen for helpful discussions; and Kim Wemmer, Elisa Kannegaard, and Jessica Feldman for careful reading of the manuscript. WFM acknowledges support from NSF grant MCB0416310, a UCSF REAC Award, a Hellman Family Award, and the Sandler Family Supporting Foundation. JRY acknowledges support from NIH grant RR11823-09 (University of Washington Yeast Resource Center).

Chlamydomonas genome sequence data were produced by the US Department of Energy Joint Genome Institute, http://www.jgi.doe.gov/ and are provided for use in this publication/correspondence only.

References

1. Beisson, J. and Wright, M. (2003) Basal body/centriole assembly and continuity. Curr Opin Cell Biol. *15*,96-104.
2. Pazour, G.J., and Rosenbaum., J.L. (2002). Intraflagellar transport and cilia dependent diseases. Trends Cell Biol. *12*,551-5.
3. Afzelius, B.A. (2004) Cilia-related Diseases. J. Pathol. *204*,470-477.
4. Li, J.B., Gerdes, J.M, Haycraft, C.J, ,Fan, Y., Teslovich, T.M, May-Simera, H, Li, H., Blacque, O.E., Li, L., Leitch, C.C., Lewis, R.A., Green, J.S., Parfrey, P.S., Leroux, M.R., Davidson, W.S., Beales, P.L., Guay-Woodford, L.M., Yoder, B.K., Stormo, G.D., Katsanis, N., and Dutcher, S.K. (2004). Comparative genomics identifies a flagellar and basal body proteome that includes the BBS5 human disease gene. Cell *117*,541-52.
5. Kim, J.C., Badano, J.L., Sibold, S., Esmail, M.A., Hill, J., Hoskins, B.E., Leitch, C.C., Venner, K., Ansley, S.J., Ross, A.J., Leroux, M.R., Katsanis, N., and Beales, P.L. (2004) The Bardet-Biedl protein BBS4 targets cargo to the pericentriolar region and is required for microtubule anchoring and cell cycle progression. Nat. Genetics. *36*,462-470.
6. Kim, J.C., Ou, Y.Y., Badano, J.L., Esmail, M.A., Leitch, C.C., Fiedrich, E., Beales, P.L., Archibald, J.M., Katsanis, N., Rattner, J.B., and Leroux, M.R. (2005) MKKS/BBS6, a divergent chaperonin-like protein linked to the obesity disorder Bardet-Biedl syndrome, is a novel centrosomal component required for cytokinesis. J Cell Sci. *118*,1007-1020.

7. Avidor-Reiss, T., Maer, A.M., Koudakjian, E., Polyanovsky, A., Keil, T., Subramaniam, S., and Zuker, C.S. (2004) Decoding cilia function: defining fgspecialized genes required for compartmentalized cilia biogenesis. Cell. *117*,527-539.

8. Andersen, J.S., Wilkinson, C.J., Mayor, T., Mortensen, P., Nigg, E., and Mann, M. (2003). Proteomic characterization of the human centrosome by protein correlation profiling. Nature *426*,570-574.

9. Snell WJ, Dentler WL, Haimo LT, Binder LI, Rosenbaum JL. (1974). Assembly of chick brain tubulin onto isolated basal bodies of *Chlamydomonas reinhardtii*. *Science 185*,357-360.

10. Dutcher, S.K. (1986). Genetic properties of linkage group XIX in Chlamydomonas reinhardtii. In "Extrachromosomal elements in lower eukaryotes", R.B. Wickner, A. hinnebusch, A.M. Lambowitz, I. Gunsalus, and A. Hollaender, Eds., pp. 303-325. Plenum Press, New York.

11. Washburn, M.P., Wolters, D., and Yates, J.R. 3rd (2001). Large-scale anslysis of the yeast proteome by multidimensional protein identification technology. Nat. Biotechnol. *19*, 242-247.

12 Schirmer, E.C., Florens, L., Guan, T., Yates, J.R. 3rd, and Gerace, L. (2003) Nuclear membrane proteins with potential disease links found by subtractive proteomics. Science. *301*,1380-1382.

13. Liu, H., Sadygov, R.G, and Yates, J.R., 3rd. (2004). A model for random sampling and estimation of relative protein abundance in shotgun proteomics. Anal. Chem. *76*,4193-4201.

14. Stephens, R.E. and Lemieux, N.A. (1998) Tektins as structural determinants in basal bodies. Cell Motility and the Cytoskeleton. *40*,379-392.

15. Norrander, J.M., deCathelineau, A.M., Brown, J.A., Porter, M.E., and Linck, R.W. (2000) The Rib43a protein is associated with forming the specialized protofilament ribbons of flagellar microtubules in *Chlamydomonas*. Mol. Biol. Cell. *11*,201-215.

16. Pfannenschmid, F., Wimmer, V.C., Rios, R.M., Geimer, S., Kröckel, U., Leiherer, A., Haller, K., Nemcová, Y,, and Mages, W. (2003) *Chlamydomonas* DIP13 and human NA14: a new class of proteins associated with microtubule structures is involved in cell division. J. Cell Sci. *116*,149-162.

17. Lechtreck, K.F., Teltenkötter, A., and Grunow, A. (2002) Analysis of *Chlamydomonas* SF-assemblin by GFP tagging and expression of antisense constructs. J. Cell Sci. *115*,1511-1522.

18. Salisbury, J.L., Suino, K.M., Busby, R., and Springett, M. (2002) Centrin-2 is required for centriole duplication in mammalian cells. Curr. Biol. *12*,1287-1292.

19. Dutcher, S.K., Morrissette, N.S., Preble, A.M., Rackley, C., and Stanga, J. (2002) Epsilon-tubulin is an essential component of the centriole. Mol. Biol. Cell. *13*,3859-3869.

20. Geimer, S., Clees, J., Melkonian, M., and Lechtreck, K.F. (1998) A novel 95

kD protein is located in a linker between cytoplasmic microtubules and basal bodies in a green flagellate and forms striated filaments in vitro. J. Cell. Biol. *140*,1149-1158.

21. Matsuura, K., Lefebvre, P.A., Kamiya, R., and Hirono, M. (2004) Bld10p, a novel protein essential for basal body assembly in *Chlamydomonas*: localization to the cartwheel, the first ninefold symmetrical structure appearing during assembly. J. Cell. Biol. *165*,663-671.
22. Kilmartin, J.V. (2003). Sfi1p has conserved centrin-binding sites and an essential function in budding yeast spindle pole body duplication. J. Cell Biol. *162*,1211-21.
23. Ostrowski, L.E., Blackburn, K., Radde, K.M., Moyer, M.B., Schlatzer, D.M., Moseley, A., and Boucher, R.C. (2002) A proteomic analysis of human cilia: identification of novel components. Mol. Cell. Proteomics. *1*,451-465.
24. Marshall, W.F. (2004) Human cilia proteome contains homolog of zebrafish polycystic kidney disease gene qilin. *14*,R913-914.
25. Stolc, V., Samanta, M.P., Tongprasit, W, and Marshall, W.F. (2005). Genome-wide transcriptional analysis of flagellar regeneration in *Chlamydomonas reinhardtii* identifies orthologs of ciliary disease genes. Proc. Natl. Acad. Sci. U.S.A. *102*,3703-7.
26. Cole, D.G. (2003) The Intraflagellar transport machinery of *Chlamydomonas reinhardtii*. Traffic. *4*,435-442.
27. Blacque, O.E., et al. (2004). Loss of *C.elegans* BBS-7 and BBS-8 protein function results in cilia defects and compromised intraflagellar transport.

Genes and Dev. *18*, 1630-1642

28. Echard, A., Hickson, G.R., Foley, E., and O'Farrell, P.H. (2004). Terminal cytokinesis events uncovered after an RNAi screen. Curr. Biol. *14*,1685-93.

29. Eggert, U.S., Kiger, A.A., Richter, C., Perlman, Z., Perrimon, N., Mitchison, T.J., and Fields, C.M. (2004). Parallel chemical genetic and genome-wide RNAi screens identify cytokinesis inhibitors and targets. PLoS Biology *2*,e379.

30. Chen, J., et al. (2005) Discovery-based science education: functional genomic dissection in *Drosophila* by undergraduate researchers. PloS Biology *3*,0207-0209.

31. Zipperlen, P., Fraser, A.G., Kamath, R.S., Martinez-Campos, M., and Ahringer, J. (2001). Roles for 147 embryonic lethal genes in C. elegans chromosome I identified by RNA interference and video microscopy. EMBO J. *20*,3984-92.

32. Piano, F., Schetter, A.J., Mangone, M., Stein, L, and Kemphues, K.J. (2000). RNAi analysis of genes expressed in the ovary of Caenorhabditis elegans. Curr. Biol. *10*,1619-22.

33. Sonnichsen, B. et al. (2005). Full-genome RNAi profiling of early embryogenesis in Caenorhabditis elegans. Nature *434*,462-9.

34. Romio, L., Wright, V., Price, K., Winyard, P.J., Donnai, D., Porteous, M.E., Franco, B., Giorgio, G., Malcolm, S., Woolf, A.S., and Feather, S.A. (2003) OFD1, the gene mutated in oral-facial-digital syndrome type 1, is

expressed in the metanephros and in human embryonic renal mesenchymal cells. J. Am. Soc. Nephrol. *14*,680-689.

35. Romio, L., et al. (2004). OFD1 is a centrosomal/basal body protein expressed during mesenchymal-epithelial transition in human nephrogenesis. J. Am. Soc. Nephrol. *15*,2556-68.
36. Hildebrandt, F., and Otto, E. (2000) Molecular genetics of nephronophthisis and medullary cystic kidney disease. J. Am. Soc. Nephrol. *11*,1753-1761.
37. Otto, E., Hoefele, J., Ruf, R., Mueller, A.M., Hiller, K.S., Wolf, M.T.F., Schuermann, M.J., Becker, A., Birkenhäger, R., Sudbrak, R., hennies, H.C., Nürnberg, P., and Hildebrandt, F. (2002). A gene mutated in nephronopthisis and retinitis pigmentosa encodes a novel protein, nephroretinin, conserved in evolution. Am. J. Hum. Genet. *71*, 1161-1167.
38. Mollet, G., Silbermann, F, Delous, M., Salomon, R., Antignac, c., and Saunier, S. (2005). Characterization of the nephocystin/nephrocystin-4 complex and subcellular localization of nephrocystin-4 to primary cilia and centrosomes. Hum. Mol. Genet. *14*,645-56.
39. Lorenzetti, D., Bishop, C.E., Justice, M.J. (2004). Deletion of the Parkin coregulated gene causes male sterility in the quaking (viable) mouse mutant. Proc. Natl. Acad. Sci. U.S.A. *101*,8402-7.
40. Ikeda, K., Brown, J.A, Yagi, T., Norrander, J.M., Hirono, M., Eccleston, E., Kamiya, R,. and Linck, R.W. (2003). Rib72, a conserved protein associated with the ribbon compartment of flagellar A-microtubules and

potentially involved in the linkage between outer doublet microtubules. J Biol Chem. *278*,7725-34

41. Lange, B.M.H., Bachi, A., Wilm, M., and González, C. (2000) Hsp90 is a core centrosomal component and is required at different stages of the centrosomal cycle in *Drosophila* and vertebrates. EMBO. *19*,1252-1262.
42. Seixas, C., Casalou, C., Melo, L.V., Nolasco, S., Brogueira, P., and Soares, H. (2003) Subunits of the chaperonin CCT are associated with Tetrahymena microtubule structures and are involved in cilia biogenesis. Exp. Cell. Res. *290*,303-321.
43. Maduro, M., and Pilgrim, D. (1995). Identification and cloning of Unc-119, a gene expressed in the Caenorhabditis elegans nervous system. Genetics *141*,977-88.
44. Rual, J.F., et al. (2004). Human ORFeome version 1.1:a platform for reverse proteomics. Genome Res. *14*(10B), 2128-2135.

Table 1. BUG proteins. *Chlamydomonas* centriole proteome components whose genes are upregulated during flagellar regeneration, presumably reflecting a role in basal body function during flagellar assembly, were designated BUG (Basal body proteins with Upregulated Genes). Protein ID numbers are as specified in version 2.0 of the *Chlamydomonas* genome sequence, available at the Joint Genomes Institute web site: http://genome.jgi-psf.org/chlre2/chlre2.home.html.

Name	protein ID	protein description
TUA1	154911	Alpha tubulin
TUB1	158210	Beta tubulin
TEK1	168881	tektin [14]
DIP13	159197	*Chlamydomonas* basal body protein [16]
RIB43a	170694	pf ribbon protein found in microtubule doublets [15]
RIB72	168675	pf ribbon protein found in microtubule doublets [40]
HSP90A	169301	chaperone protein associated with cilia [41]
CCT3	156617	CCT T-complex protein 1 gamma [42]
BUG1	155336	novel protein
BUG2	159506	novel protein
BUG3	166521	novel protein expressed in mouse testis
BUG4	171153	novel protein
BUG5	153027	nucleoside diphosphate kinase similar to NDK-7
BUG6	155819	IQ domain protein
BUG7	157731	DnaJ domain protein

BUG8	154693	novel protein
BUG9	156034	novel protein
BUG10	156969	EF-hand protein similar to centrin-2
BUG11	157801	LisH-domain protein orthologous to OFD1
BUG12	160014	novel protein
BUG13	161556	P-loop protein
BUG14	168135	WD40 domain protein, FABP motility class
BUG15	169308	novel protein expressed in mouse testis
BUG16	171275	novel protein
BUG17	162106	novel protein
BUG18	158310	novel protein
BUG19	161985	novel gene
BUG20	168906	cgcr-4 protein encoded in GC-rich genome region
BUG21	162703	PACRG ortholog (Parkin co-regulated gene)
BUG22	153184	novel protein
BUG23	156421	coiled coil protein
BUG24	157337	proline-rich domain protein
BUG25	159666	coiled coil protein
BUG26	160224	novel protein
BUG27	161716	coiled coil protein

Table 2. POC proteins. Centriole proteome components whose potential association with centrioles is supported either by comparative genomics [4,7] or by proteomics of the human centrosome [8], were designated POC (Proteome of Centriole) proteins. In this table FABP refers to the comparative genomics studies of Li et al. and Avidor-Reiss et al [4,7]. Prototypical cilia class refers to the class of genes conserved in all ciliated organism including those lacking motile cilia [7].

Name	protein ID	protein description
POC1	162499	FABP "prototypical cilia" class protein, in human centrosomes
POC2	156598	novel P-loop protein found in FABP
POC3	163597	ortholog of human centrosome protein cep290 (3H11 antigen)
POC4	163629	similar to centrin-interacting protein SFI1 (5 SFI repeats)
POC5	155108	ortholog of human centrosome protein FLJ35779
POC6	155808	EF-hand protein similar to centrin-3
POC7	158560	FABP, ortholog of C. elegans gene UNC-119 [43]
POC8	159663	14-3-3 protein found in human centrosome proteome
POC9	166376	FABP protein with DM10 domain, similar to Rib72
POC10	164333	FABP protein, ortholog of nephronophthisis gene NPHP-4

POC11	164517	hypothetical protein found in human centrosome proteome
POC12	169453	FABP protein similar to human protein FLJ20345
POC13	153900	FABP protein with SH3 domain
POC14	152990	14-3-3 epsilon-like protein found in human centrosome
POC15	153659	novel EF-hand protein in FABP
POC16	161892	WD40 protein found in FABP
POC17	164452	human centrosome proteome protein
POC18	167712	FABP "prototypical cilia class" protein in human centrosome

Figure Legends

Figure 1. Isolation of *Chlamydomonas* basal bodies. (A) Western blot of Nycodenz gradient probed for acetylated-tubulin. Blot shows 15 fractions out of 35, with peak centriole concentration limited to three sequential fractions. (B,C) Enrichment of basal bodies during isolation (1st lane – whole cell lysates, last two lanes – peak fraction from second sucrose step gradient and from Nycodenz gradient, respectively). (B) Equal protein loaded in each lane indicated by Coomassie stain. (C) Western blot for acetylated-tubulin, a centriole marker, showing progressive enrichment relative to total protein. (D) Immunofluorescence image of isolated basal bodies stained with anti-acetylated-tubulin antibodies. Inset: negative stain electron micrograph of isolated basal bodies, showing that typical centriole ultrastructure remains intact during the procedure. (E) 2D PAGE analysis of isolated basal bodies.

Figure 1. Isolation of Chlamydomonas Basal Bodies

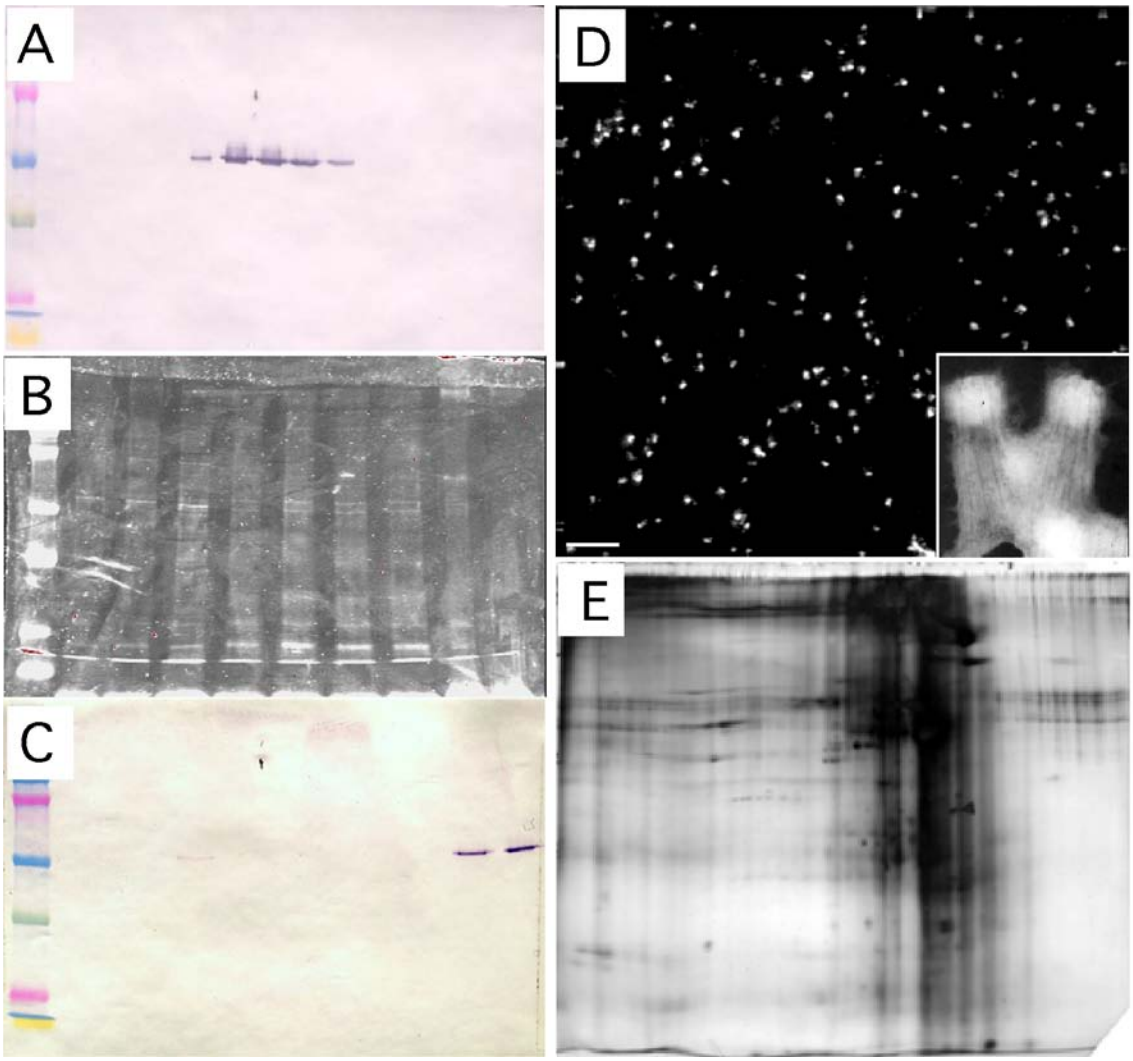

Figure 2. Mass spectrometry confirms enrichment of centriole proteins in peak fraction relative to control fractions. Graph indicates the fraction of known proteins of different types found in each sample. (Red) control fraction running above peak fraction in Nycodenz gradient. (White) control fraction running below peak fraction in Nycodenz gradient. (Blue) peak centriole fraction as judged by immunofluorescence and Western blotting. As indicated by the graph, the peak centriole fraction contains the majority of known centriole proteins, while none were found in either control fraction. Chloroplast and mitochondria were major components of the two control fractions and were also found in peak fraction.

Figure 2. Mass Spectrometry Confirms Enrichment of Centriole Proteins in the Peak Fraction Relative to Control Fractions

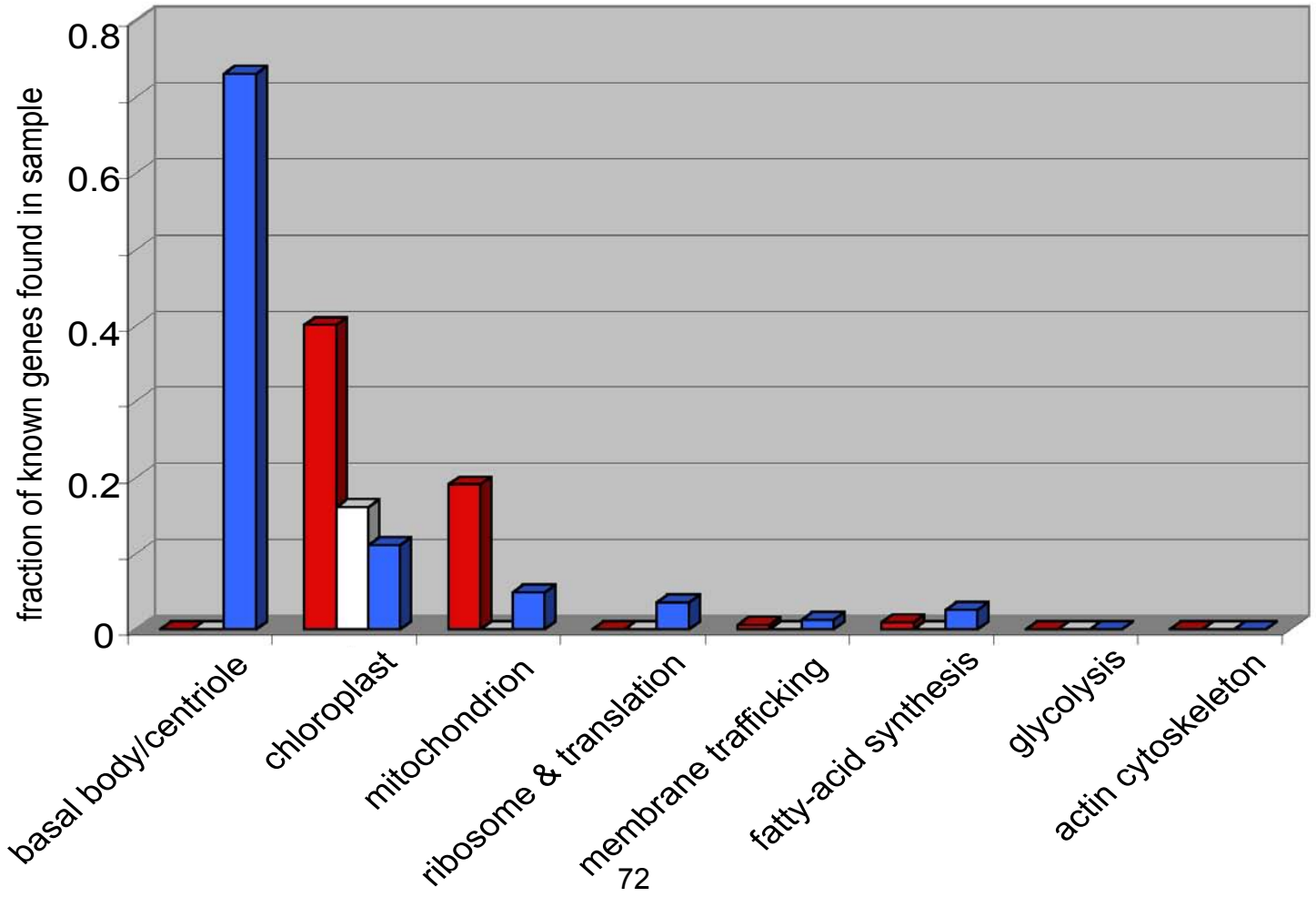

Figure 3. Protein composition of isolated basal bodies. (A) Pie chart showing fraction of proteins classified according to predicted localization. (B) Venn diagram illustrating the overlap between the sets of proteins scored positive by the three different methods of bioinformatic cross-validation. The total set of 195 proteins also includes unknown and other categories indicated in panel A, but these did not overlap any of the cross-validated categories were therefore not included in the Venn diagram.

Figure 3. Protein Composition of Isolated Basal Bodies

A

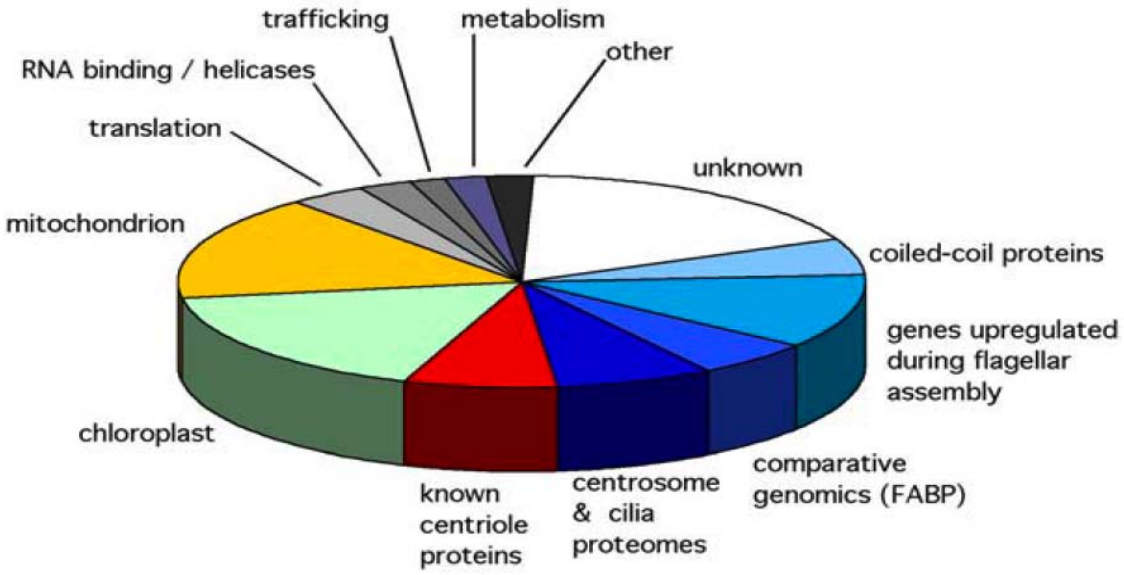

B

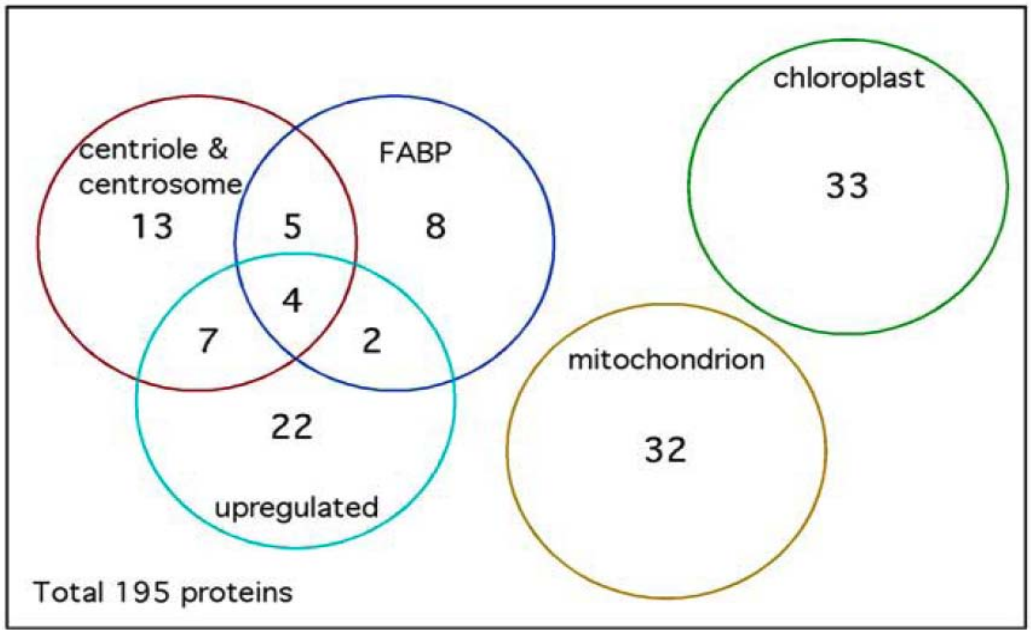

Figure 4. Localization of candidate centriole proteins. (A,E,I,M,Q) gamma-tubulin antibody stain showing centrosomes. Arrowheads, when present, indicate untransfected cells. (B,F,J,N,R) Localization of GFP-fusion proteins corresponding to human homologs of *Chlamydomonas* centriole candidate proteins (Tektin, PACRG/BUG21, POC1, POC12, and BUG14) after transient transfection into HeLa cells. (C,G,K,O,S) DAPI stain to show DNA in cells. (D,H,L,P,T) Merge indicating that each GFP-fusion protein colocalizes to a pair of dots within the centrosome in HeLa cells, confirming centriolar localization. Insets are enlarged approximately five times relative to panel. Bar 5μm.

Figure 4. Localization of Candidate Centriole Proteins

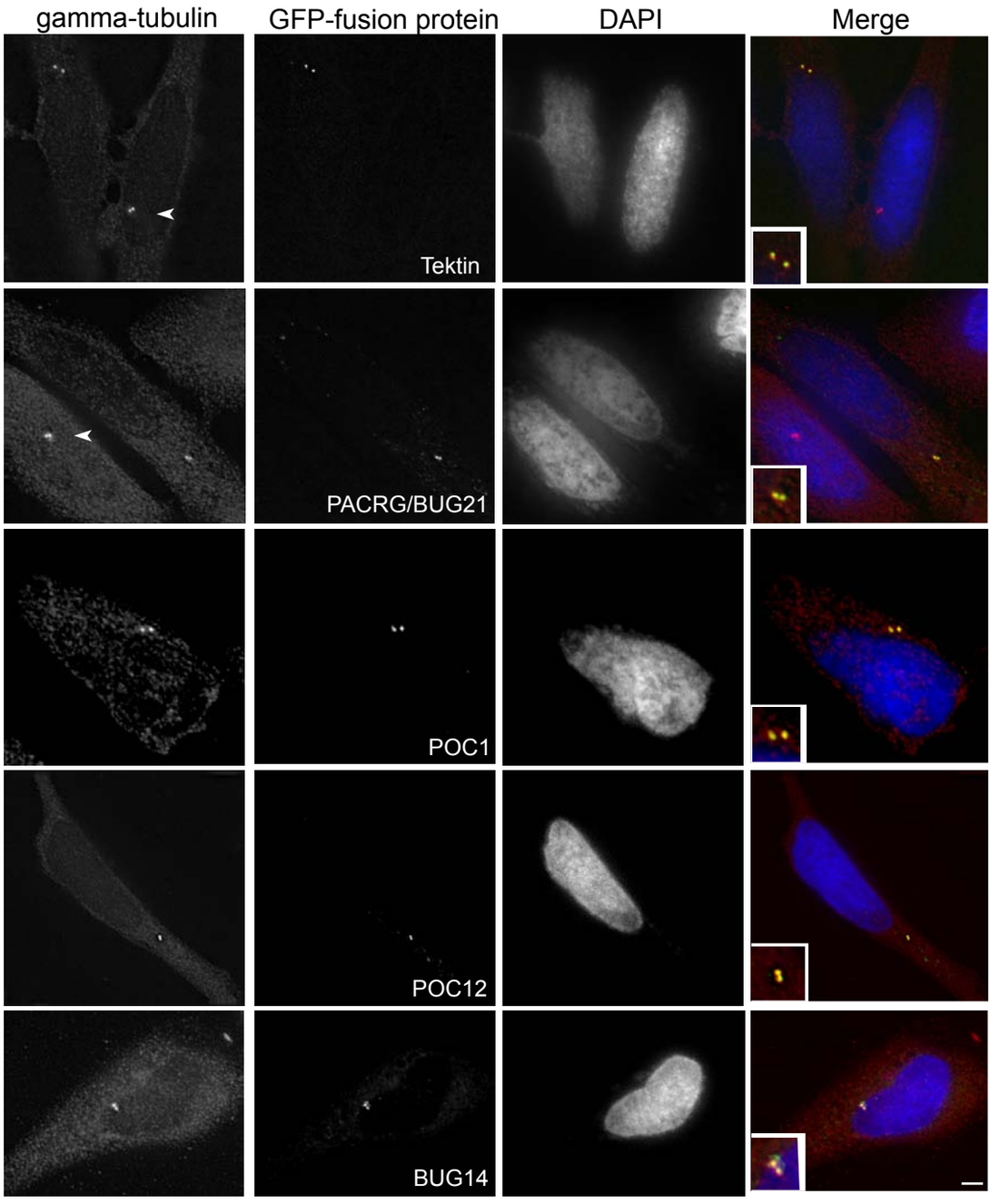

Supplementary Figure/Table Legends

Supplementary Figure 1. Diagram of procedure for isolating*Chlamydomonas* basal bodies. (A) Cell-wall-deficient mutants of *Chlamydomonas reinhardtii* were grown in 8L bottles with constant aeration. (B) All four 8L bottles were combined and concentrated into approximately 100mL deflagellation buffer. (C) Deflagellation was induced by pH shock followed by isolation of cell bodies away from flagella. (D) Cell bodies were lysed by addition of detergent and subsequent homogenization. (E and F) Velocity sedimentation. Clarified lysate was separated in a 40%/50% sucrose step gradient (E) followed by a 50%/60%/70%/80% sucrose step gradient (F). Peak fractions from (F) were separated in a continuous Nycodenz gradient centrifuged for 18 hours at 14000 x g. Peak fractions were assessed by Western-blot analysis and immunofluorescence. Peak fractions from Nycodenz gradient were washed twice with TE and pelleted before mass-spectrometry analysis. Control fractions were taken just above or below peak fractions and were treated with same way before subtractive mass-spectrometry analysis.

Figure S1. Purification Method of Chlamydomonas Basal Bodies

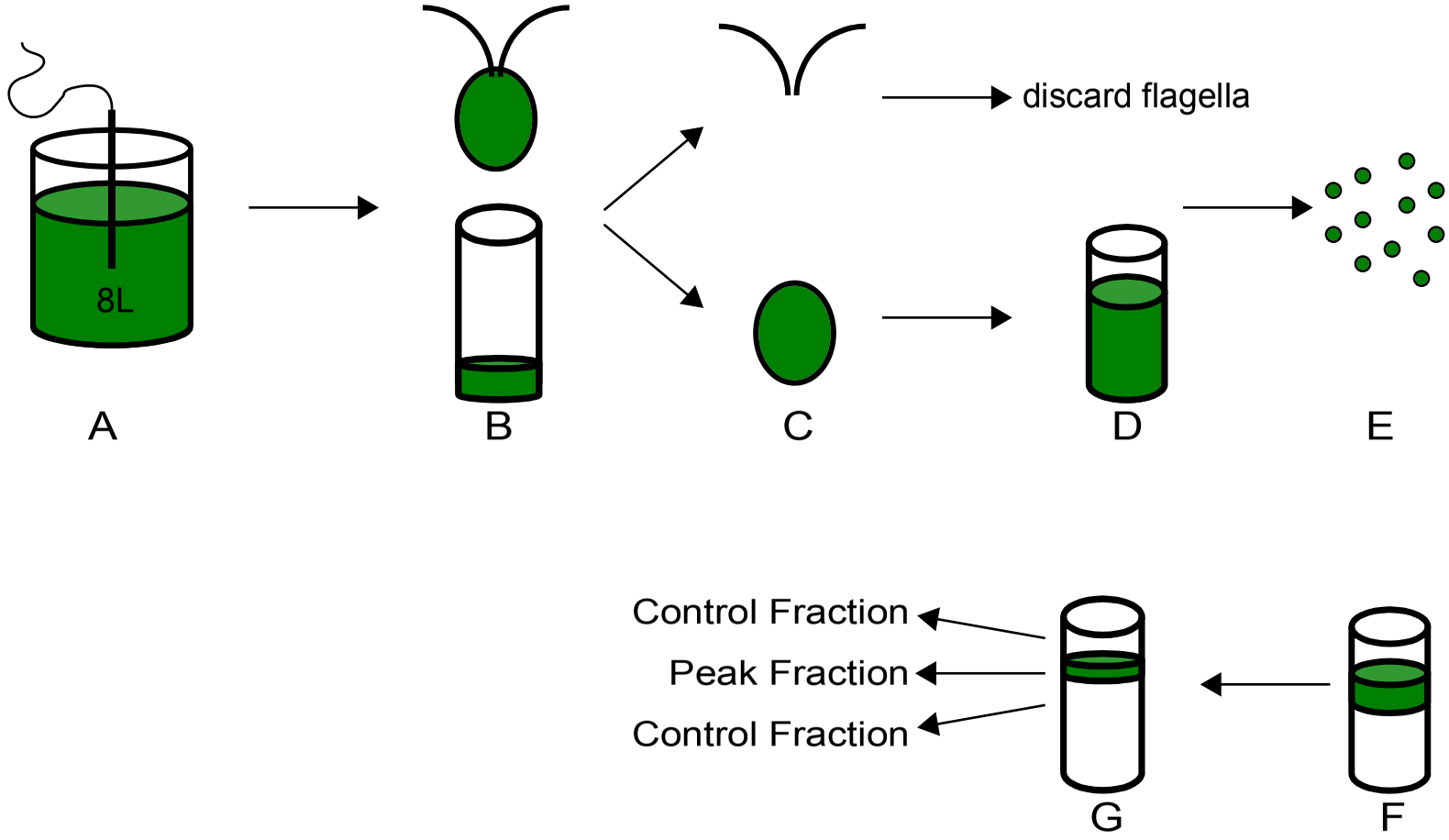

Table S1. Enrichment of basal bodies during isolation procedure.

BB/total protein column calculated as ratio of BB/field of view to concentration of protein. Fold-change in this quantity during a purification step should be equal to the fold enrichment of basal bodies relative to total protein. Due to interference by large particulate matter and other contaminants, measurements for the Crude lysate are likely to be inaccurate and are presented here for reference only. Calculation of total enrichment during the isolation procedure is found to be 5600-fold, based on comparison of data for clarified lysate and the peak of the final Nycodenz gradient.

	Total Protein (mg/mL)	Volume (mL)	BB/field of view (average 5 fields)	BB/total protein (BB/field/mg)
Crude Lysate	8400	100	1 ± 0.7	0.0001
Clarified Lysate	3020	25	3 ± 1.4	0.001
Peak 2nd gradient	40	2	175 ± 6	4.4
Peak Nycodenz	30	1	168 ± 8	5.6

Supplemental Table 2. The Centriole Proteome. Annotated list of proteins found in peak basal body fraction following subtractive analysis using flanking control fractions. The first column indicates the *Chlamydomonas* protein ID number. The second and third columns shows spectral count divided by the predicted protein mass and the number of peptides hit per protein respectively. The fourth column indicates proteins that were also identified in the FABP (*) (Li et al., 2004), in the prototyical cilia class (#), or in the comparative genomic analysis of Avidor-Reiss et al., 2004 ($). The fifth column indicates any protein that was also identified in human cilia (□) or in the human centrosome (■). The sixth column indicates any protein in Drosophila whose gene gives a rough eye phenotype when mutated (RE), a binucleate RNAi phenotype (Bi) or a cytokinesis RNAi phenotype (cyto). The seventh column indicates any protein that gives a worm RNAi phenotype of embryonic lethal (Emb), cytokinesis (cyto), spindle defective (spd), dye-filling (dyf), or location of vulva (lov). The eighth column indicates any protein that was also identified as being upregulated (*) or not upregulated confirmed by quantitative RT-PCR (-) during flagellar regeneration. The & sign means that these proteins were upregulated by 1.5 fold at both 30 and 45min. The last three columns show the accession numbers if homologs exist in fly, worm, and human. Lines highlighted blue refer to previously reported centriolar proteins. Any writing in bold refers to proteins which we verified as centriolar, based on our cross-validation bioinformatics approach. Chlamy ID numbers were prveiously assigned by the JGI Assembly October 2003, release 2.0 (http://genome.jgi-psf.org/chlre2/chlre2.home.html).

Chlamy ID	Counts/kDa	# peptides hit	Comparative Genomics	Human cilia/Centrosome	Fly Phenotype	Worm Phenotype	Upregulated by Flagellar Assembly	Protein Identify	fly homolog	worm homolog	human homolog
154911	**5**	**113**		□			*	**TUA1, TUA2 alpha tubulin**	CG1913	CE24843	NP_006000.2
158210	**3**	**93**		●□			*	**Tubulin beta chain TUB1, TUB2 beta tubulin**	CG9277	CE00850	NP_006079.1
152450	**1**	**9**			RE	Emb		**Ef1A1- localizes to cilia in tetrahymena**	CG8280	CE01270	NP_001949.1
152719	**0.6**	**4**						**SF-assemblin**	NONE	CE07306	NP_958784.1
160224	0.5	2					*	novel upregulated gene	NONE	NONE	NONE
162499	**0.5**	**20**	#$	●				**protocilia-class FABP protein in human centr.**	CG10191	CE00901	NP_758440.1
168881	**0.5**	**20**	*				*	**tektin**	CG3085	CE04781	NP_444515.1
155336	**0.4**	**9**					*	**novel upregulated gene**	NONE	NONE	NONE
158741	0.4	5			RE	Emb		putative eukaryotic IF4A subunit	CG9075	CE01341	NP_001958.1
171701	0.4	13				Emb		putative RNA helicase	CG10077	CE18785	NP_004387.1
156421	0.4	9					*	novel upregulated gene	NONE	CE27084	NP_055490.2
161716	0.4	3					*	coiled coil- novel upregulated gene	NONE	CE28848	NONE
156598	**0.3**	**35**	*			Emb		**FABP P-loop protein**	CG7852	CE25697	NP_653213.4
159197	**0.3**	**2**	*	●			*	**DIP13 (localizes to BB and flagella)**	NONE	CE31598	NP_003722.1
159506	**0.3**	**2**					*	**novel upregulated gene**	NONE	NONE	NONE
162352	**0.3**	**16**						**homology with Spermatozopsis BAp95**	NONE	CE09197	NP_006176.1
163597	**0.3**	**18**		●				**human cep290**	CG17927	CE09349	NP_079390.2
163629	**0.3**	**10**						**SFI1-like (5 sfi repeats)**	NONE	NONE	NP_001007468.1
166521	**0.3**	**7**					*	**novel upregulated gene, in mouse testis**	NONE	NONE	NONE
167674	0.3	9						Fibrillarin and related nucleolar proteins	CG9888	CE12920	NP_001427.2

170694	**0.3**	**4**	*#			Cyto	*	**Rib43a pf ribbon protein**	CG7264	CE03434	NP_056468.1
171153	**0.3**	**5**					*	**strongly upregulated during flagellar reg.**	NONE	NONE	NONE
153027	**0.2**	**3**		●□			*	**NDPK (NDK7-like)- Upreg. Also in human centr.**	CG8362	CE09650	NP_932076.1
155108	**0.2**	**11**		●			-	**hypothetical protein FLJ35779- in human centr.**	NONE	CE17428	NP_689621.1
155808	**0.2**	**3**		●		Emb		**centrin3 homolog**	CG31802	CE13902	NP_004356.2
157337	0.2	3					*	weak homology, expressed in mouse testis	NONE	CE21047	NONE
155819	**0.2**	**2**					*	**novel upregulated gene**	NONE	NONE	NONE
157074	0.2	7						CAT1 catalase	CG6871	CE22476	NP_001743.1
157731	**0.2**	**2**		●	RE	Spd	*	**DnaJ chaperone- Upreg. Also in human centr.**	CG8863	CE16015	NP_001530.1
158560	**0.2**	**2**	*$			Dyf		**UNC119 (mammalian form expressed in retina)**	CG1659	CE06203	NP_005139.1
158737	**0.1**	**2**			RE	Emb		**FAP3 flagellar proteome protein**	CG2922	CE32821	NP_054757.1
159663	**0.1**	**11**		●□			-	**14-3-3 epsilon -like protein. In human centr.**	CG31196	CE03389	NP_006752.1
162471	0.1	2			Bi	Emb		40S ribosome protein S3	CG6779	CE01810	NP_000996.2
163162	0.1	2						peptidylprolyl isomerase (cyclophilin)	CG9916	CE20371	NP_005720.1
166376	**0.1**	**2**	*					**Rib72-like DM10 containing protein**	CG11048	CE37648	NP_060570.1
168675	**0.1**	**7**	*	□			*	**Rib72 pf ribbon protein**	CG8959	CE36724	NP_060570.1
155021	0.2	2					*	novel	NONE	NONE	NONE
159666	0.2	11					*	weak homology to Treacher-Collins Syndrome gene	NONE	CE21470	NP_001008656.1
164333	**0.1**	**35**	*			Lov		**NPH4 nephrocystin-4 a.k.a. nephroretinin**	NONE	CE35605	NP_055917.1
153012	0.1	2				Emb		Adenylate kinase 1	CG17146	CE29198	P_037543.1
154693	**0.1**	**3**					*	**novel upregulated gene**	NONE	CE11848	NONE
155337	0.1	2				Emb		Ribosomal protein Sa	CG14792	CE00854	NP_002286.2
156034	**0.1**	**2**					*	**novel upregulated gene**	NONE	NONE	NONE
156177	**0.1**	**2**		□				**VFL2 (centrin)**	CG8472	CE13387	NP_004335.1
156856	0.1	2						ribosomal 60S L28 protein	NONE	NONE	NP_000982.2
156969	**0.1**	**4**		●			*	**centrin 2 EF-hand protein/centrin 2 (mouse)**	NONE	CE29674	NONE
157396	0.1	7				Emb		EFG2 elongation factor	CG2238	CE15900	NP_001952.1
157786	0.1	3		●	Bi			calcium dependent protein kinase CaMKI	CG1495	CE28054	NP_003647.1
157801	**0.1**	**4**		●			*	**OFD1**	NONE	CE27084	NP_003602.1
160014	**0.1**	**2**					*	**strongly upregulated during flagellar regen**	NONE	NONE	NONE
161252	0.1	2				Emb		RPS2; Cytosolic 80S ribosomal protein S2	CG5920	CE04237	NP_002943.2
161556	**0.09**	**2**					*	**P-loop protein, strongly upregulated**	NONE	NONE	NONE
164517	**0.09**	**2**	*	●				**hypothetical protein. In human centr.**	NONE	NONE	NP_115734.1
166267	0.09	9						elongation factor EF3	CG9330	CE18971	NP_009120.1
166666	0.08	2				Emb		KH domain rna binding protein	CG8144	CE05266	NP_127503.1
167486	0.08	6		□	RE			BIP1 ER chaperone same as 167717	CG4147	CE08177	NP_005338.1
168135	**0.08**	**7**	$				*	**FABP, motility class, WD40 repeat. In testis**	CG10064	CE11748	NP_659491.2
168432	**0.08**	**10**	*			Emb		**Bld10**	CG3493	CE27133	NP_055490.2
169308	**0.07**	**2**					*	**upregulated gene, expressed in mouse testis**	NONE	NONE	NONE
171275	**0.07**	**2**					*	**strongly upregulated during flagellar reg.**	NONE	NONE	NONE
153184	0.1	2					*	novel upregulated gene	CG5343	CE33367	NP_037374.1
167800	0.07	2						VP55a sortin nexin (ER to golgi transport)	NONE	CE07927	NP_003091.2
169301	**0.07**	**4**			RE	Emb	&	**HSP90A**	CG1242	CE05441	NP_005339.2

169453	0.07	3	*					FABP169453, hypothetical protein FLJ20345	NONE	CE17428	NP_060247.1
153900	0.07	2	*					FABP153900 , SH3 domain	NONE	NONE	NONE
162106	0.07	2					*	novel upregulated gene	NONE	NONE	NONE
164604	0.07	2				Emb		Small G protein superfamily	CG5771	CE11006	NP_004654.1
170731	0.06	2						phosphate acetyltransferase	NONE	NONE	NONE
152346	0.06	2			cyto	sterile		COPB1 beta cop vesicle protein	CG6223	CE21472	NP_057535.1
152990	0.06	2		●□			-	14-3-3 epsilon -like protein. In human centr.	CG31196	CE03389	NP_006752.1
153659	0.06	30	*					EF-hand protein	CG8472	CE35164	NONE
153868	0.06	2				Emb		RNA helicase, Arabidopsis At5g63120.2	CG10279	CE27427	NP_006377.2
156617	0.06	4		●		Emb	*	CCT3 T-complex protein 1 gamma. Upreg.	CG31548	CE31540	NP_005989.2
158310	0.06	2					*	unknown upregulated gene	NONE	NONE	NONE
161985	0.06	2					*	strongly upregulated during flagellar reg.	NONE	NONE	NONE
165705	0.06	2						rice centromere MT-binder, yeast cbf5 65%	CG3333	CE16195	NP_001354.1
168906	0.06	2					&	cgcr-4-like protein, mouse Nischarin homolog?	NONE	CE17428	NONE
156739	0.06	2	*					hypothetical human protein (in FABP)	NONE	NONE	NONE
159078	0.06	2			RE	Emb		putative Rna helicase	CG7269	CE00839	NP_542165.1
161892	0.06	10	*					FABP161892, WD40 protein	CG13956	CE35164	NP_694971.2
162703	0.06	2	*#				*	PACRG (parkin co-regulated gene)	CG15120	CE01214	NP_689623.1
164452	0.06	2		●	Bi	Emb		hypothetical protein. In human centrosome	CG15081	CE02883	NP_009204 B
165702	0.06	2						BLD2 epsilon-tubulin	NONE	NONE	NP_057346.1
167712	0.06	4	*#$	●				FABP protocilia class. In human centrosome	CG16896	CE27084	NP_663622.1
168551	0.06	4						Malate Synthase	NONE	CE23521	NONE

Supplemental Table 3. Annotated list of proteins found in control fractions 1 and 2. Lines highlighted in light green or orange refer to proteins in control fractions that are found in the chloroplast or mitochodria respectively.

153056		Lhca7
153074		2-oxoglutarate dehydrogenase E2 subunit (mito)
153214		hypothetical protein
153236		coiled coil
153399		putative kinase
153794	hit in both control fractions	LhcbM1
154002	hit in both control fractions	LhcbM5
154320		hypothetical protein
154442		COX5b (mito)
154579		hypothetical protein
155433		Lhca5
155702		hypothetical protein
155786		*light harvesting complex protein*
155800		Lhca1
155816		LhcbM8
155818	hit in both control fractions	LhcbM4
155892		quinone-oxidoreductase QR2 (chloroplast)
156442		glycine rich cell wall protein
156523		At1g54780
156749		PSB28
156755		endosomal membrane protein
156901		FTSH1 (chloroplast divisionprotein)
156924		PSAL
157292		SET domain protein SETj
157843		PSBW photosystem II reaction center W protein
158548	hit in both control fractions	PSAF
158876	hit in both control fractions	*cp29 (chloroplast)*
159580		*chloroplast thylakoid lumen protein*
159888		hypothetical protein
159939		coiled coil
159948		hypothetical protein
160046		mitochondrial outer membrane porin
160616		coiled coil
160619		hypothetical protein

161585		hypothetical protein
161987		putative protein kinase
161994		mitochondrial porin
162061		hypothetical protein
162239	hit in both control fractions	LhcbM6
162826		PSAD
163127	hit in both control fractions	PSBB
163166		COP1 chlamy opsin
163240		PSBY
163278		NUO5 (mito)
163297		Lhca4
163724		PSBR
163755		helicase
164607		Nudix hydrolase
164620	hit in both control fractions	TUA1 alpha tubulin
165373		ER cargo receptor
165429		hypothetical protein
165563		hypothetical protein
166067		Lhca2
166088		rubredoxin-like
166657	hit in both control fractions	*CP26 (chloroplast)*
166829		NUOS4 (mito)
166949		MDH1 malate dehydrogenase (cytosolic)
167161		hydroxyproline rich glycoprotein (cell wall?)
167490		FAP24
167744	hit in both control fractions	glycine rich cell wall protein
168321		ACP1(mitochondrial)
168666		FUO1 (mitochondrial)
168807		no good homology
168826		putative cation channel
168914		cAMP dependent kinase
169140		NUOP6 (mito)
169269	hit in both control fractions	DYRK2
169338		flagellar membrane glycoprotein FMG1B
169341		flagellar membrane glycoprotein FMG1A
169436		cAMP dependent kinase

169442		FAS2 (extracellular?)
169944		LhcbM7
170161		plasma membrane-type proton ATPase
170203		cgcr-4 protein-like
170258		COX90 (mito)
170462		lipase
170511		Algal-CAM - Volvox carteri
170760		coiled coil
170820		PSBP
171094		proton-translocating inorganic pyrophosphatase
171419		NUOB13 (mito)
171502	hit in both control fractions	PSBO
171588		NUOB10 mitochondrial NADH:ubiquinone oxidoreductase
171987		COX12 (mitochondrial)
159358		LhcbM3
159050		granule bound starch synthase (chloroplast)
152451		DEGP15 protease found in thylakoid membrane
160535		glycine rich protein
162110		glycine rich protein
170431		putative guanylate cyclase
161007		pherophorin dz-1 protein (cell wall)
163064		putative protein kinase
158804		coiled coil protein
156044		coiled coil protein
164641		coiled coil protein
154562		coiled coil protein
156771		putative calcium channel
171993		putative PI kinase
156279		coiled coil protein
154794		coiled coil protein
168593		hypothetical protein

Table S4. Upregulation of genes encoding centriole proteome proteins during flagellar regeneration assesed by RT-PCR. Genes were considered upregulated if their expression increased by at least 1.75-fold, the same criterion used to assess upregulation by microarray analysis in Table S1 column 8. Upregulated genes are highlighted in bold. The first five entries are positive and negative controls using genes not represented in the centriole proteome. Fold upregulation was computed using the delta delta Ct method, using the RBCS2 gene as the normalizing standard.

Genes	Ct predeflag	30 min Ct	ΔCt	ΔΔCt	fold change
168391 RBCS2	25.81257	25.59854	-0.21403	0.00000	1.00000
168391 RBCS2 (replicate)	25.74535	25.35485	-0.39050	-0.17647	1.13012
158239 non-upregulated FABI	33.53523	33.51039	-0.02484	0.18919	0.87710
167776 Dpy-30 (+ ctrl)	**36.23739**	**32.00906**	**-4.22833**	**-4.01430**	**16.15938**
156724 Reptin (+ ctrl)	**37.66290**	**34.16789**	**-3.49501**	**-3.28098**	**9.72016**
152368	40.31860	41.38560	1.06700	1.28103	0.41150
152523	35.02641	35.15020	0.12379	0.33782	0.79124
152650	33.49668	33.90743	0.41075	0.62478	0.64852
152838	39.66195	41.28777	1.62582	1.83985	0.27935
152990 POC14	32.00897	32.15882	0.14985	0.36388	0.77707
153184 BUG22	**34.22979**	**31.86743**	**-2.36236**	**-2.14833**	**4.43314**
153417	40.62858	39.63957	-0.98901	-0.77498	1.71117
155021	30.53926	29.85536	-0.68390	-0.46987	1.38498
155318	31.14481	32.00088	0.85607	1.07010	0.47629
156421 BUG23	**41.71044**	**39.80831**	**-1.90213**	**-1.68810**	**3.22232**
157337 BUG24	**40.86049**	**39.74535**	**-1.11514**	**-0.90111**	**1.86750**
159054	28.70566	29.43291	0.72725	0.94128	0.52077
159663 POC8	35.49382	35.79667	0.30285	0.51688	0.69888
159666 BUG25	**39.66846**	**38.52414**	**-1.14432**	**-0.93029**	**1.90566**
160224 BUG26	**35.35369**	**34.24571**	**-1.10798**	**-0.89395**	**1.85826**
160538	39.42904	40.01514	0.58610	0.80013	0.57430
160684	41.66401	44.09111	2.42710	2.64113	0.16030
161716 BUG27	**46.51726**	**43.37167**	**-3.14559**	**-2.93156**	**7.62935**
162703 BUG21 (PACRG)	**36.28742**	**32.86834**	**-3.41908**	**-3.20505**	**9.22181**
168853	36.76611	36.94135	0.17524	0.38927	0.76352

Chapter 4

Molecular Architecture of the Centriole Proteome: The Conserved WD40 Domain Protein POC1 is Required for Centriole Duplication and Length Control

Abstract

Centrioles are intriguing cylindrical organelles composed of triplet microtubules. Proteomic data suggest that a large number of proteins besides tubulin are necessary for the formation and maintenance of a centriole's complex structure. Expansion of the pre-existing centriole proteome from the green alga, *Chlamydomonas reinhardtii*, revealed additional human disease genes, emphasizing the significance of centrioles in normal human tissue homeostasis. We found that two classes of ciliary disease genes were highly represented among the basal body proteome: cystic kidney disease (especially nephronophthisis) syndromes including Meckel/Joubert-like and oral-facial-digital syndromes caused by mutations in CEP290, MKS1, OFD1, and AHI1/Jouberin proteins and cone-rod dystrophy syndrome genes including UNC-119/HRG4, NPHP4, and RPGR1. We further characterized POC1, a highly abundant WD40 domain containing centriole protein. We found that POC1 is recruited to nascent pro-centrioles and localizes in a highly asymmetrical pattern in mature centrioles corresponding to sites of basal-body fiber attachment. Knockdown of POC1 in human cells caused a reduction in centriole duplication while overexpression caused the appearance of elongated centriole-like structures. Together these data suggest that POC1 is involved in early steps of centriole duplication as well as in the later steps of centriole length control.

Introduction

Centrioles are barrel-shaped structures composed of nine triplet microtubules. They are necessary for recruitment of pericentriolar material (PCM) to form a complete centrosome and act as basal bodies during the formation of cilia and flagella. In most quiescent cells, centrioles move to and dock on the apical plasma membrane during ciliogenesis and provide a template for the extension of doublet microtubules, which make up the ciliary axoneme (Ringo, 1967; Sorokin, 1968; Snell *et al*., 1974; Vorobjev and Chentsov, 1982; Dawe *et al*., 2007). Centrioles that template cilia are known as basal bodies and the proteins that compose them have received increased attention in recent years because of their role in ciliary diseases. Ciliary diseases, or ciliopathies, result in symptoms ranging from obesity and retinal degeneration to polydactyly and cystic kidneys (Pazour and Rosenbaum, 2002; Afzelius, 2004; Badano *et al*., 2006; Yoder, 2007; Marshall, 2008). Ciliopathies arise from mutations in not only ciliary genes but also in genes encoding proteins within the basal body (Ansley *et al*., 2003; Keller *et al*., 2005; Marshall, 2008). Proteomic analyses of centrioles from a number of diverse organisms reveal the presence of ciliary-disease genes (Keller *et al*., 2005; Broadhead *et al*., 2006; Kilburn *et al*., 2007). Because having a properly anchored basal body is required for a functional cilium, mutations in any protein involved in the formation and maintenance of centriole or basal body integrity have the potential to lead to ciliary diseases.

The structure of the centriole is complex and highly precise, with centriole length tightly controlled but the molecular mechanisms governing centriole

assembly, length control, and maturation into basal bodies remain mysterious. Genetic screens in *Chlamydomonas*, *Drosophila*, and *C. elegans* have given clues to how centrioles assemble by providing mutants that act as premature stops in the centriole assembly pathway and have provided insights into such questions as how the nine-fold symmetry of centrioles is established, what other tubulin isoforms are necessary for triplet microtubule formation, and how initial steps of centriole assembly progress in various species (Dutcher *et al*., 1998; Dutcher *et al*., 2002; Dammermann *et al*., 2004; Bettencourt-Dias *et al*., 2005; Delattre *et al*.,2006; Pelletier *et al*., 2006; Hiraki *et al*., 2007; Nakazawa *et al*., 2007). Although these studies reveal crucial steps in centriole assembly at the ultrastructural scale, we have only just begun to learn how steps in basal body assembly are reflected in individual protein recruitment events. Detailed localizations and determination of the order of assembly of particular centriole proteins are pertinent for a detailed depiction of how centrioles form and duplicate once per cell cycle, but thus far few centrioles proteins have been characterized in detail.

In this report, we have expanded the *Chlamydomonas* centriole proteome based on new genomic data and the identification of additional centriole proteins. In order to begin to learn how the centriole proteome is put together, we investigated POC1, one of the most abundant proteins from our centriole proteome, and found it to be a proximal and very early marker of centriole duplication. Additionally, POC1 has a unique localization on intact mature centrioles, being found to co-localize with attachment points of multiple distinct

fiber systems that contact the centriole/basal body. This is the first protein to date to have been localized to both early duplicating centrioles and to places of centriole fiber attachment, indicating that POC1 may be involved in multiple distinct aspects of centriole biology. Furthermore, knockdown of POC1 in human U2OS cells prevented overduplication of centrioles while overexpression of POC1 caused the appearance of numerous elongated centriole-like structures. Based on these results, we suggest that POC1 is involved in the early stages of centriole duplication and also plays a role in the enigmatic process of centriole length control.

Materials and Methods

Human Cell Culture

Hela and U2OS cells were grown in DME medium (GIBCO) supplemented with 10% fetal calf serum as in Keller *et al*., 2005.

Generation of GFP-expressing Cell Lines

C-terminally tagged POC1B-GFP (Keller *et al*., 2005) was transfected with Lipofectamine™ 2000 according to manufacturers guidelines. Using a limited dilution method in the presence of 500μg/ml Geneticin (GIBCO), stable clones expressing the POC1B-GFP fusion protein were isolated. Multiple independent clones were analyzed. The centrioles in each clone had no differences in known centriole markers when compared to parental cell lines.

POC1A cDNA was cloned by RT-PCR from a cDNA library constructed from unsynchronized Hela cells. The cDNA was then sub-cloned into the pEGFP-C1 vector (Clontech), which added a C-terminal GFP tag. Cells were transiently transfected with Lipofectamine™ 2000 according to manufacturers guidelines.

Human Cell Fixation and Immunofluorescence

Cells were grown on coverslips in 12 or 24-well plates, fixed, and visualized according to Keller *et al*., 2005. Cells were stained with either anti gamma-tubulin (GTU-88, Sigma) 1:100, centrin-2 (a generous gift from M. Bornens) 1:2000, acetylated-tubulin (clone 6;11B-1, Sigma) 1:500, polyglutamylated-tubulin ([B3] ab11324, abcam) 1:1000, or GFP (11 814 460 001, Roche) 1:250. The following

secondary antibodies from Jackson Immuno-Research were used at 1:1000: FITC-conjugated AffiniPure Goat Anti-Mouse IgG (115-095-003), TRITC-conjugated AffiniPure Goat Anti-Mouse IgG (115-025-003), or TRITC-conjugated AffiniPure Goat Anti-Rabbit IgG (111-025-144). Cells were then stained with DAPI for five minutes and mounted with Mowiol mounting media. DeltaVision deconvolution fluorescence microscopy was used with Olympus PlanApo 60 and 100X objectives and 0.2μm steps in the z-axis were used to make quick projections of deconvolved images. Intensity plots were made by choosing a region of interest followed by use of DeltaVision 3D graph data inspector software. Centriole lengths were measured using the Distance tool with standard two point settings.

To facilitate the visualization of GFP-localization to centrioles, U2OS cells were occasionally treated with aphidicolin (3.2μg/ml) for 50-72 hours to induce S-phase arrest and an accompanying overduplication of centrioles.

RNAi

Synthetic siRNA oligonucleotides were obtained from Qiagen. Transfection of siRNAs using HiPerFect Transfection Reagent (Qiagen) was performed according to manufacturer's instructions. Qiagen's thoroughly tested and validated AllStars Negative Control siRNA was used as a negative control. The following predesigned siRNAs were ordered and used from Qiagen: Hs_WDR51A_2, Hs_WDR51A_4, Hs_WDR51B_2, AND WDR51B_4. Coverslips were fixed and stained as above after 55 hours of treatment. For S-phase

arrested cells, aphidicolin (3.2μg/ml) was added to cells two hours after siRNA transfection. Cells were examined 55 hours later.

Human Cell Transient Transfection and Overexpression

Hela and/or U2OS cells were seeded the day before transfection onto coverslips. The day of transfection, cells were transfected with the following constructs: full-length POC1A-Cherry, POC1B-Cherry, POC1A-WD40-GFP, POC1A-WD40-Cherry, POC1B-WD40-Cherry, POC1A-Cterm-Cherry, or POC1B-Cterm-Cherry. For S-phase arrested cells, aphidicolin (3.2ug/ml) was added to cells two hours after transfection and cells were examined 55-72 hours later. Mammalian cDNAs from the human ORF collection in the form of Gateway entry vectors were purchased from Open Biosystems: POC4 (CV030533), POC6 (CV027317), POC7 (CV025021), POC8 (CV023168), POC9 (CV-029168), POC17 (CV023450), Rib43A (CV023821), CCT3 (CV027136), BUG5 (CV027392), BUG7 (CV025099), BUG22 (CV-026100). The follows cDNAs in the form of Gateway entry vectors were purchased from GeneCopoeia: POC2 (GC-E0364), POC3 (GC-T7752), POC11 (GC-V0935), POC20 (GC-F0087), DIP13 (GC-Q0661), Hsp90 (GC-M0233), BUG11 (GC-U0139), BUG30 (GC-E0925), BUG32 (GC-V1413).

Chlamydomonas Cell Culture and Immunofluorescence

Chlamydomonas reinhardtii wildtype (strains cc125 and cc124), basal body-deficient strains bld2 (cc478), uni3 (cc2508), and bld10 (cc4076), and

temperature-sensitive flagellar assembly mutant strain fla10 (fla10-1 allele, cc1919) were obtained from the *Chlamydomonas* Genetics Center (Duke University, Durham, NC). Cells were grown and maintained in TAP media (Harris, 1989). Growth was at 25˚C with continuous aeration and constant light except for the *fla10* mutant, which was grown at 34˚C as the restrictive temperature.

To study the localization and properties of *Chlamydomonas* POC1, a peptide antibody against the following peptide was raised and affinity purified: RAGRLAEEYEVE (Bethyl Laboratories). This peptide was designed using Invitrogen antigen design tool (www.invitrogen.com) and the Open Biosystems antigenicity prediction tool (www.openbiosystems.com). The peptide is located within the last 150aa of *Chlamydomonas* POC1 but does not overlap with the C-terminal POC1 domain and does not share homology with any other organisms (Figure 3A). The antibody detects a single polypeptide and specific antibody staining *in vivo* was completely abolished after incubation with the peptide used for antibody preparation (Supplementary Figure 3).

Chlamydomonas immunofluorescence followed the standard procedure of Cole *et al*., 1998. Cells were allowed to adhere to poly-lysine-coated coverslips prior to fixation in cold methanol for five minutes. Coverslips were then transferred to a solution of 50% methanol; 50% TAP for an additional five minutes. After fixation, cells were blocked in 5% BSA, 1% fish gelatin and 10% normal goat serum in PBS. Cells were then incubated in primary antibodies overnight: anti POC1 1:200, anti acetylated-tubulin (T6793, Sigma) 1:500, anti-

Bld10p (a generous gift from M. Hirono) 1:100, and anti-centrin (a generous gift from J. Salisbury). Secondary antibodies used are as stated above.

Chlamydomonas Flagellar Manipulations

Flagellar splay assays were conducted according to Johnson, 1998. Following fixation, coverslips were blocked in 5% BSA, 1% fish gelatin and 10% normal goat serum in PBS. Coverslips were then incubated in primary antibodies: anti POC1, 1:200 and acetylated-tubulin, (T6793, Sigma) 1:500 overnight. Secondary antibodies used are as stated above.

In order to test if POC1 is a component of the intraflagellar transport (IFT) machinery, the fla10-ts mutant was temperature shifted from 25˚C to 34˚C for 45 minutes. It has previously been shown that this mutant stops IFT (Kozminski, 1995) and loses IFT proteins from its flagella (Cole *et al*., 1998) within 100 minutes after shifting to the non-permissive temperature. Cells were stained with POC1, 1:200 and IFT172.1, an IFT complex B protein, 1:200 (a generous gift from D. Cole).

Quantitative PCR

All quantitative PCR was performed according to Keller *et al*., 2005.

Western Blot

For POC1 Western blots, purified basal bodies were mixed 1:1 with sample buffer and loaded onto a 10% polyacrylamide gel. Blots were probed with the

Chlamydomonas POC1 peptide antibody at a concentration of 1:250 followed by staining with a rabbit HRP-conjugated secondary (Jackson Labs, 1:20000). Human cells were grown in 6-well dish and treated with 3.2ug/ml aphidicolin for 55-72 hours to achieve S-phase arrest. Cells were then collected in wash buffer (10mM Hepes, 1% Triton-X, and 1mM PMSF) and centrifuged for 15 minutes at 24,000xg. Pellets were then resuspended in wash buffer and equal amounts of protein were loaded onto a 10% polyacrylamide gel. Blots were probed with an anti-GFP antibody (11 814 460 001, Roche) 1:250 followed by staining with a mouse HRP-conjugated secondary (Jackson Labs; 1:20000).

Fluorescence Intensity Quantification

All images were scaled identically to maintain quantitative information. 50x50 pixel boxes surrounding each basal body image were then analyzed. Background was estimated from the average intensity of pixels on the edge of the box. A threshold was then applied such that all pixels with intensity less than half the dynamic range of the image were set to zero. The total intensity of the remaining pixels was added and then the estimated background contribution was subtracted.

Immuno-Electron Microscopy

All immuno-electron microscopy was done as described in Geimer and Melkonian, 2005 with the following changes. Serial-sections (50nm) were cut with a Leica Ultracut UCT microtome (Leica Microsystems, Vienna, Austria) and

collected on pioloform-coated gold gilded copper grids. Incubation with POC1 primary antibody was done for 90 minutes at room temperature at a dilution of 1:250 followed by goat anti-rabbit IgG labeled with 15 nm colloidal gold (Jackson ImmunoResearch Laboratories). Sections were imaged with a Zeiss CEM 902 transmission electron microscope (Carl Zeiss, Oberkochen, Germany) operated at 80 kV using SO-163 EM film (Eastman Kodak, Rochester, NY).

Results

Extending the Chlamydomonas *Centriole Proteome*

The original centriole proteome from *Chlamydomonas reinhardtii* (Keller *et al*., 2005) was determined by using MudPIT (multidimensional protein identification technology), a mass-spectrometry-based method in which complex mixtures of proteins can be analyzed without prior electrophoretic separation (Washburn *et al*., 2001). This method was combined with matching individual peptides to predicted gene models in the *Chlamydomonas* genome sequence (Keller *et al*., 2005). However, since the time of the first centriole proteome study, the *Chlamydomonas* genome has been refined and extensively re-annotated (Merchant *et al*., 2007), with many new and revised gene-model predictions added. We therefore re-analyzed our initial mass-spectrometry data using the new *Chlamydomonas* version 3.0 gene model predictions to search for additional centriole proteins. This analysis identified seven additional candidate centriole proteins (Figure 1A). Six of these proteins have human orthologs, three of which

are associated with known human diseases, revalidating the importance of the centriole proteome.

Utilizing our previously established criteria for determining if genes are upregulated during flagellar regeneration, we characterized the novel proteins as either core components of the centriole (POCs- proteome of the centriole) or as basal body proteins with upregulated genes (BUGs- basal body proteins with up-regulated genes) (Keller *et al*., 2005). The latter category indicates proteins encoded by genes whose expression (as judged by quantitative real-time PCR and/or microarray analysis) increases during flagellar assembly, implicating them in the process of ciliogenesis. Figure 1A demonstrates that five of the seven novel centriole proteins have genes that are upregulated during flagellar regeneration and are thus annotated as BUGs (BUG28-BUG32). A full list of cross-validated POCs and BUGs from the *Chlamydomonas* centriole proteome appears in Supplemental Table 1. Two proteins, POC13 and BUG6, were not re-annotated in the version 3.0 genome and are indicated as such in Supplemental Table 1.

In order to validate centriole proteins we constructed C-terminal GFP fusion proteins and analyzed their localizations during transient transfections in both Hela and U2OS cells. We previously published the localizations of four centriole proteins from the centriole proteome in human cells (POC1, BUG21/PACRG, POC12/MKS1, and BUG14) (Keller *et al*., 2005). We have now succeeded in localizing twenty-eight of the POCs and BUGs at the centriole in our on-going effort to verify our cross-validated groups of centriole proteins (Supplementary

Table 1). POC20/FAP124, BUG30/Sjogrens autoantigen (Ro/SSA), and BUG32 are among the new proteins in the centriole proteome that we have shown to be centriolar by GFP localization in human cells (Figure 1B). Co-staining with gamma-tubulin to mark the centrosome reveals that each of the examined proteins localizes to a pair of dots representing the centrioles embedded in a matrix of PCM. The results of the GFP-localizations for all POCs are summarized in Supplemental Figure 1. Results of GFP-localizations for all BUGs are summarized in Supplemental Figure 2. Furthermore, other groups have demonstrated centriole localizations for additional POCs and BUGs, in both mammalian cells and in other organisms. BUG28/RPGR1 has been demonstrated to localize to centrioles and basal bodies in cells with primary cilia (Shu *et al*., 2005) and recently, POC10/NPHP-4 has also been shown to localize to the transition zone, a distal modification of the basal body that is required for ciliogenesis, in *C .elegans* sensory cilia (Jauregui *et al*., 2008). Additionally, both POC5 and POC19 localize to centrioles in mammalian cells (J. Azimzadeh and M. Bornens, personal communication). A number of proteins from the centriole proteome did not have a mammalian homologue which prevented us from checking their localization using human GFP-tagged constructs. Overall, the localization data confirm the validity of our centriole proteome data and allow us to expand our centriole proteome by seven proteins.

Due to the large number of cilia and centriole proteomes that have been published since our original centriole proteome we sought to examine which of the POCs and BUGs are also found in the proteomes from mouse photoreceptor

complexes, *Chlamydomonas* flagella, *Tetrahymena* centrioles and cilia, and *Trypanosome* flagella (Pazour *et al*., 2005; Smith *et al*., 2005; Broadhead *et al*., 2006; Liu *et al*., 2007; Kilburn *et al*., 2007). The number of proteins overlapping between POCs and BUGs and these other proteomes are shown in Supplemental Table 1. It is noteworthy that when compared with the flagellar proteome from *Chlamydomonas*, the majority of overlap occurs within the BUGs, corresponding to genes upregulated during flagellar assembly, compared to the POCs whose genes are not upregulated during flagellar assembly (Figure 1C). We hypothesize that these BUG proteins are components of a common structural motif based on microtubule doublets that is shared between centrioles and flagella. In contrast, POCs have a larger overlap than BUGs when compared with the *Tetrahymena* centriole proteome suggesting that POCs do indeed constitute core structural components of the centriole (Figure 1C).

Human Disease Proteins are highly represented in the Centriole Proteome

Due to the ubiquitous distribution of cilia in the human body, mutations in genes encoding for proteins localized in cilia and basal bodies can result in systemic diseases that involve a wide-range of symptoms including but not limited to polydactyly, polycystic kidney disease, and retinal degeneration. In particular, two classes of ciliary disease genes are highly represented among the basal body proteome (Table 1): cystic kidney disease syndromes and cone-rod dystrophy syndrome genes. Mutations in POC3 (CEP290/NPHP6), POC10 (NPHP4), POC12 (MKS1), BUG29 (AHI1/Jouberin), and BUG11 (OFD1) cause a

broad spectrum of phenotypes with cystic kidney disease being among the most common. The diseases which are caused by mutations in these genes (Nephronopthhsis, Meckel syndrome, Joubert's syndrome and oral-facial-digital syndrome) are all known ciliopathies (King *et al*., 1984; Feather *et al.,* 1997; Ferrante et al., 2006; Kyttala *et al*., 2006; den Hollander *et al*., 2006; Parisi *et al*., 2006; Valente *et al*., 2006; Tory *et al*., 2007; Jauregui *et al*., 2008) and we hypothesize that these diseases arise from defects in centriole structure and/or function.

In addition to gene products implicated in cystic kidney disease syndromes, our basal body proteome also includes products of genes connected with retinal degeneration. Mutations in BUG28 (RPGR1) and POC7 (UNC119) are associated with cone-rod dystrophy, a name given to a wide range of eye conditions causing deterioration of the cones and rods in the retina which often leads to blindness (Kobayashi *et al*., 2000; Gerber *et al*., 2001; Koenekoop, 2005; Adams *et al*., 2008; Hameed *et al*., 2003). All human diseases represented by the centriole proteome are summarized in Table 1. Due to the heterogeneity of ciliopathies, many proteins are associated with more than one human disease.

POC1 is a Conserved Protein that uses WD40 Repeats to Localize to Centrioles

The kidney and retinal disease gene products outlined above must act in the context of the overall complex structure of the basal body. A key goal at present is thus to know how all basal body proteins fit into this structure. As a first step

towards this goal, we have focused on POC1 which is the most abundant centriole protein besides tubulin and tektin, based on spectral counts in the basal body proteome (Keller *et al*., 2005). Since tubulin and tektin are both centriole structural proteins (Hinchcliffe and Linck, 1998) we reasoned that POC1 might also be an important part of the centriole structure. The POC1 protein is evolutionarily conserved in all organisms from *Chlamydomonas* to humans, excluding *C. elegans* which has a highly unusual centriole structure that is shorter than normal centrioles. All organisms with standard triplet microtubule-containing centrioles in at least part of their life cycle have a POC1 gene (Figure 2A). There is a gene duplication of POC1 in all vertebrates, and we will refer to the two paralogs in humans as POC1A (NP_056241.2) and POC1B (NP_758440.1). POC1 has seven WD40 repeats in the N-terminal half of the protein and the last 50 or so amino acids form a coiled coil based on the COILS server prediction (Figure 2B). Sequence alignment of the last 50 amino acids of POC1 reveals a novel consensus sequence we have termed the POC1-domain (Figure 2C).

We previously confirmed that POC1B is a centriolar protein in HeLa cells (Keller *et al*., 2005). We cloned the POC1A gene from HeLa cell cDNA by reverse transcription and verified that it is also centriolar by POC1A-GFP transfection (Supplemental Figure 1). In order to identify what part of POC1 is necessary for centriolar localization, we constructed C-terminally tagged GFP pieces of POC1A and POC1B (Figure 2D). Our results indicate that besides full-length protein, only the WD40 domain at the N-terminus (aa 1-298) is involved in

targeting POC1 localization to centrioles in human cells (Figure 2E). Sequences including only parts of the WD40 domain (aa 1-98 and aa 87-276) are not sufficient for POC1 localization to the centriole, suggesting that the entire WD40 domain, including all seven repeats are necessary for localization to centrioles, probably due to the fact that these repeats are likely to assemble into a single beta-propellar. This is consistent with WD40 repeats being involved in protein-protein interactions necessary for centriolar localization of other proteins (Hartman *et al*., 1998). The conserved POC1-domain consensus sequence is neither necessary nor sufficient for centriole localization, and we therefore hypothesize it may be involved in interactions with other proteins.

POC1 Localizes to Basal Bodies in human cells and in Chlamydomonas

We found that POC1 remains localized to centrioles when they become basal bodies in ciliated human cells (Supplemental Figure 5). To more carefully explore POC1 localization within the basal body, we turned to *Chlamydomonas* where the basal body cytology is extremely well defined (Ringo, 1967; O'Toole et al., 2003; Geimer and Melkonian, 2005). The *Chlamydomonas* POC1 peptide antibody (Figure 3A) stains the basal bodies of wild-type cells (Figure 3B). The POC1 positive spots colocalize with both acetylated-tubulin and centrin (Figure 3B) indicating that POC1 is a specific marker for centrioles in *Chlamydomonas*. The antibody appears to be specific to POC1 and only recognizes one polypeptide (Supplemental Figure 3). This polypeptide has the predicted molecular weight of POC1 (54.4kD). As a further control for antibody specificity,

we have shown that pre-incubation with a POC1 peptide used for antibody production completely abolishes all basal body and flagellar staining demonstrating that the antibody is specific to the POC1 protein in *Chlamydomonas* (Supplemental Figure 3).

During spindle formation, POC1 exclusively stains centrioles near the spindle poles. More specifically, POC1 was visualized in two spots at either pole of the spindle representing the four centrioles that are present in wildtype *Chlamydomonas* spindles (Figure 3B). At higher magnification POC1 appears to stain the entire basal body from which acetylated-tubulin positive cilia extend (Figure 3C).

We also observed a faint punctate staining along the length of the flagella. Interestingly, the flagellar staining was dramatically increased in flagella that had become detached from the cell body (data not shown). Similar epitope behavior was reported with antibodies to the axonemal microtubule-associated protein BUG21/PACRG (Ikeda *et al*., 2007) suggesting that the POC1 epitope may be inaccessible in attached flagella.

POC1 Localizes to Newly Duplicating Centrioles

We are particularly interested in investigating proteins involved in the early steps of centriole assembly because these may give clues to the unexplained process of centriole duplication. We used both the *Chlamydomonas* POC1 antibody and human POC1-GFP constructs to ask if POC1 localizes to newly duplicating daughter centrioles in addition to fully developed mother centrioles. In

Chlamydomonas, careful examination demonstrated that POC1 localizes to four distally located spots in wildtype cells (Figure 4A). This is reminiscent of both Bld10p and Vfl1p localizations, both of which show two to four dots at the base of the flagella in positions that resemble the basal bodies and probasal bodies (proBBs) (Silflow *et al*., 2001; Matsuura et al., 2004). To confirm the POC1 proBB localization in *Chlamydomonas*, we performed immuno-electron microscopy (immmunoEM) on isolated nucleoflagellar apparatuses (NFAps), which are cytoskeletal complexes containing the basal bodies, proBBs, axonemes, rootlet microtubules, and other fibrous structures tightly associated with the basal bodies (Wright *et al*., 1985). Gold particles conjugated to the secondary antibody were found associated not only with mature mother centrioles (Figure 4B1-4B3) but also with proBBs (Figure 4B3, 4B5, and 4B6). POC1 is therefore a novel proBB protein in *Chlamydomonas* and part of a very small group of proteins that are known to be present in daughter proBBs and are likely essential for proper centriole assembly.

Since *Chlamydomonas* POC1 localizes to both mother and daughter centrioles, we wanted to further investigate human POC1 localization. We looked at both POC1A-GFP and POC1B-GFP constructs that had been transiently and stably transfected into HeLa and U2OS cells. Costaining with the early centriole marker, centrin 2 (Cetn2) revealed POC1 localization to both mother centrioles and newly forming daughter centrioles (Figure 4C). Centrin is known to localize to the distal lumen of mature centrioles (Azimzadeh and Bornens, 2007), in contrast POC1 localizes along the entire length of the microtubule-based

centriole structure, consistent with the localization in *Chlamydomonas*. To further clarify POC1 position within the centriole, we examined centrioles during S-phase before procentriole elongation. These images indicate that POC1 localizes to the whole centriole, while centrin occupies only the distal ends in both mature centrioles and in procentrioles (Figure 4C). Relative intensity plots were constructed to demonstrate that POC1 and centrin are slightly shifted from one another and to show that the mature mother centriole has higher fluorescence intensity then the daughter procentriole (Figure 4D). POC1 is therefore a component of both mother and daughter centrioles in both *Chlamydomonas* and in human cells.

POC1 Recruitment in Centriole Mutants with Ultrastructural Defects

To investigate when POC1 becomes recruited to centrioles during the assembly process we took advantage of previously described *Chlamydomonas* centriole mutants which block specific steps in the centriole assembly pathway. Mutations in delta-tubulin (UNI3) and epsilon-tubulin (BLD2) cause basal bodies to have doublet and singlet microtubules respectively, unlike the wild-type triplet microtubules (Goodenough and StClair, 1975; O'Toole *et al.,* 2003). Centrioles in *bld2* mutants are also much shorter than wildtype centrioles suggesting a defect in centriole length control (Goodenough and StClair, 1975). Additionally, the *bld10* mutant has been reported to completely lack centrioles, however on very rare occasions cells have fragments of centrioles, which stain positively with an acetylated-tubulin antibody (Matsuura *et al*., 2004).

We compared POC1 localizations in mutants with doublet, singlet, or fragments of centrioles to its expression in wildtype *Chlamydomonas* (Figure 5). POC1 localizes to centrioles composed of only doublet or only singlet microtubules (Figure 5B, 5C). The majority of *bld10* cells had diffuse POC1 with no particular localization, however whenever cells stained positively for acetylated-tubulin, indicating the presence of centriole fragments, POC1 was precisely colocalized (Figure 5D). Fluorescence intensity quantification showed that wildtype basal bodies have a significantly higher amount of total POC1 than any of the three mutants ($p<0.005$). This suggests that POC1 is incorporated into the core microtubule structure of basal bodies since it is reduced in mutants with either doublet or singlet microtubules. The mutant with the shortest centrioles, *bld2*, had the least POC1 recruited. This analysis demonstrates that POC1 can localize to centrioles lacking many of the structures found in mature centrioles, consistent with the above data indicating early recruitment of POC1 to proBBs and procentrioles.

POC1 Localizes to Sites of Basal Body Fiber Attachment

In order to get higher resolution information about POC1 localization we utilized immunoEM on isolated *Chlamydomonas* nucleoflagellar apparatus (NFap) preparations (Wright et al., 1985). POC1 protein was found to associate with the entire microtubule-based barrel structure that constitutes the basal body. Specifically, POC1 localizes to triplet microtubules (Figure 6A, 6B), axonemal doublet microtubules (Figure 6C), and rootlet microtubules near the basal bodies

(Figure 6B, 6D, and 6E). Tangential sections confirm localization to the walls of the microtubule-based barrel (Figure 6F-6H). POC1 is absent from the centriole lumen, the transition zone, and the central pair microtubules in the axoneme (Figure 6A, 6G, 6C). Serial sections allowed us to examine where POC1 is found in detail throughout a centriole both in cross-section and in tangentially cut sections. Serial sections indicate that POC1 is highly enriched in regions where fibers attach to the basal bodies. In particular, POC1 localizes to both proximal and distal connecting fibers at the regions of attachment (Figure 6I). In fact, there is POC1 enrichment at the site of attachment of all fibers that are interacting with the basal body (Figure 6I). The basal body localization of POC1 to fiber attachment points demonstrates that the protein localizes in a highly asymmetric pattern on mature basal bodies. POC1 does not specifically localize to the cartwheel as was reported for *Tetrahymena* POC1 protein (Kilburn *et al*., 2007). This is seen for example in panel I2 of Figure 6 shown by gold particles located distal to the cartwheel, which is at the very base of the basal bodies (Ringo, 1967). In fact, POC1 localizes to both inner and outer-walls of centrioles and is present on the entire length of the centriole but is completely absent from the centriole lumen (quantification of gold particle distribution given in Supplemental Figure 4). The pattern of POC1 localization implies that POC1 may be involved in establishing, maintaining, or stabilizing specialized microtubular structures. We suggest that POC1 is necessary for either formation or maintenance of doublet and triplet microtubules and is involved at the attachment site of fibers to the microtubule-based basal body structure.

POC1 Localizes to Axonemal Doublet Microtubules

The localization of POC1 to microtubule triplets, which structurally resemble the axonemal microtubule doublets, led us to re-examine the localization of POC1 within the axoneme. We conducted a flagellar splay assay, which uses the ability of flagella to rip themselves apart (Johnson, 1998) to investigate whether POC1 localizes only to doublet microtubules. These experiments reveal that the doublet microtubules colocalize with POC1 whereas the singlet central pair microtubules fail to associate with POC1 (Figure 7A). This result, together with the complete lack of POC1 associated with cytoplasmic microtubules indicates that POC1 is not simply a general microtubule binding protein.

The punctate staining of POC1 in *Chlamydomonas* flagella resembles the staining pattern of many intraflagellar transport (IFT) proteins (Cole *et al*., 1998; Rosenbaum and Witman, 2002; Scholey, 2003). IFT proteins also localize in the vicinity of the basal body (Deane *et al., 2001*). Those similarities in localization raised the possibility that POC1 might be associated with IFT. To test whether POC1 is a structural component of the axoneme or a transitory IFT protein, we utilized a temperature sensitive mutation in the axonemal-specific kinesin II motor subunit, FLA10. This *fla10* mutant is wildtype at 21˚C but loses IFT protein in the axoneme and starts absorbing its flagella within 40 minutes at 34˚C (Kozminski *et al*., 1995). We stained this temperature sensitive mutant at 21˚C and after 45 minutes at 34˚C when all IFT proteins should be absent from flagella. Our results indicate that POC1 is in the flagella in both cases, unlike the IFT 172.1 protein

which disappears at 34˚C, demonstrating that POC1 is a component of the axoneme rather than an IFT-associated protein (Figure 7B).

RNAi of POC1 Reduces Centriole Duplication

We took advantage of the fact that human U2OS cells overduplicate centrioles when S-phase arrested, to examine the effect of POC1 depletion on centriole duplication (Habedanck et al., 2005). We were successfully able to knock down POC1 in a U2OS line stably expressing POC1-GFP, indicated by both fluorescence intensity quantification of GFP (data not shown) and by Western blot (Figure 8A). In untreated U2OS cells S-phase arrest caused cells to accumulate between 2 and 12 centrioles per cell (Figure 8B) so that a substantial fraction of cells have more than four centrioles, the maximum number seen in normal dividing cells. In contrast, the percent of cells with more than four centrioles was significantly decreased ($p<0.05$) in POC1 siRNA-treated cells in comparison to treatment with a negative control siRNA (Figure 8C). The POC1 depleted cells also had a significant increase in the percent of cells that had only two centrioles. These data demonstrate that POC1 is necessary for centriole overduplication in U2OS cells and may suggest that POC1 plays a critical role in centriole duplication in cells that are not S-phase arrested.

Overexpression of POC1 leads to Elongated Centriole-like Structures

In order to gain functional insight into the role of POC1 in centriole assembly we overexpressed POC1-Cherry constructs to investigate the possibility of a

dominant negative effect. Overexpression of full-length POC1 or the C-terminal POC1-domain resulted in no measurable loss of POC1-GFP or centrin at the centrioles of stably expressing POC1-GFP Hela or U2OS cells. Overexpression of POC1-WD40 resulted in a slight reduction (<30%) of POC1-GFP at the centriole (data not shown), but we failed to identify any associated phenotype with this slight loss of POC1-GFP at centrioles. However, we noticed that approximately 5-10% of the full length POC1 overexpressing cells, showed a remarkable increase in centriole length indicated by both POC1-GFP and by centrin 2 staining (Figure 9A).

Upon S-phase arrest in POC1-GFP overexpressing U2OS cells, we found that a large proportion of cells (>45%) that had elongated centriole-like structures that were positive for POC1-GFP but also stained with centrin (Figure 9A). These elongated centriole-like structures also stain with antibodies against acteylated-tubulin and polyglutamylated-tubulin, both which mark the more stable microtubules that constitute the centriole (Supplemental Figure 6) (Kann et al., 2003; Piperno et al., 1987). Additionally, gamma-tubulin, which can associate specifically with centrioles and is a component of the pericentriolar material, but its not found within cilia (Fuller et al., 1995; Dibbayawan et al., 1995), colocalizes with these POC1-GFP positive elongated centriole-like structures. The distal appendage marker ODF2 (Ishikawa et al., 2005) fails to colocalize along the length of these elongated structures and rather localizes to only the mother centriole (Supplemental Figure 6). The average length of these elongated centriole-like structures was over 1mm and in some instances extended several

microns in length (Figure 9B). These structures are very similar to the phenotype seen by depletion of either Cep97 or CP110 (Spektor et al., 2007) although those authors interpreted the structures as primary cilia. Due to the presence in these structures of centrin, which localizes to centrioles and only in the transition zone of axonemes (Laoukili et al., 2000), and of gamma-tubulin, we argue that these elongated centriole-like structures are not primary cilia but rather elongated centrioles.

To confirm that the presence of elongated centriole-like structures was dependent on POC1 levels, we transfected cells with siRNA targeting either POC1B alone or simultaneous knockdown of POC1A and POC1B. Depletion of either POC1B or simultaneous depletion of both POC1A and POC1B caused a significant reduction in percent of cells with elongated centriole-structures (<10%) in comparison to negative control siRNA (>45%) ($p<0.05$) (Figure 9B). Additionally the average length of centrin-staining structures within cells was reduced from over 1mm to approximately 0.2mm in both POC1 siRNA-treatments (Figure 9B). Wildtype centriole length, measured by both POC1-GFP and centrin fluorescence, is approximately 0.2mm, which is similar to the POC1-depleted cells (data not shown). These data together suggest that overexpression of POC1 leads to an elongation of centrioles. This phenotype appears to be dependent specifically on POC1 because reduced expression of POC1 restores centrioles to their normal length. We therefore suggest that POC1 is involved in both centriole duplication and in centriole length control.

Discussion

Importance of the Centriole Proteome is Shown by Presence of Human Diseases

Here, we document an expansion of the *Chlamydomonas* centriole proteome based on version three of the *Chlamydomonas* genome (Merchant *et al*., 2007). The total expanded proteome includes twelve potential human disease proteins (summarized in Table 1), confirming the importance of a thorough investigation of centrioles. In fact, known human disease genes encode more than 17% of the cross-validated *Chlamydomonas* centriole proteins (Supplemental Table 1). One possibility is that the disease genes found in the centriole proteome encode for structurally conserved core centriole proteins that are necessary for establishing or maintaining the integrity of the complex triplet microtubules structure. Another possibility is that these proteins are involved in ciliogenesis-related functions like IFT docking. In the future it will be important to not only examine the composition of centrioles, but also to understand their precise function in regards to the cell cycle and ciliogenesis.

POC1 may be Specific to Motile Cilia

It is interesting to note that the POC1 gene is apparently absent from the *C. elegans* genome. This is intriguing because *C. elegans* lacks both triplet microtubules and motile cilia, suggesting that POC1 may be directly associated with motility. Motile cilia are much more structurally complex than non-motile cilia

and have a large number of proteins, such as outer and inner dynein arms, that are necessary to confer movement. Additionally, motile cilia always have an associated triplet microtubule centriole. *C. elegans* basal bodies have only singlet microtubules during early development and doublets during the formation of sensory cilia (Inglis *et al*., 2007). Worms have lost other conserved centriole proteins and structures, such as centrin and epsilon and delta-tubulin along with the cartwheel structure, indicating that nematodes are highly divergent when it comes to both centrioles and cilia (Pelletier *et al*., 2006; Azimzadeh and Bornens, 2007). It is formally possible that other proteins in *C. elegans* play the function of POC1. Additionally, *Drosophila* POC1 mRNA is highly upregulated (more than 4 times higher expression than in any other adult tissue) in testes (Chintapalli et al., 2007). Testes are the only location in *Drosophila* that contain known motile cilia, so the upregulation of POC1 in this tissue type would be consistent with a role in forming basal bodies of motile cilia/flagella.

Basal bodies, which have the appearance of a symmetrical cylinder, also have an inherent asymmetry due to the asymmetric attachment of various fibers and appendages. Proteins such as VFL1 and Centrin are known to localize on mature basal bodies in an asymmetric manner and have been hypothesized to confer orientational information to the two adjacent mature basal bodies and to the newly duplicating probasal bodies (Salisbury *et al*., 1998; Silflow *et al*., 2001; Geimer and Melkonian, 2005). The distribution of POC1 on these fibrous attachment points confers a rotational asymmetry that may be important for either setting up basal body orientation that is essential for subsequent ciliary

beating or for establishing the cytoplasmic location of probasal body formation, which is also determined by the inherent asymmetry of the mature basal body. POC1 thus may play a role in establishing and maintaining the connections between basal bodies which has implications for ciliary beat patterns and planar cell polarity.

POC1 is Involved in Centriole Duplication and Centriole Length Control

The Vienna *Drosophila* RNAi Center reports that a line expressing an RNA-interference construct encoding for POC1 is lethal (Dietzl *et al*., 2007) suggesting POC1 may be essential. Consistent with this, we have not been able to obtain sustained knock-down of POC1 in *Chlamydomonas* or in human cells by stable expression of RNA-interference constructs. Thus, to investigate the function of POC1 we turned to methods such as overexpression and transient siRNA knockdown in human cells. We have demonstrated that POC1 is necessary for the formation of newly duplicated daughter centrioles. Using the standard U2OS centriole-overduplication system we found that depletion of POC1 strongly reduces the amount of newly formed daughter centrioles. This is exciting because there are only a handful of candidate centriole proteins known to be involved in centriole duplication (Pelletier et al., 2006; Dobbelaere et al., 2008). The fact that cells depleted for both POC1A and POC1B show the absence of centrin-staining procentrioles, together with the localization of POC1 protein to procentrioles that we have demonstrated, suggest that POC1 may be involved in an early stage of centriole assembly.

Overexpression of POC1 in S-phase arrested cells causes a large increase in the percent of cells with elongated centriole-like structures. These elongated centrioles are unique for a number of reasons. Firstly, they stain with centrin and gamma-tubulin, which are both specific for centrioles, indicating they are not simply abnormal cilia or microtubule bundles. Secondly, these fibers, despite having an average length of about 1mm can extend over several microns, far longer than normal centrioles can ever become. Thirdly, the elongated centriole-like structures are caused directly by the overexpression of POC1 because subsequent depletion of the protein almost completely eliminates these fibers.

Since POC1 is an early recruited protein to the centriole which is subsequently found along the whole length of the centriole barrel, it is possible that it is intimately involved in determining and influencing centriole length. The total amount of POC1 that becomes incorporated into a centriole may be directly proportional to the length of centrioles, which could explain why overexpression of POC1 causes such a drastic increase in centriole length. Future ultrastructural analysis of these elongated structures using electron microscopy will be required to further define the nature of the elongation defect.

We have shown that POC1 is likely to play a key role in determining many aspects of centriole biology. The localization of POC1 to *Chlamydomonas* centrioles at sites of fibrous attachments suggest that it may play a central role in establishing centriole orientation within the context of a cell and/or organism. Additionally, POC1 localizes to and appears to be essential for the emergence of newly formed daughter centrioles during centriole duplication. POC1, which

localizes along the entire triplet microtubule structure of mature centrioles is also directly involved in determining centriole length. Future studies focusing on POC1 interacting proteins and how it becomes incorporated into centrioles to determine length control will help provide insights into the complex triplet microtubules structure that epitomizes a centriole.

Acknowledgements

We would like to thank the Marshall lab for invaluable discussion and critical review of the manuscript, J. Salisbury, M. Hirono, T. Ikeda, R. Kamiya, M. Bornens, J. Azimzadeh, and D. Cole for reagents, and E. Harris and the *Chlamydomonas* Genetics Center for providing strains. A special thanks to C. Carroll for help with a number of experimental details. LCK is supported by an American Heart Association Predoctoral Fellowship. WFM acknowledges support from National Institutes of Health grant RO1 GM077004, a W.M. Keck Foundation Distinguished Young Scholar in Medical Research award, and the Searle Scholars Program.

References

Adams, M., Smith, U.M., Logan, C.V., and Johnson, C.A. (2008). Recent advances in the molecular pathology, cell biology and genetics of ciliopathies. J. Med. Genet. *45*, 257-267.

Afzelius, B.A. (2004). Cilia-related diseases. J. Pathol. *204*, 470-477.

Ansley, S.J. *et al*. (2003). Basal body dysfunction is a likely cause of pleiotropic Bardet-Biedl syndrome. Nature. *425*: 628-633.

Azimzadeh, J. and Bornens, M. (2007). Structure and duplication of the centrosome. J. Cell Sci. *120*: 2139-2142.

Badano, J.L., Mitsuma, N., Beales, P.L., and Katsanis, N. (2006). The ciliopathies: an emerging class of human genetic disorders. Annu. Rev. Hum. Genet. *7*, 125-148.

Bettencourt-Dias, M., Rodrigues-Martins, A., Carpenter, L., Riparbelli, M., Lehmann, L., Gatt, M.K., Carmo, N., Balloux, F., Callaini, G., and Glover, D.M. (2005). SAK/PLK4 is required for centriole duplication and flagella development. Curr. Biol. *15*: 2199-2207.

Broadhead, R., *et al*. (2006). Flagellar motility is required for the viability of the bloodstream trypanosome. Nature. *440*, 224-227.

Chintapalli, V.R., Wang, J., and Dow, J.A. (2007). Using FlyAtlas to identify better *Drosophila melanogaster* models of human disease. Nat. Genet. *39*(6):715-720.

Cole, D.G., Diener, D.R., Himelblau, A.L., Beech, P.L., Fuster, J.C., and Rosenbaum, J.L. (1998). *Chlamydomonas* kinesin-II-dependent intraflagellar

transport (IFT): IFT particles contain proteins required for ciliary assembly in Caenorhabditis elegans sensory neurons. J. Cell Biol. *141*, 993-1008.

den Hollander, A.I. *et al*. (2006). Mutations in the CEP290 (NPHP6) gene are a frequent cause of Leber congenital amaurosis. Am. J. Hum. Genet. *79*, 556-561.

Dammermann, A., Muller-Reichert, T., Pelletier, L., Habermann, B., Desai, A., and Oegema, K. (2004). Centriole assembly requires both centriolar and pericentriolar material proteins. Dev. Cell. *7*: 815-829.

Dawe, H.R., Farr, H. and Gull, K. (2007). Centriole/basal body morphogenesis and migration during ciliogenesis in animal cells. J. Cell Sci. *120*, 7-15.

Deane, J.A., Cole, D.G., Seeley, E.S., Diener, D.R., and Rosenbaum, J.L. (2001). Localization of intraflagellar transport protein IFT52 identifies basal body transitional fibers as the docking site for IFT particles. Curr. Biol. *11*, 1586-1590.

Delattre, M., Canard, C., and Gonczy, P. (2006). Sequential protein recruitment in *C. elegans* centriole formation. Curr. Biol. *16*, 1844-1849. Cell Biol. Int. *19*(7): 559-567.

Dibbayawan, T.P., Harper, J.D.I., Elliott, J.E., Gunning, B.E.S., and Marc, J. (1995). A gamma-tubulin that associated specifically with centrioles in Hela cells and the basal body complex in *Chlamydomonas*.

Dietzl, G. *et al*. (2007). A genome-wide transgenic RNAi library for conditional gene inactivation in *Drosophila*. Nature. *448*, 151-156.

Dobbelaere, J., Josue, F., Suijkerbuijk, S., Baum, B., Tapon, N., and Raff, J.

(2008). A genome-wide RNAi screen to dissect centriole duplication and centrosome maturation in Drosophila. PLoS Biol. *6*, e224.

Dutcher, S.K., Morrissette, N.S., Preble, A.M., Rackley, C., and Stanga, J. (2002). Epsilon-tubulin is an essential component of the centriole. Mol. Biol. Cell. *13*, 3859-3869.

Dutcher, S.K. and Trabuco, E.C. (1998). The UNI3 gene is required for assembly of basal bodies of Chlamydomonas and encodes delta-tubulin, a new member of the tubulin superfamily. Mol. Biol. Cell. *9*, 1293-1308.

Feather, S.A., Winyard, P.J.D., Dodd, S., and Woolf, A.S. (1997). Oral-facial digital syndrome type 1 is another dominant polycystic kidney disease: clinical, radiological and histopathological features of a new kindred. Nephrol Dial Transplant. *12*: 1354-1361.

Ferrante, M.I., Zullo, A., Barra, A., Bimonte, S., Messaddeq, N., Studer, M., Dolle, P., and Franco, B. (2006). Oral-facial-digital type I protein is equired for primary cilia formation and left-right axis specification. Nat. Cell Biol. *38*(1): 112-117.

Fuller, S.D., Gowen, B.E., Reinsch, S, Sawyer, A, Buendia, B., Wepf, R., and karsenti, E. (1995). The core of the mammalian centriole contains gamma-tubulin. Curr. Biol. *5*, 1384-93.

Geimer, S. and Melkonian, M. (2005). Centrin scaffold in *Chlamydomonas reinhardtii* revealed by immunoelectron microscopy. Euk. Cell. *4*, 1253-1263.

Gerber, S., *et al*. (2001). Complete exon-intron structure of the RPGR-interacting

protein (RPGRIP1) gene allows the indentification of mutations underlying Leber congenital amaurosis. Eur. J. Hum. Genet. *9*, 561-571.

Goodenough, U.W. and StClair, H.S. (1975). BALD-2: a mutation affecting the formation of doublet and triplet sets of microtubules in Chlamydomonas reinhardtii. J. Cell Biol. *66*: 480-491.

Habedanck, R., Stierhof, Y.D., Wilkinson, C.J., and Nigg, E.A. (2005). The polo kinase Plk4 functions in centriole duplication. Nat. Cell Biol. *7*(11):1140-1146.

Hameed, A., Abid, A., Aziz, A., Ismail, M., Mehdi, S.Q., and Khaliq, S. (2003). Evidence of RPGRIP1 gene mutations associated with recessive cone-rod dystrophy. J. Med. Genet. *40*, 616-619.

Harris, H. (1989). The Chlamydomonas sourebook: A comprehensive guide to biology and laboratory use. San Diego, Academic Press, Inc.

Hartman, J.J., Mahr, J., McNally, K., Okawa, K., Iwamatsu, A., Thomas, S., Cheesman, S., Heuser, J, Vale, R.D., McNally, F.J. (1998). Katanin, a microtubule-severing protein, is a novel AAA ATPase that targets to the centrosome using a WD40-containing subunit. Cell. *93*, 277-287.

Hinchcliffe, E.H. and Linck, R.W. (1998). Two proteins isolated from sea urchin sperm flagella: structural components common to the stable microtubules of axonemes and centrioles. J. Cell Sci. *111*, 585-595.

Hiraki, M., Nakazawa, Y., Kamiya, R., and Hirono, M. (2007).Bld10p constitutes the cartwheel-spoke tip and stabilizes the 9-fold symmetry of the centriole. Curr. Biol. *17*, 1-6.

Ikeda, K., Ikeda, T., Morikawa, K., and Kamiya, R. (2007). Axonemal localizations of Chlamydomonas PACRG, a homologue of the human Parkin-Coregulated gene product. Cell. Motil. Cytoskeleton. *64*, 814-821.

Inglis, P.N., Ou, G., Leroux, M.R., and Scholey, J.M. (2007). The sensory cilia of *Caenorhabditis elegans*. *8*, 1-22.

Ishikawa, H., Kubo, A., Tsukita, S., and Tsukita, S. (2005). Odf2-deficient mother centrioles lack distal/subdistal appendages and the ability to generate primary cilia. Nat. Cell Biol. *7*, 517-24.

Jauregui, A.R., Nguyen, K.C.Q., Hall, D.H., and Barr, M.M. (2008). The *Caenorhabditis elegans* nephrocystins act as global modifiers of cilium structure. J. Cell. Biol. *180*, 973-988.

Johnson, K. (1998). The axonemal microtubules of the Chlamydomonas flagellum differ in tubulin isoform content. J. Cell Sci. *111*, 313-320.

Kann, M., Soues, S., Levilliers, N., and Fouquet, J. (2003). Glutamylated tubuilin: diversity of expression and distribution of isoforms. Cell Motil Cytoskeleton. *55*: 14-25.

Keller, L.C., Romijn, E.P., Zamora, I., Yates III, J.R., and Marshall, W.F. (2005). Proteomic analysis of isolated Chlamydomonas centrioles reveals orthologs of ciliary-disease genes. Curr. Biol. *15*, 1090-1098.

Kilburn, C.L., Pearson, C.G., Romijn, E.P., Meehl, J.B., Giddings, T.H., Culver,

B.P., Yates III, J.R., and Winey, M. (2007). New Tetrahymena basal body protein components identify basal body domain structure. J. Cell Biol. *178*, 905-912.

King, M.D., Dudgeon, J., and Stephenson, J.B. (1984). Joubert's syndrome with retinal dysplasia: neonatal tachypnoea as the clue to a genetic brain-eye malformation. Arch. Dis. Child. *59*: 709-718.

Kobayashi, A., Higashide, T., Hamasaki, D., Kubota, S., Sakuma, H., An, W., Fujimaki, T., McLaren, M.J., Weleber, R.G., and Inana, G. (2000). HRG4 (UNC119) mutation found in cone-rod dystrophy causes retinal degeneration in a transgenic model. Invest. Ophthalmol. Vis, Sci. *41*, 3268-3277.

Koenekoop, R.K. (2005). RPGRIP1 is mutated in Leber congenital amaurosis: a mini-review. Ophthalmic. Genet. *26*, 175-179.

Kozminski, K.G., Beech, P., and Rosenbaum, J.L. (1995). The Chlamydomonas FLA10 gene encodes a novel kinesin-homologous protein. J. Cell Biol. *131*, 1517-1527.

Kyttala, M., Talila, J., Salonen, R., Kopra, O., Kohischmidt, N., Paavola-Sakki, P., Peltonen, L., and Kestila, M. (2006). MSK1, encoding a component of the flagellar apparatus basal body proteome, is mutated in Meckel syndrome. Nat Genetics. *38*, 155-157.

Laoukili, J., Perret, E., Middendorp, S., Houcine, O., Guennou, C., Marano, F., Bornens, M., and Tournier, F. (2000). Differential expression and cellular

distribution of centrin isoforms during human ciliated cell differentiation in vitro. J. Cell Sci. *113*: 1355-1364.

Liu, Q., Tan, G., Levenkova, N., Li, T., Pugh, E.N. Jr., Rux, J.J., Speicher, D.W., and Pierce, E.A. (2007). The proteome of the mouse photoreceptor sensory cilium complex. Mol. Cell Proteomics. *6*: 1299-1317.

Marshall, W.F. (2008). The cell biological basis of ciliary disease. J. Cell Biol. *180*, 17-21.

Matsuura, K., Lefebvre, P.A., Kamiya, R., and Hirono, M. (2004). Bld10p, a novel protein essential for basal body assembly in Chlamydomonas: localization to the cartwheel, the first ninefold symmetrical structure appearing during assembly. J. Cell Biol. *165*: 663-671.

Merchant, S.S. *et al*. (2007). The Chlamydomonas genome reveals the evolution of key animal and plant functions. Science. *318*: 245-250.

Nakazawa Y., Hiraki, M., Kamiya, R., and Hirono, M. (2007). SAS-6 is a cartwheel protein that establishes the 9-fold symmetry of the centriole. Curr. Biol. *17*, 2169-2174.

O'Toole, E.T., Giddings, T.H., McIntosh, J.R. and Dutcher, S.K. (2003). Three dimensional organization of basal bodies from wild-type and delta-tubulin strains of Chlamydomonas reinhardtii. Mol. Biol. Cell. *14*, 2999-3012.

Parisi *et al*., (2006). AHI1 mutations cause both retinal dystrophy and renal cystic disease in Joubert syndrome. J. Med. Genet. *43*, 334-339.

Pazour, G.J., Agrin, N., Leszyk, J., and Witman, G.B. (2005). Proteomic analysis of a eukaryotic cilium. J. Cell Biol. *170*, 103-113.

Pazour, G.J. and Rosenbaum, J.L. (2002). Intraflagellar transport and cilia-dependent diseases. Trends Cell Biol. *12*, 551-555.

Pelletier, L., O'Toole, E., Schwager, A., Hyman, A.A., and Muller-Reichert, T. (2006). Centriole assembly in Caenorhabditis elegans. Nature. *444*, 619-623.

Piperno, G., LeDizet, M., and Chang, X. (1987). Microtubules containing acetylated alpha-tubulin in mammalian cells in culture. J. Cell. Biol. *104*: 289-302.

Ringo, D.L. (1967). Flagellar motion and fine structure of the flagellar apparatus in *Chlamydomonas*. J. Cell Biol. *33*: 543-571.

Rosenbaum, J.L. and Witman, G.B. (2002). Intraflagellar transport. Nat. Rev. Mol. Cell Biol. *3*, 813-825.

Salisbury, J.L. (1998). Roots. J. Eukaryot. Microbiol. *45*, 28-32.

Scholey, J.M. (2003). Intraflagellar transport. Annu. Rev. Cell Dev. Biol. *19*, 423-443.

Shu, X., *et al*. (2005). RPGR ORF15 isoform co-localizes with RPGRIP1 at centrioles and basal bodies and interacts with nucleophosmin. Hum. Mol. Genet. *14*, 1183-1197.

Silflow, C.D., LaVoie, M., Tam, L., Tousey, S., Sanders, M., Wu, W., Borodovsky, M., and Lefebvre, P.A. (2001). The Vfl1 protein in *Chlamydomonas* localizes in a rotationally asymmetric pattern at the distal ends of the basal bodies. J. Cell Biol. *153*, 63-74.

Smith, J.C., Northey, J.G.B., Gary, J., Pearlman, R.E., Michael Siu, K.W. (2005). Robust method for proteome analysis by MS/MS using an entire translated genome: Demonstartion on the ciliome of Tetrahymena thermophila. J. Proteome Res. *4*, 909-919.

Snell, W.J., Dentler, W.L., Haimo, L.T., Binder, L.I., and Rosenbaum, J.L. (1974). Assembly of chick brain tubulin onto isolated basal bodies of *Chlamydomonas reinhardtii*. Science *26*, 357-360.

Sorokin, S.P. (1968). Reconstruction of centriole formation and ciliogenesis in mammalian lungs. J. Cell Sci. *3*: 207-230.

Spektor, A., Tsang, W.Y., Khoo, D., and Dynlacht, B.D. (2007). Cep197 and CP110 suppress a cilia assembly program. Cell *130*: 678-690.

Tory, K., *et al*. (2007). High NPHP1 and NPHP6 mutation rate in patients with Joubert syndrome and nephronophthisis: potential epistatic effect of NPHP6 and AHI1 mutations in patients with NPHP1 mutations. Clin. J. Am. Soc. Nephrol. *18*, 1566-1575.

Uetake, Y., Loncarek, J., Nordberg, J.J., English, C.N., La Terra, S., Khojakov, A., and Sluder, G. (2007). Cell cycle progression and de novo centriole assembly after centrosomal removal in untransformed human cells. J. Cell Biol. *176*, 173-182.

Valente, E.M., *et al*. (2006). Mutations in CEP290, which encodes a centrosomal protein, cause pleiotropic forms of Joubert syndrome. Nat. Genetics. *38*, 623-625.

Vorobjev, I.A. and Chentsov, Y.S. (1982). Centrioles in the Cell Cycle. I. Epithelial Cells. J. Cell Biol. *98*: 938-949.

Washburn, M.P., Wolters, D., Yates III, J.R. (2001). Large-scale analysis of the yeast proteome by multidimensional protein identification technology. Nat. Biotechnol. *19*, 242-247.

Wright, R.L., Salisbury, J., and Jarvik, J.W. (1985). A nucleus-basal body connector in Chlamydomonas reinhardtii that may function in basal body localization or segregation. J. Cell Biol. *101*, 1903-1912.

Yoder, B.K. (2007). Role of primary cilia in the pathogenesis of polycystic kidney disease. J. Am. Soc. Nephrol. *18*, 1381-1388.

Tables

Table 1. Human diseases represented by the centriole proteome.

Proteins Involved in Cystic Kidney Diseases	Proteins Involved in Cone-Rod Dystrophies	Proteins Involved in Other Human Diseases
POC3 (CEP290/NPHP6)	POC3 (CEP290/NPHP6)	POC9 (Rib72-like protein)- Juvenile myoclonic epilepsy
POC10 (NPHP4)	POC10 (NPHP4)	DIP13- Sjogrens antigen
POC12 (MKS1)	BUG28 (RPGR1)	BUG30 (Ro/SSA)- Sjogrens antigen
BUG29 (AHI1/Jouberin)	BUG29 (AHI1/Jouberin)	BUG11 (OFD1)- Oral-Facial-Digital syndrome
BUG11 (OFD1)- Oral-Facial-Digital syndrome	POC7 (UNC119)	BUG21 (PACRG)- Male infertility

Figures

Figure 1. Expansion of the *Chlamydomonas* centriole proteome reveals additional human disease genes. (A) Table of newly discovered POCs and BUGs. Version three gene identification numbers are as specified in v3.0 of the *Chlamydomonas* genome sequence, available at the Joint Genomes Institute web site: http://genome.jgi-psf.org/Chlre3/Chlre3.home.html. Table also indicates protein name, human Refseq ID numbers, localization of proteins to other proteomes of interest, GFP-localization to centrioles in human cells, and any associated human diseases. (B) Localization of GFP-fusion proteins corresponding to human homologs of *Chlamydomonas* centriole candidate proteins (POC20/FAP124, BUG30/Ro/SSA, and BUG21/Mns1) after transient transfection into Hela cells. Gamma-tubulin antibody stain shows centrosomes, DAPI stain shows DNA. Each GFP-fusion protein colocalizes to a pair of dots within the centrosome in Hela cells, confirming centriolar localization. The scale bar represents 5μm. (C) Venn diagrams illustrating the overlap of POC and BUG proteins with the *Chlamydomonas* flagellar proteome (Pazour *et al*., 2005) and with the *Tetrahymena* centriole proteome (Kilburn *et al*., 2007). Percent of POC and BUG proteins overlapping with the specified proteomes are indicated.

Figure 1. Expansion of the Chlamydomonas centriole proteome

A

POC/BUG	v.3 Gene ID	Protein Name	Human Refseq ID	Photoreceptor Complex Proteome	Flagellar Proteome	Tetrahymena Centriole Proteome	Tetrahymena Cilia Proteome	Trypanosome Flagellar Proteome	GFP Localized	Associated Human Disease
POC20	191903	UBA1 (FAP124)	NP_003325.2	X	X				X	
POC21	182582	AGG3 (FAP142)	none		X					
BUG28	13859	RPGR1	NP_065099.3	X						Retinitis pigmentosa
BUG29	146617	AHI1/Jouberin	NP_008993.1	X						Joubert's syndrome
BUG30	138565	Ro/SSA	NP_004591.2						X	Sjogrens antigen
BUG31	24810	NESG1	NP_036469.2			X	X	X		
BUG32	36430	Mns1	NP_060835.1					X	X	

B

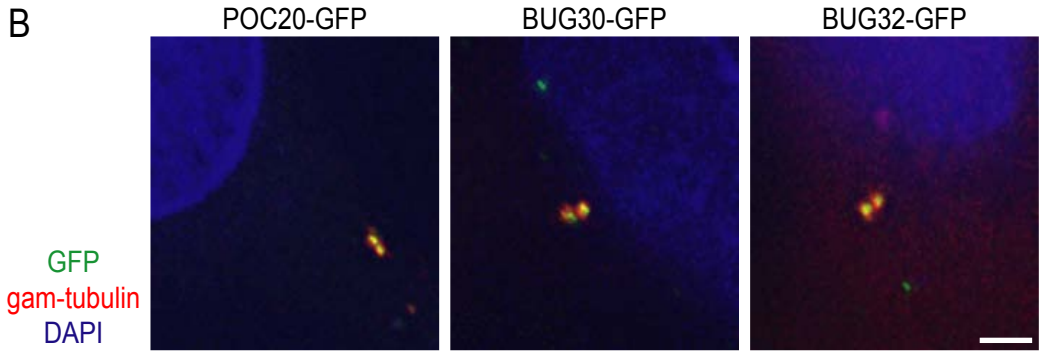

C

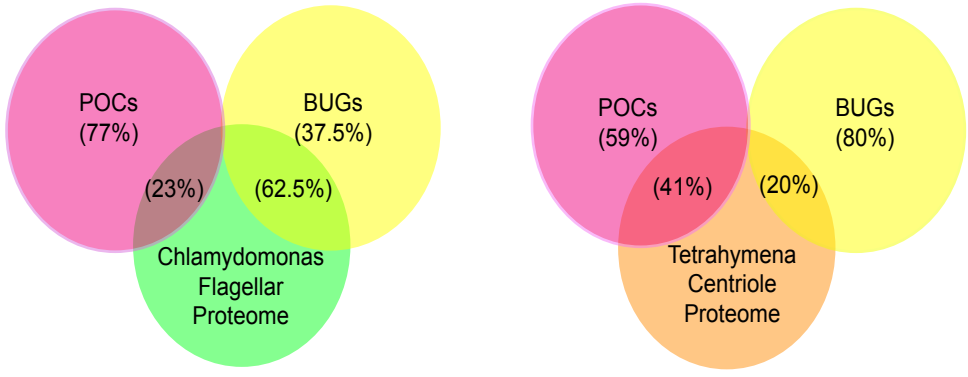

Figure 2. POC1 is a conserved centriole protein that is recruited to the centriole through the N-terminal WD40 repeat domain. (A) Phylogenetic unrooted tree showing that POC1 is conserved from *Chlamydomonas* to humans. The POC1 protein underwent a gene duplication in vertebrates as shown. (B) Coiled-coil prediction analysis of POC1 illustrates that there is a coiled-coil domain at the C-terminus of the protein (COILS server; ch.EMBnet.org). (C) The POC1-domain is a conserved sequence at the C-terminus of all conserved POC1 sequences. The POC1 consensus sequence is indicated at the bottom of the sequence alignment. (D) POC1 domain architecture. The WD40 repeat domain contains seven repeats (labeled wd1-wd7) and is sufficient for localization to centrioles in human cells (depicted by red star). Numbers represent amino acid positions. Coiled-coil domain indicated by purple box. (E) POC1-WD40-GFP (green, middle panel) colocalizes with gamma-tubulin (red, left panel) in transiently transfected Hela cells. Right panel is a merged image with nuclear stain (blue, DAPI). Scale bar, 5μm.

Figure 2. POC1 is a conserved centriole protein

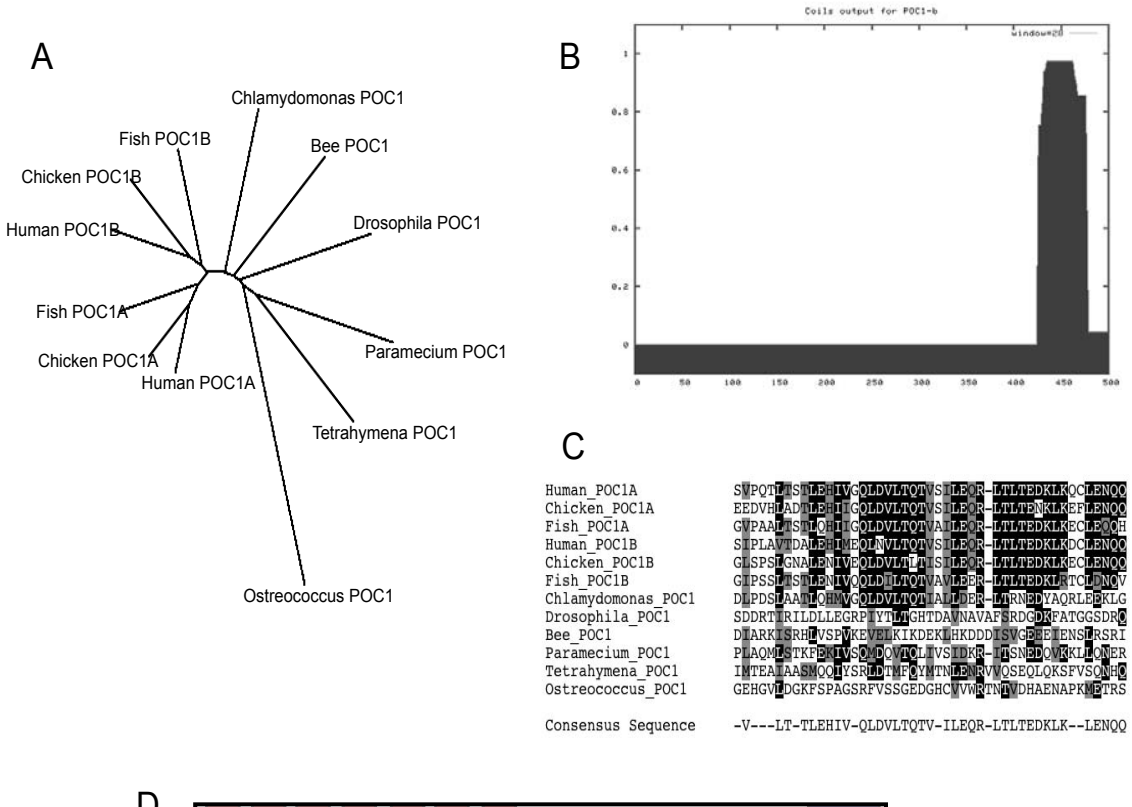

Figure 3. *Chlamydomonas* POC1 immunofluorescence. (A) Illustration depicting the position and sequence of the POC1 peptide that was used to create the *Chlamydomonas* POC1 antibody. Numbers represent amino acid positions. (B) POC1 (red) localizes to the basal bodies of wild-type *Chlamydomonas* cells, as shown by colocalization with acetylated-tubulin antibody (green, top panel). Merged image is with nuclear stain (blue, DAPI). Middle panel indicates that POC1 (red) colocalizes with centrin (green) antibody only at the basal body. POC1 is absent from the centrin-based nuclear-attachment fibers. Bottom panel demonstrates that POC1 (red) costains with acetylated-tubulin (green) to mark two centrioles at each pole of the mitotic spindle. Merged image is stained with a nuclear stain (blue, DAPI). (C) POC1 localizes to centrioles in a distinct pattern. Illustration of *Chlamydomonas* basal bodies (red), flagella (green), and inner-rootlet microtubules (smaller green lines). The boxed region represents the area of high magnification in the next panels. Merged images demonstrate that POC1 (red) forms a cylindrical structure at the base of the flagella (green). Scale bar, 1μm.

Figure 3. Chlamydomonas POC1 Immunofluorescence

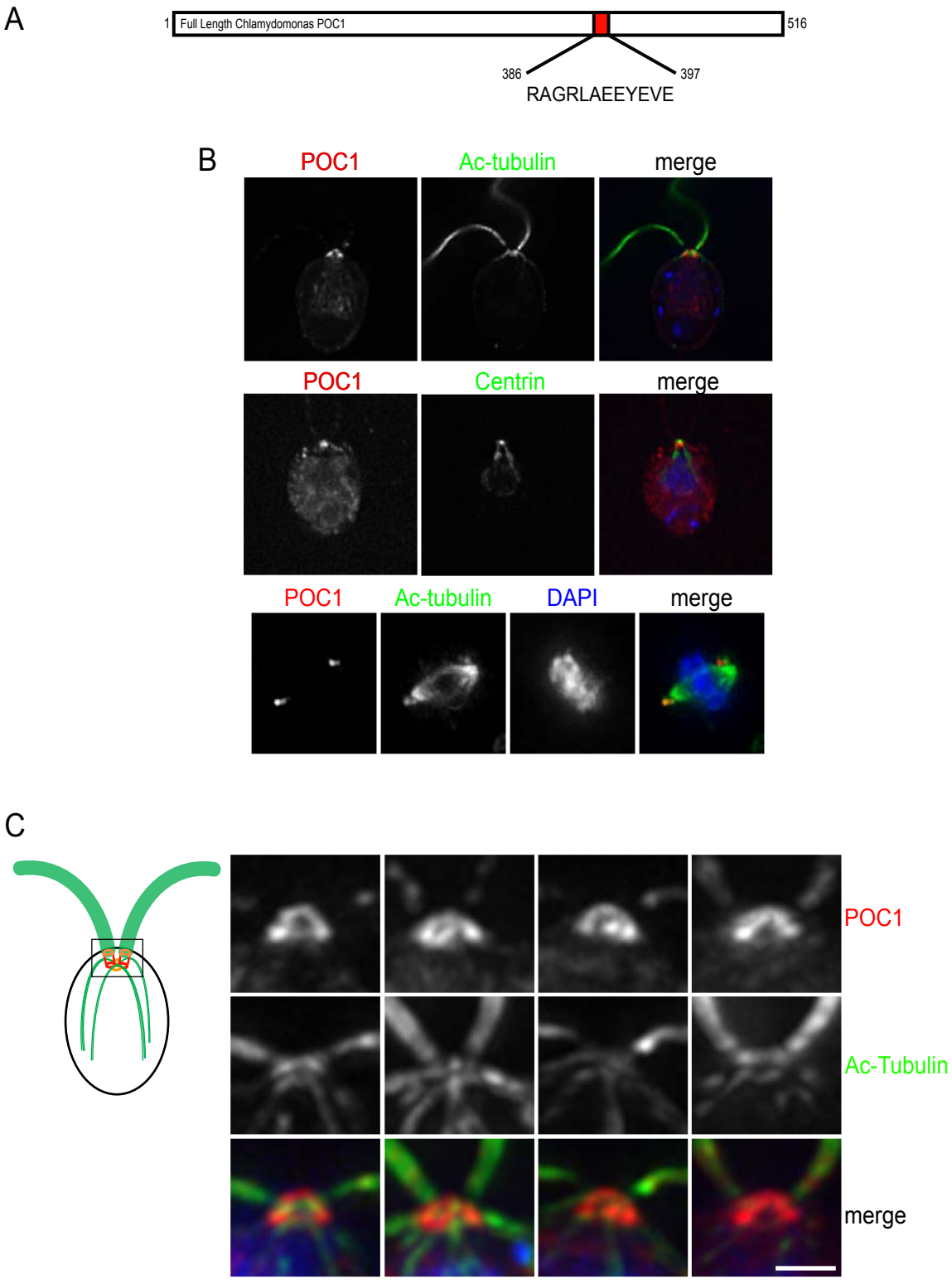

Figure 4. POC1 localizes to newly duplicating centrioles in both *Chlamydomonas* and in human cells. (A) *Chlamydomonas* POC1 (red) localizes to both mature basal bodies and proBBs, indicated by the appearance of four dots at the base of the flagella (green) as shown in the higher magnification images. Scale bar, 1μm. (B) ImmunoEM of *Chlamydomonas* basal body sections. Cells were labeled with anti-POC1 antibody and gold-conjugated secondary antibodies. Localization of POC1 to probasal bodies is highlighted with arrowheads. B1-B3 are serial sections, as are B4-5. Scale bar, 250nm. (C) Immunofluorescence of stably expressing human POC1-GFP (green). Hela cells with centrosomes stained with Cetn2 (red). Merged images show two mature centrioles (top panels) and two mature centrioles along with their newly duplicating daughter centrioles from their proximal ends (bottom panels). Overlay images demonstrate proximal and distal ends of the mature centrioles along with newly duplicating daughter centrioles. Scale bar, 1μm. (D) Fluorescence intensity quantification of boxed images in (C). Large peak represents mature basal body; smaller peak represents newly duplicating daughter centriole. Note the smaller peak in the Cetn2 graph is shifted farther (more distal) from the mature centriole than the smaller peak in the POC1 graph.

Figure 4. POC1 Localizes to Newly Duplicating Centrioles

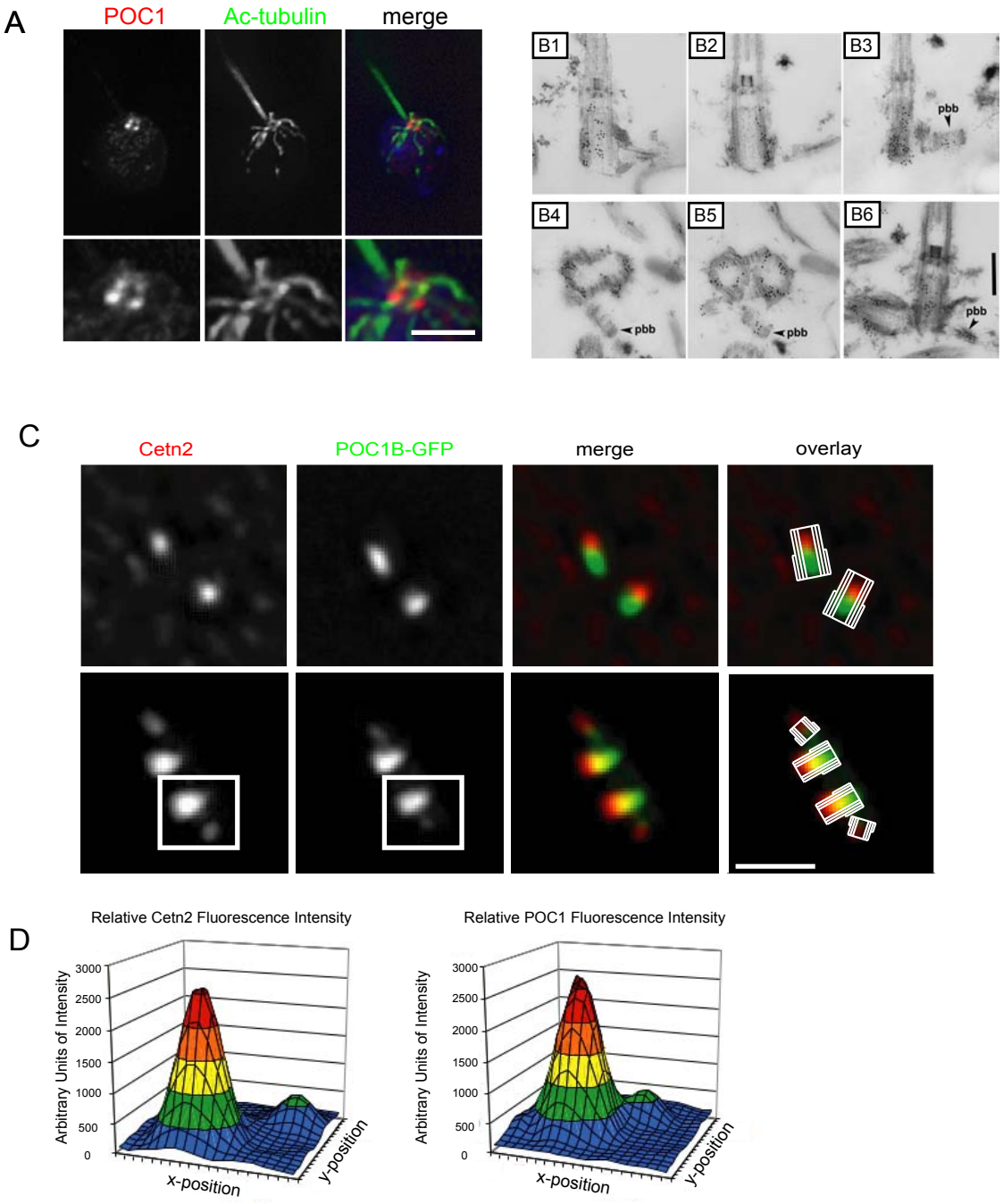

Figure 5. POC1 localization in *Chlamydomonas* basal body mutants. (A) Wildtype *Chlamydomonas* cells stained with POC1 (red) and acetylated-tubulin (green). Note staining at the base of the flagella (green). (B) uni3 cells stained with POC1 (red) and acetylated-tubulin (green) demonstrating that POC1 stains doublet microtubules. (C) bld2 cells stained with POC1 (red) and acetylated-tubulin (green) indicating that POC1 stains singlet microtubules. (D) bld10 cells stained with POC1 (red) and acetylated-tubulin (green) showing that POC1 always colocalizes with acetylated-tubulin positive centrioles. Merged images were stained with a nuclear stain (blue, DAPI). (E) Histogram of POC1 staining intensity indicating reduced POC1 recruitment levels in mutant basal bodies.

Figure 5. POC1 localization in Chlamydomonas basal body mutants

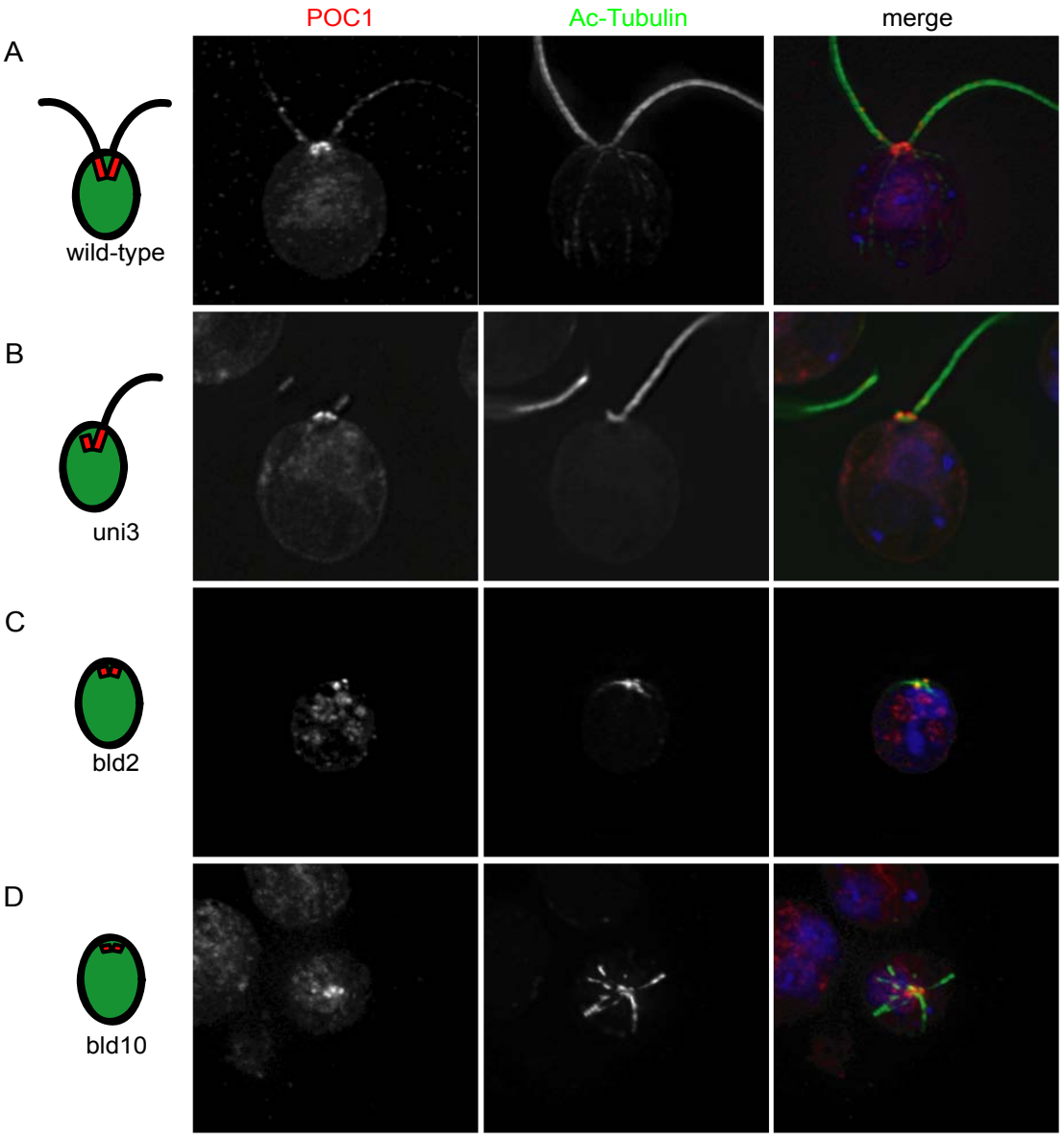

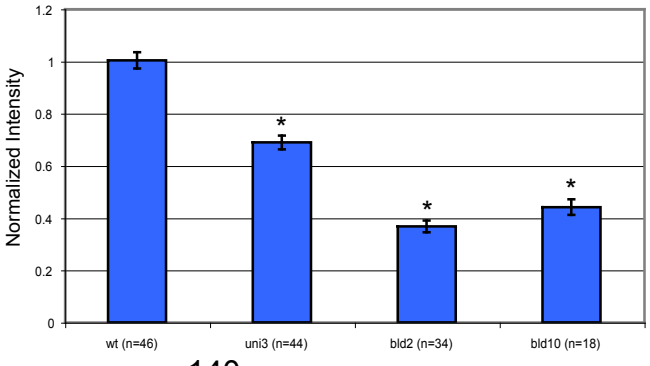

Figure 6. ImmunoEM of *Chlamydomonas* POC1 reveals localization to triplet microtubules and sites of fiber attachment. (A1-A4) ImmunoEM of basal body serial sections showing POC1 localization throughout the length of the triplet microtubules. (B1-B3) Serial sections showing POC1 localization to triplet microtubules and rootlet microtubules (root mt's). (C) POC1 localizes to doublet microtubules of axonemes but is absent from central pair microtubules. (D,E) POC1 localizes to rootlet microtubules that are nearby and/or attached to centrioles. (F,G,H) Sections demonstrating that POC1 localizes to proBBs and occasionally at the cartwheel (carwheel indicated by black box). (I1-I5) Serial sections through a longitudinally sectioned basal body. POC1 localizes to sites of rootlet microtubule attachment and sites where proximal and distal connecting fibers attach to the basal body (root mt's, rootlet microtubules; pcf proximal connecting fiber, arrow shows a high density of POC1 at rootlet microtubule connection and at proximal connecting fiber). All sections were labeled with anti-POC1 antibody and gold-conjugated secondary antibodies. Scale bar, 250nm.

Figure 6. ImmunoEM with of Chlamydomonas POC1

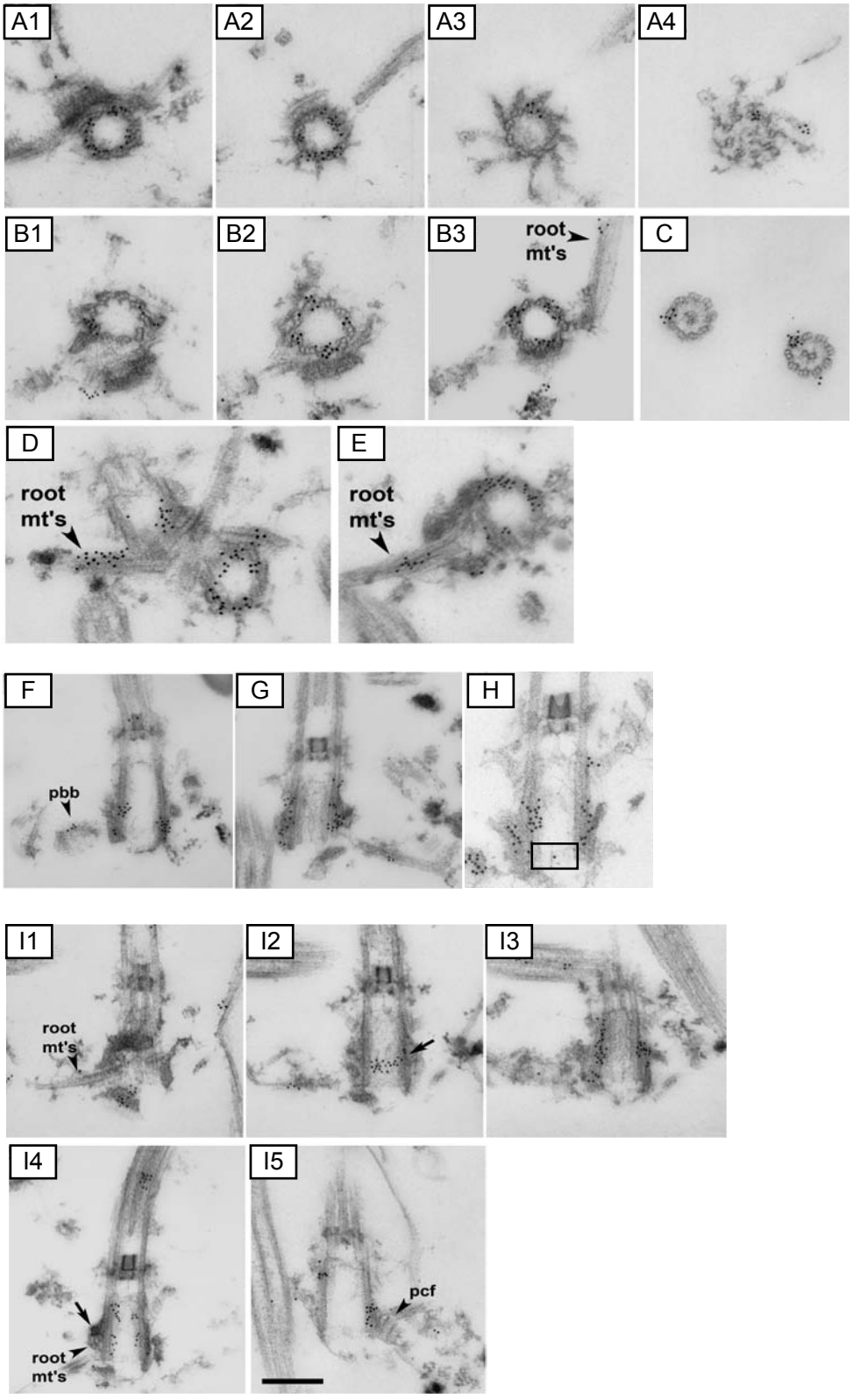

Figure 7. *Chlamydomonas* POC1 associates with doublet microtubules in the axoneme and is not a component of the IFT machinery. (A) Flagellar splay assay demonstrates that POC1 (red) localizes specifically to the doublet microtubules (arrowhead) and is absent from central pair microtubules (arrow). Note basal body staining at the base of the splayed flagella with both POC1 and acetylated-tubulin antibodies. Scale bar, 5μm. (B) POC1 (red) localizes to flagella in *fla10*^{ts} *Chlamydomonas* cells at both 21°C and 34°C, unlike the IFT protein, IFT172.1, which is absent at 34°C.

Figure 7. Chlamydomonas POC1 Associates with Doublet Microtubules in the Axoneme and is not a component of the IFT machinery

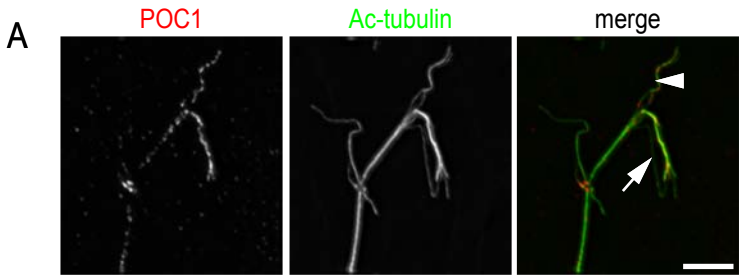

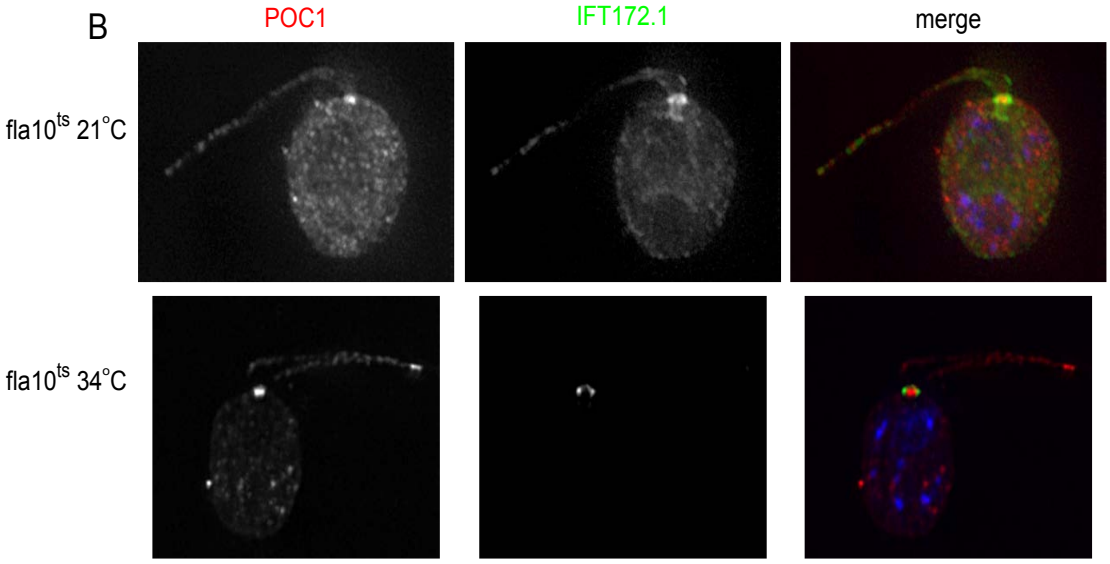

Figure 8. POC1 depletion leads to a reduction in centriole overduplication. (A) Western blot of POC1-GFP in RNAi-treated U2OS cell lysate. Ponceau stain was used as a loading control (data not shown). Quantification of Western blot normalized to 100%, indicated approximately 75% and 60% knockdown of POC1B-GFP by POC1B siRNA and POC1A/B siRNA respectively. (B) S-phase arrested U2OS cells have overduplicated centrioles, but when POC1 is depleted this overduplication is suppressed (green, POC1B; red, Cetn2). (C)The percent of cells with overduplicated centrioles is reduced in the presence of POC1 siRNA, while the number of cells with wildtype number of two centrioles increases. Scale bar, 5μm

Figure 8. POC1 Depletion leads to a Reduction in Centriole Overduplication

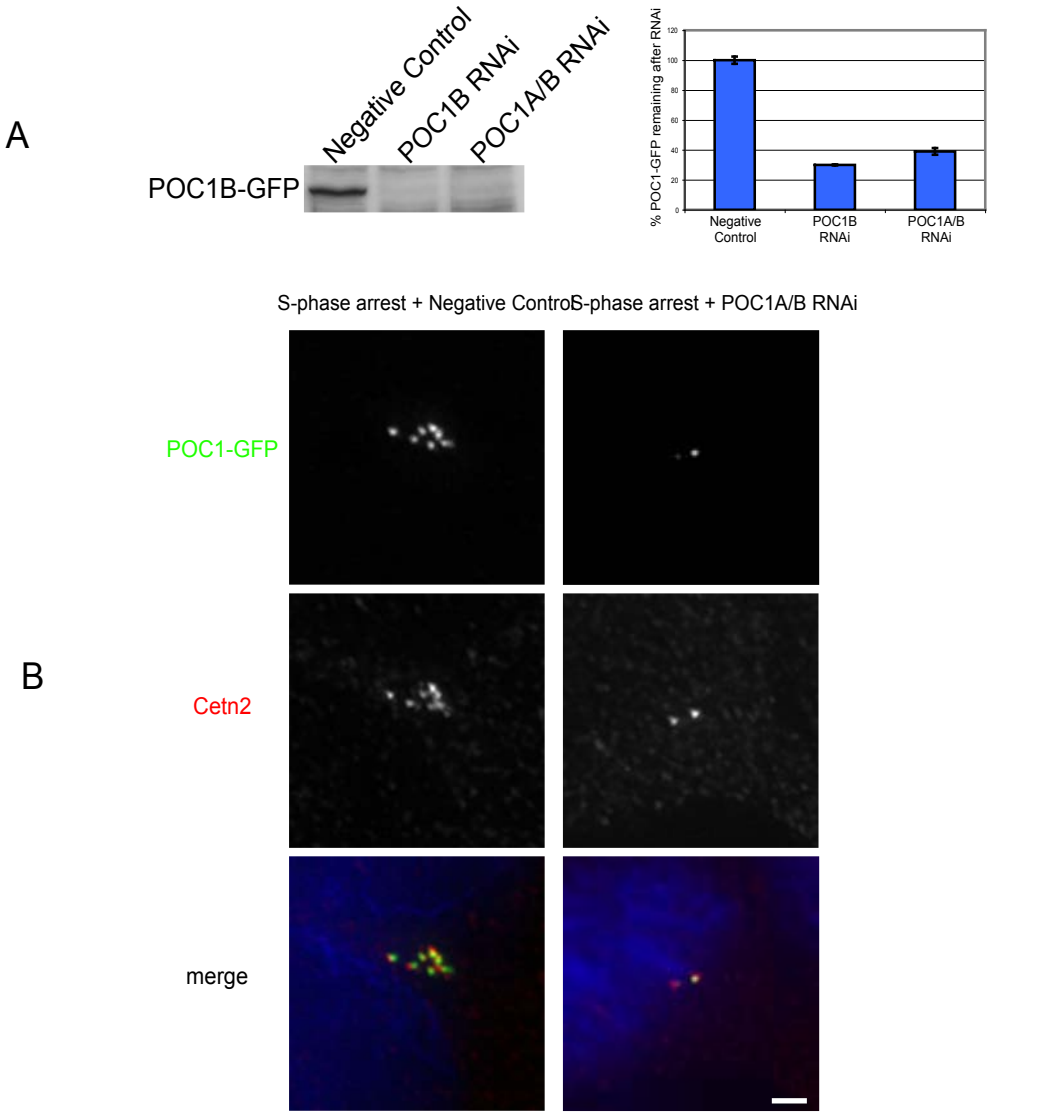

Figure 9. POC1 overexpression in human cells leads to elongated centriole-like structures, which is abolished when POC1 is knocked down by POC1 siRNA. (A) POC1B-GFP-expressing U2OS cells grown and treated with 3.2mg/ml aphidicolin show a large percent of cells with elongated centriole-like structures which are POC1B-GFP positive and stain with Cetn2 (red). This overexpression phenotype is abolished in the presence of POC1 siRNA. (B) The percent of cells with elongated centriole-like structures is dramatically reduced in the presence POC1 siRNA (left graph). The length of the elongated centriole-like structures was quantified and is also dramatically reduced in the presence of POC1 siRNA (right graph).

Figure 9. POC1 Overexpression leads to elongated centriole-like structures

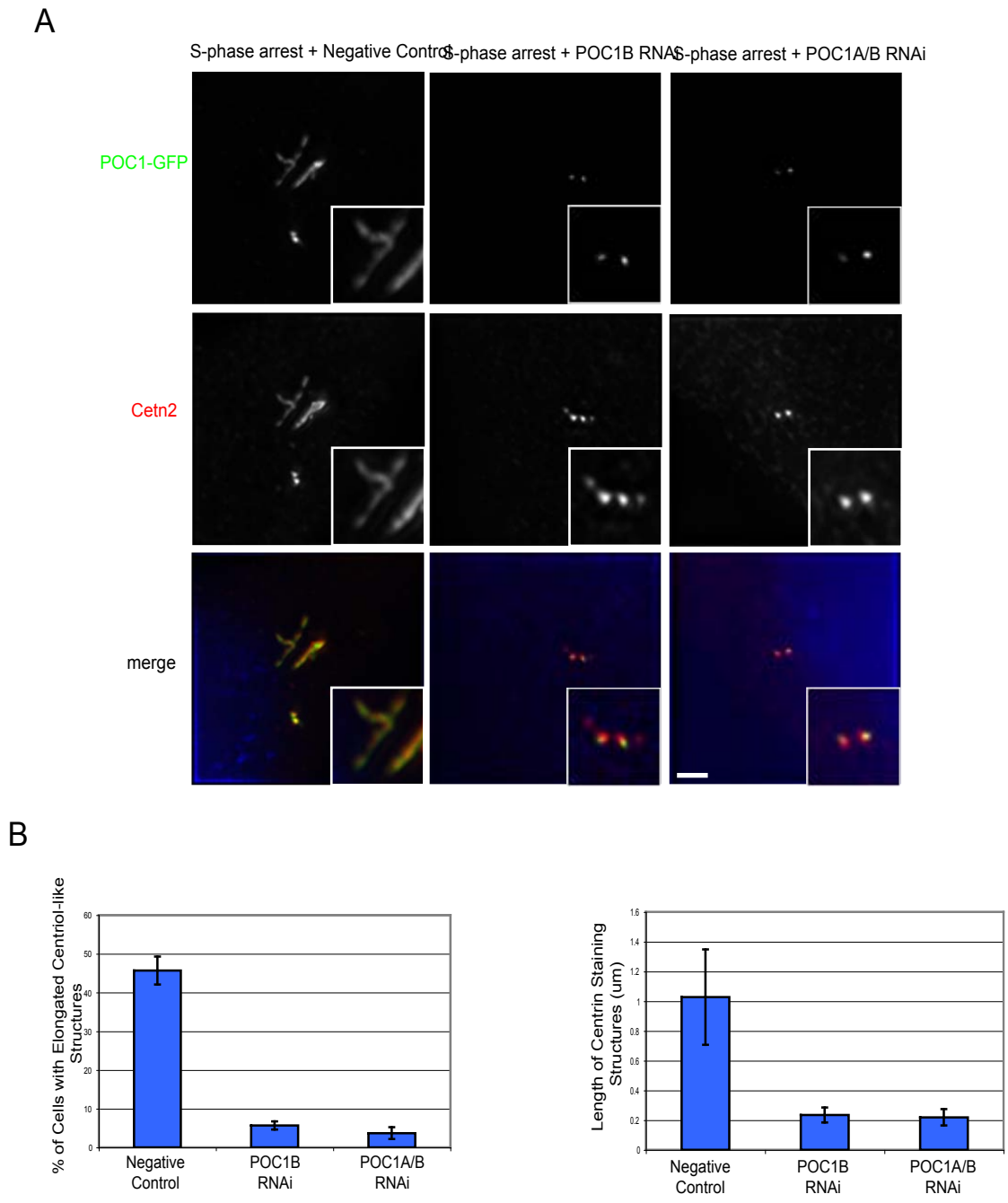

Supplemental Figures/Tables

Supplemental Table 1. Expansion of the cross-validated *Chlamydomonas* centriole proteome. Table of all POC and BUG proteins including version three gene identification numbers which are as specified in v3.0 of the *Chlamydomonas* genome sequence, available at the Joint Genomes Institute web site: http://genome.jgi-psf.org/chlre2/chlre2.home. Table also indicates protein name, human Refseq ID numbers, localizations of the protein to other proteomes of interest, GFP-localization to centrioles in human cells, and any associated human diseases. Bold **X**s indicate that localization was done by another group, ♦ symbol indicates that this gene was found only in the version two *Chlamydomonas* genome and has not yet been annotated in the version three genome.

Supplemental Table 1. Expanded list of cross-validated POCs and BUGs in the *Chlamydomonas* centriole proteome

POCs	v3 Chlamy ID	Protein Name	Human Refseq ID	Blastp e-value	Photoreceptor Complex Proteome	Flagellar Proteome	Tetrahymena Centriole Proteome	Tetrahymena Cilia Proteome	Trypanosoma Flagellar Proteome	GFP Localized	Associated Human Disease
POC1A	112249	POC1/WDR51A	NP_056241.2	2.E-97	X		X		X	X	
POC1B	112249	POC1/WDR51B	NP_758440.1	3.E-93			X		X	X	In JBTS5 locus
POC2	144289	POC2	NP_653213.4	3.E-157						X	
POC3	9715	CEP290/NPHP6	NP_079390.3	5.E-89	X					X	Meckel/Joubert
POC4	9658	POC4/SFI1-like	NP_001007468.1	1.E-08						X	
POC5	9798	POC5	NP_689621.2	2.E-02	X					X	
POC6	104097	POC6	NP_004356.2	4.E-26	X		X		X	X	
POC7	132861	UNC119	NP_005139.1	4.E-41	X					X	Cone-rod dystrophy
POC8	187228	POC8/14-3-3	NP_006752.1	1.E-81	X	X	X			X	
POC9	177558	Rib72-like	NP_060570.2	4.E-65			X		X	X	Juvenile myoclopic epilepsy
POC10	32880	NPH4	NP_055917.1	4.E-81	X					X	Renal-retinal syndrome
POC11	13542	POC11	NP_115734.1	6.E-34						X	
POC12	20204	POC12/MKS1	NP_060247.2	7.E-32	X					X	Meckel syndrome
POC13	153900•	FAP186	none			X					
POC14	185967	POC14/14-3-3	NP-006752.1	2.E-104	X	X	X			X	
POC15	185306	EF-hand protein	none				X				
POC16	18900	POC16	NP_694971.2	5.E-30			X		X		
POC17	141462	POC17	NP_009204 B	1.E-85	X		X	X		X	
POC18	6466	POC18	NP_663622.1	7.E-79							
POC19A	169402	POC19A•	NP_115556.2	1.E-03		X				X	
POC19B	169402	POC19B•	NP_689658.1	2.E-02		X				X	
POC20	191903	POC20/UBA1	NP_003325.2	0.E+00	X	X				X	
POC21	182582	POC21/AGG3	none			X					

BUGs	v3 Chlamy ID	Chlamy Name	Human Refseq ID	Blastp e-value	Photoreceptor Complex Proteome	Flagellar Proteome	Tetrahymena Centriole Proteome	Tetrahymena Cilia Proteome	Trypanosoma Flagellar Proteome	GFP Localized	Associated Human Disease
TUA1	128523	TUA1, TUA2	NP_006000.2	0.E+00	X	X	X	X		**X**	
TUB1	129876	TUB1, TUB2	NP_006079.1	0.E+00	X	X	X	X	X	**X**	
tektin	24358	Tektin	NP_444515.1	1.E-14		X				X	
DIP13	131284	DIP13	NP_003722.1	3.E-22		X			X	X	Sjogrens antigen
Rib43a	77703	Rib43a	NP_056468.1	1.E-24		X			X	X	
Rib72	126286	Rib72	NP_060570.2	4.E-96		X	X	X	X	X	
Hsp90a	138117	Hsp90	NP_005339.2	0.E+00	X	X	X			X	
CCT3	127904	CCT3	NP_005989.2	0.E+00	X					X	
BUG1	181854	BUG1	none			X					
BUG2	29687	BUG2	none			X					
BUG3	156094	BUG3	none			X	X	X	X		
BUG4	191360	BUG4	none			X					
BUG5	180221	BUG5/NDPK	NP_932076.1	1.E-84	X	X			X	X	
BUG6	155819•	BUG6	none								
BUG7	170453	DNJ1	NP_001530.1	6.E-86	X					X	
BUG8	190617	BUG8	none			X					
BUG9	194240	BUG9	none			X					
BUG10	187818	BUG10	none			X					
BUG11	31640	OFD1	NP_003602.1	3.E-14	X					X	Oral-facial-digital syndrome
BUG12	182707	BUG12	none			X					
BUG13	181900	BUG13	none			X					
BUG14	128114	BUG14	NP_659491.3	9.E-163		X			X	X	
BUG15	34449	BUG15	none			X			X		
BUG16	190291	BUG16	none			X					
BUG17	146275	BUG17	none			X			X		
BUG18	136677	BUG18	none				X		X		
BUG19	32222	BUG19	none			X					
BUG20	193134	BUG20	none			X					
BUG21	97201	PACRG	NP_689623.2	6.E-69		X	X	X	X	X	Parkinsons
BUG22	189631	BUG22	NP_037374.1	5.E-100	X	X			X	X	
BUG23	8784	BUG23	NP_055490.3	8.E-13	X						
BUG24	176257	BUG24	none								
BUG25	19751	BUG25	NP_001106674.1	1.E-31							
BUG26	191828	BUG26/ASA8	none								
BUG27	142067	BUG27	none								
BUG28	13859	RPGR1	NP_065099	1.E-38	X						Retinitis pigmentosa
BUG29	19372	AHI1/Jouberin	NP_060121.3	3.E-12	X						Jouberin syndrome
BUG30	138565	Ro/SSA	NP_004591	1.E-110						X	Sjogrens antigen
BUG31	24810	BUG31/NESG1	NP_036469	2.E-15			X	X	X		
BUG32	36430	BUG32/Mns1	NP_060835	3.E-35					X	X	

X Localized by Others

•v2 Chlamy ID, removed by new annotation

Liu *et al* ., 2007- Photoreceptor Complex Protoeome

Pazour *et al*., 2005- *Chlamydomonas* Flagellar Proteome

Kilburn *et al*., 2007- Tetrahymena Centriole Proteome

Smith *et al*., 2005- Tetrahymena Cilia Proteome

Broadhead *et al*., 2006- Trypanosome Flagellar Proteome

Supplemental Figure 1. POC C-terminal GFP fusion protein localizations in Hela, U2OS or RPE-1 cells. Immunofluorescence of human cells expressing GFP fusion proteins: GFP alone, POC1A, POC2, POC3, POC4, POC6, POC7, POC8, POC9, POC11, POC17, POC20. In all cases, the GFP fusion proteins (green) co-localizes with gamma-tubulin (red, except POC8). All cells are U2OS except for the panels depicting POC1A and POC8, which were imaged in Hela and RPE-1 cells respectively. Note the cilia in the RPE-1 cell staining of POC8 and the colocalization of the GFP-signal at the base of the acetylated-tubulin stain (red). POC8 and POC14 both had the same mutual best match human homolog as did POC9 and POC6, thus only one picture is represented for both of these sets of proteins. Scale bar, 10μm.

Supplemental Figure 1. POC protein C-terminal GFP fusion protein localizations in Hela, U2OS, or RPE-1 cells

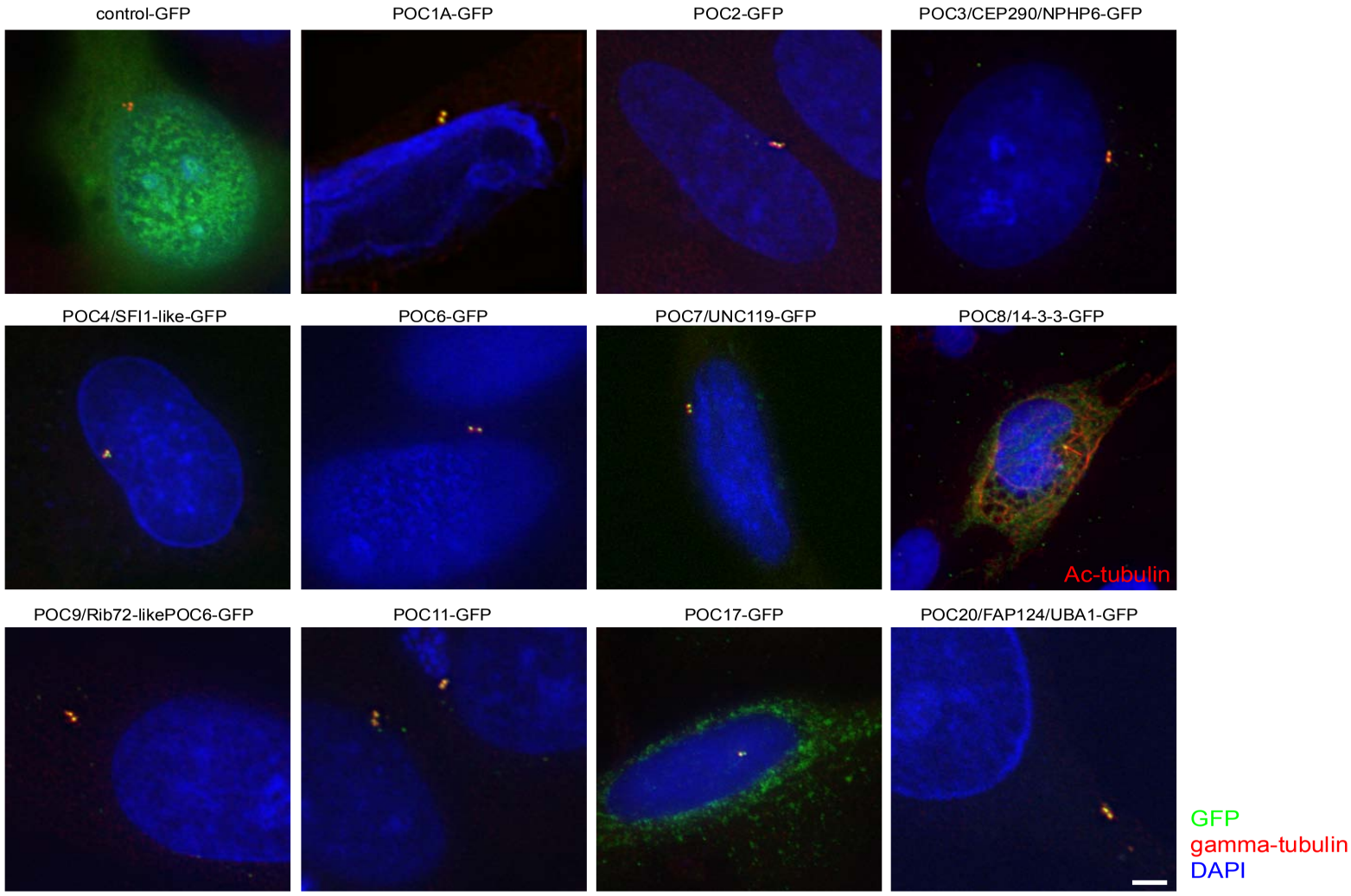

Supplemental Figure 2. BUG protein C-terminal GFP fusion protein localizations in U2OS cells. Immunofluorescence of human cells expressing GFP fusion proteins: DIP13, Rib43a, Hsp90, CCT3, BUG5, BUG7, BUG11, BUG22, BUG30, BUG32. In all cases, the GFP fusion proteins (green) colocalizes with gamma-tubulin (red). Scale bar, 10μm.

Supplemental Figure 2. BUG protein C-terminal GFP fusion protein localizations in U2OS cells

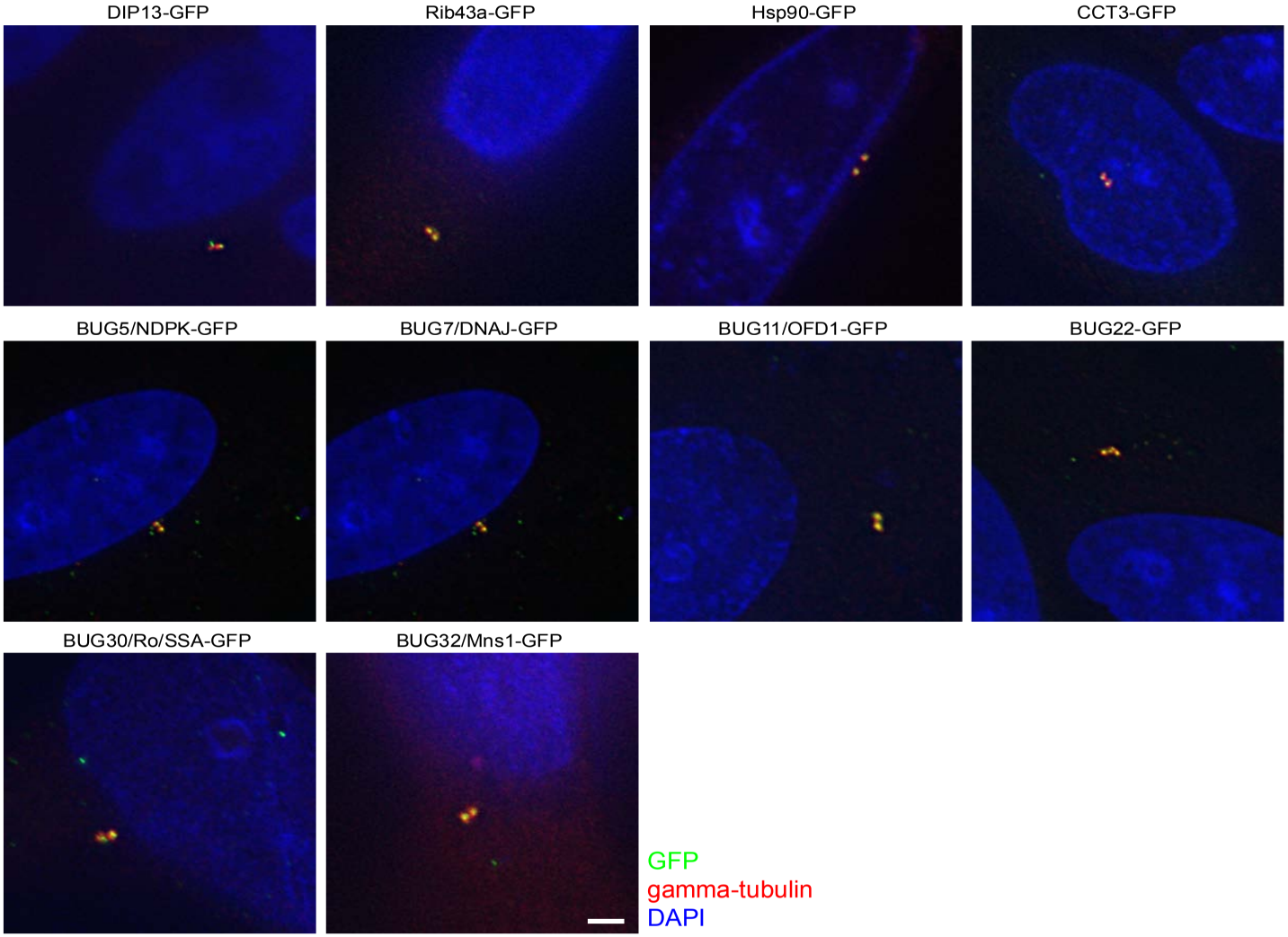

Supplemental Figure 3. *Chlamydomonas* POC1 antibody specificity. *Chlamydomonas* POC1 peptide antibody recognizes one clear band in purified basal bodies. The molecular weight of this band is comparable to the predicted molecular weight of POC1, which is 54.4kD. No other bands were visible with this antibody. In addition to biochemical specificity as judged by Western blotting, we also analyzed immunochemical staining specificity using peptide blocking controls. *Chlamydomonas* cells were stained with POC1 antibody (red) that was previously incubated with either a control peptide that is not within the POC1 protein sequence or with the peptide that was made to produce the POC1 antibody. Merged images were stained with a nuclear stain (blue, DAPI). ImmunoEM images show a pair of basal bodies with POC1 localizing to the triplet microtubule barrel. The images indicate that POC1 antibody staining is completely abolished when the antibody was preincubated with the POC1 peptide, while the control peptide had no effect on staining, thus supporting specificity of staining. Scale bar, 250nm.

Supplemental Figure 3. Chlamydomonas POC1 Antibody Specificity

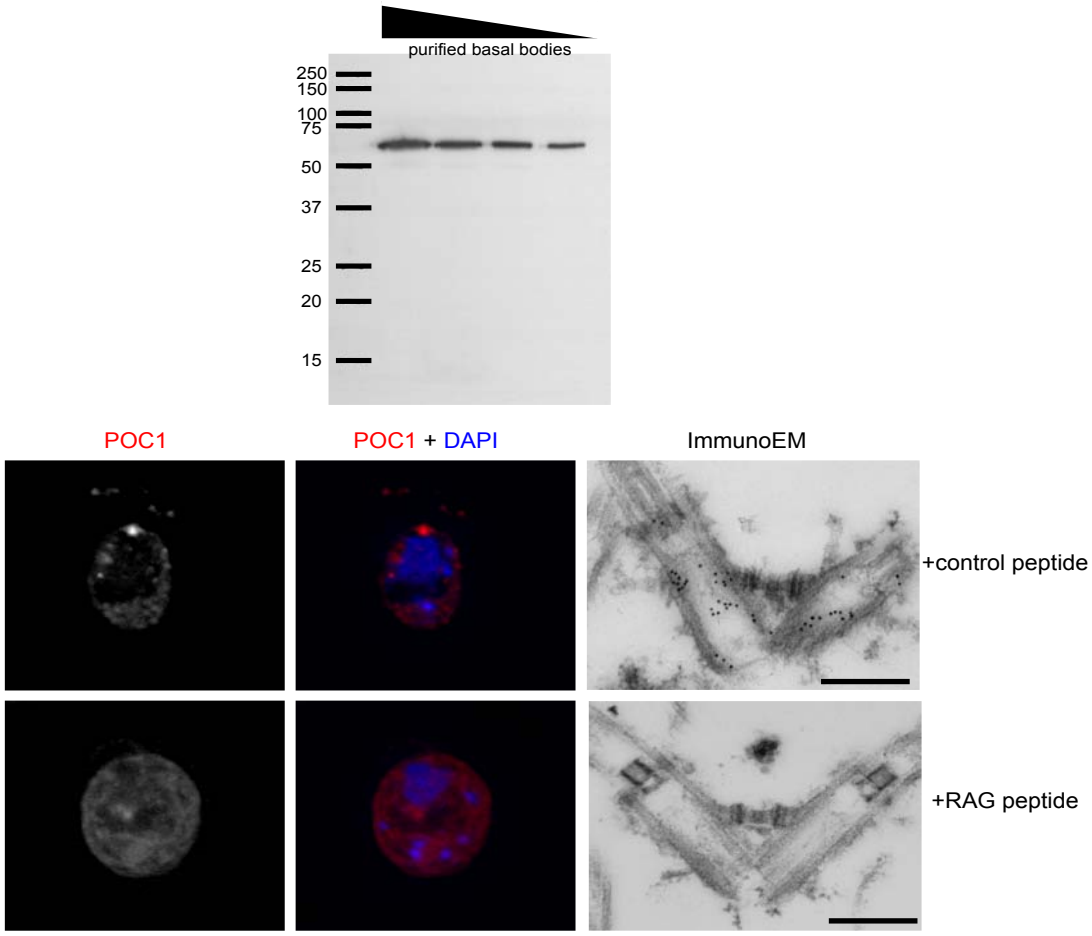

Supplemental Figure 4. Quantification of POC1 localization within centrioles from *Chlamydomonas*. (A) POC1 is highly concentrated in the basal bodies of *Chlamydomonas* but is still present in flagellar axonemes but at a reduced amount. (B) Quantification of gold-conjugated particles representing POC1 localization. Particles were quantified as being either in the distal or proximal half and either in the inner or outer walls of the triplet microtubules. The percent of all gold particles that localized to the lumen, sites of attachment, or the cartwheel structure were also quantified.

Supplemental Figure 4. Quantification of POC1 localization within centrioles and flagellar axonemes

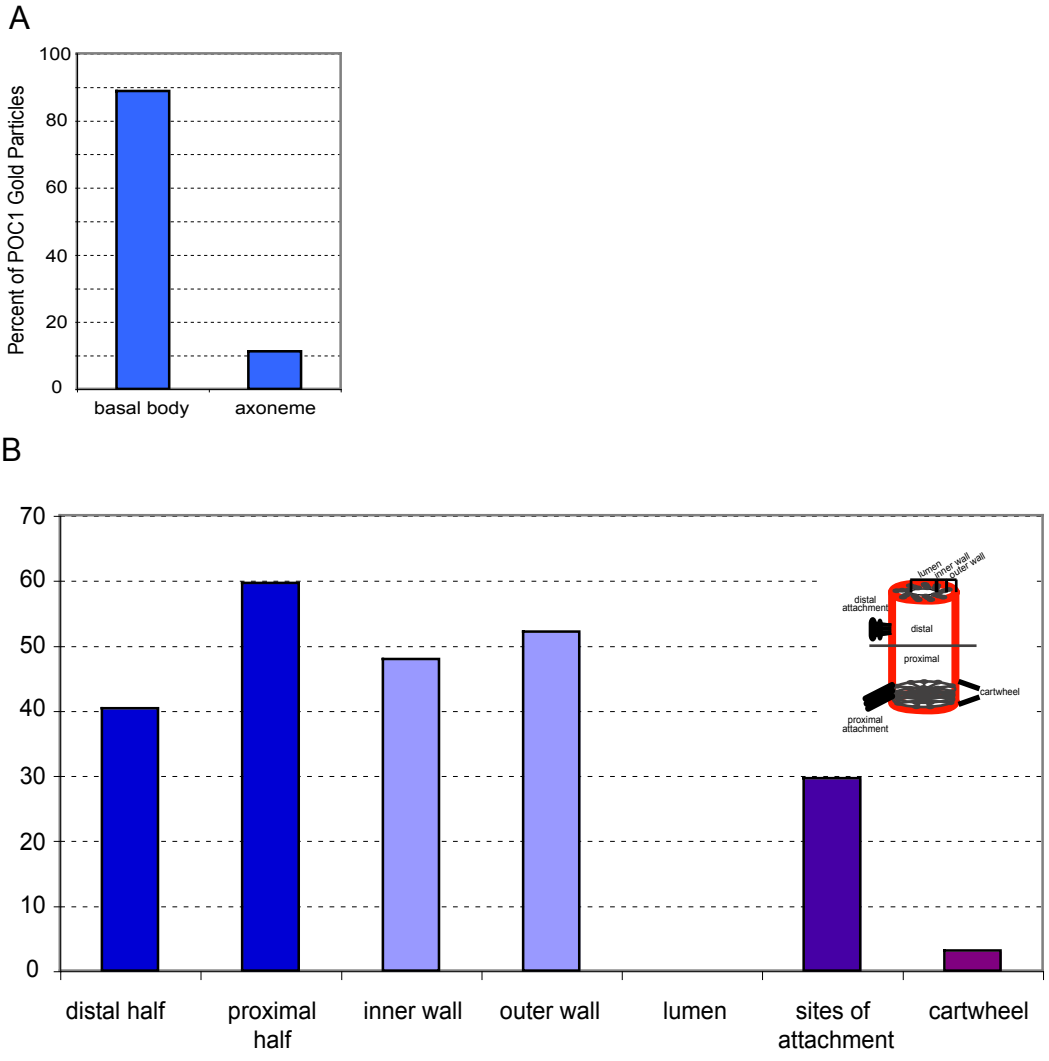

Supplemental Figure 5. POC1 is present at the basal bodies of human primary cilia. Transient transfection of POC1B-GFP into human RPE-1 cells demonstrate that POC1 localizes specifically to basal bodies (POC1B-GFP, green) and does not extend in the ciliary axoneme (actylated-tubulin, red).

Supplemental Figure 5. POC1 localizes to Basal Bodies but not to Primary Cilia

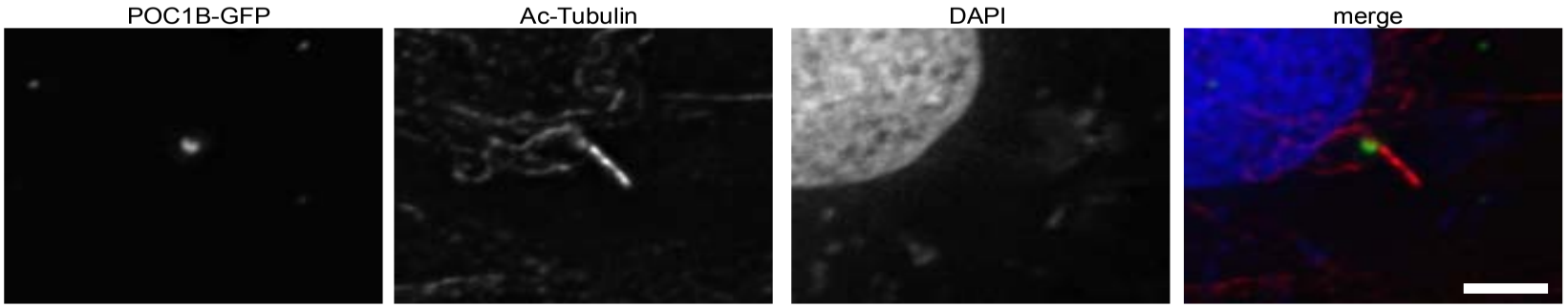

Supplemental Figure 6. Elongated centriole-like structures stain with both centriole and pericentriolar material markers. A stably expressing U2OS POC1B-GFP line shows a large percent of cells with elongated centriole-like structures after S-phase arrest. These structures stain with Centrin 2, acetylated-tubulin, polyglutamylated-tubulin, and gamma-tubulin. ODF2, which specifically stains the distal appendages of the mother centriole, fails to colocalize with the elongated centriole-like structures. Scale bar, 5mm.

Supplemental Figure 6. Elongated centriole-like structures stain with both centriole and pericentriolar material markers

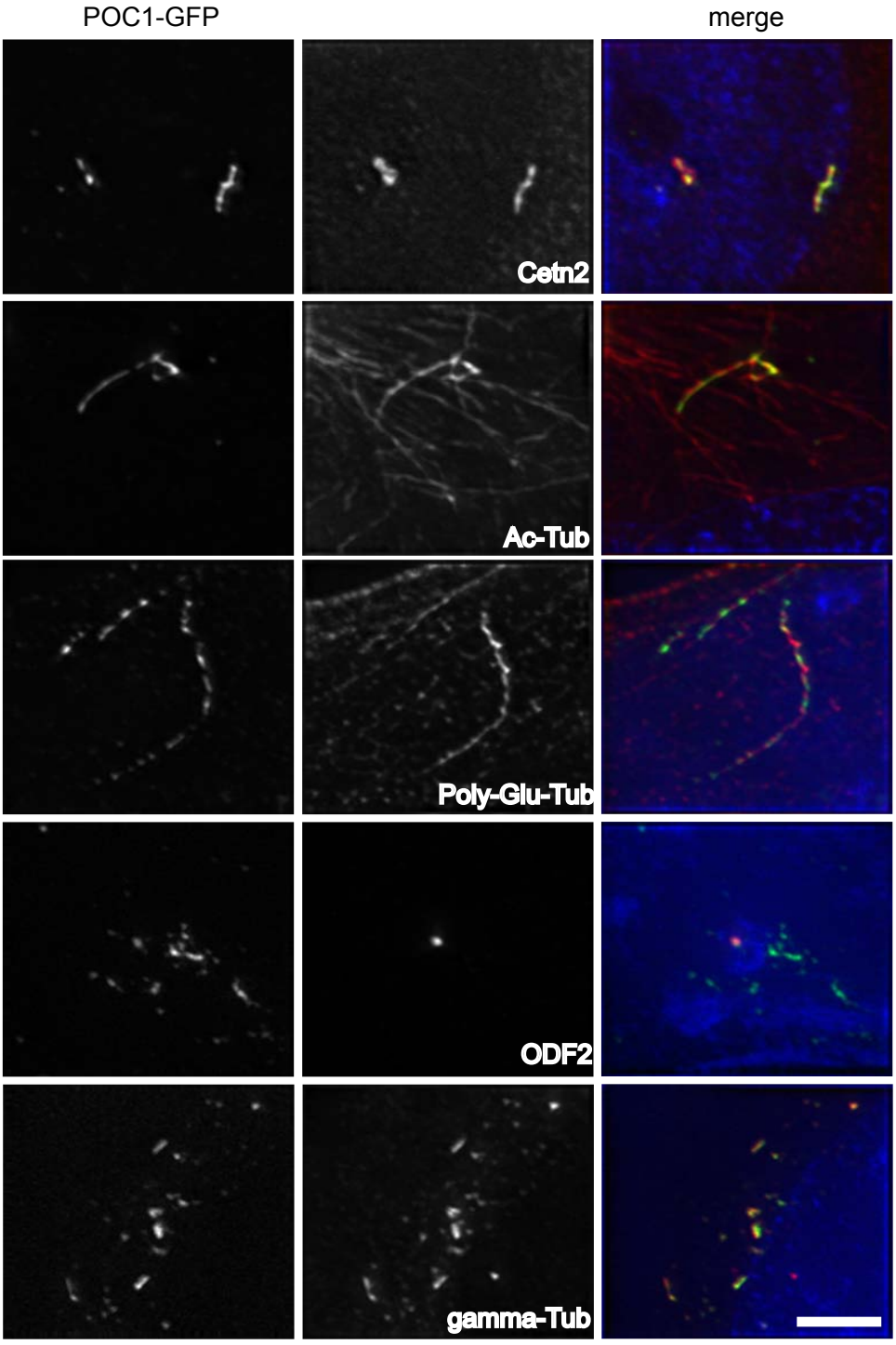

Chapter 5

Influence of Centriole Number on Spindle Morphology and Cell Division in *Chlamydomonas reinhardtii*

Abstract

The role of centrioles in cell division is a long standing question in cell biology that remains controversial. It is well established that centrioles are not required for mitosis, but does this mean centriole play no role when they are present? Here we analyze mitosis, cytokinesis, and cell size in mutants of Chlamydomonas with defective centriole segregation, such that cells contain variable numbers of centrioles. By correlating cell division defects with centriole number on a cell by cell basis, we provide evidence that centrioles play a role in biasing spindle morphology towards a bipolar arrangement, in promoting symmetry of tubulin content between the two half-spindles, and in promoting completion of cytokinesis. Absence of centrioles was found to be generally much more deleterious than the presence of supernumerary centrioles, despite the apparent absence of a centriole-clustering process in this organism. We also find that cells lacking centrioles are substantially larger than cells that contain centrioles, suggesting a link between centrioles and cell size control.

Introduction

Abnormal numbers of centrioles and centrosomes are a hallmark of cancer cell biology. Virtually all types of solid tumors contain cells with abnormal centriole numbers (Pihan et al., 1998; Lingle and Salisbury, 1999; Nigg, 2006; Sankaran and Parvin, 2006). In 1914, Theodor Boveri proposed that abnormal centrosome numbers could play a causal role in the development of cancer by contributing to chromosome instability (Boveri, 1929; Kramer et al., 2002). The idea behind this proposal is that supernumerary centrioles would lead to formation of multipolar spindles, resulting in massive chromosome mis-segregation during mitosis. But this model contains a potential paradox: massive mitotic failure would result in a few dead cells, rather than a proliferating tumor. The question thus arises of whether variation in centriole number would actually have a significant impact on spindle assembly.

The effect of centriole numerical abnormalities on mitosis hinges on the robustness of the spindle assembly process. It has been known for some time that bipolar spindles can form without centrioles or centrosomes (Heald, 1996; de Saint Phalle and Sullivan, 1998; Compton, 2000; Basto et al., 2006) suggesting a high degree of robustness in spindle self-organization in the absence of centrioles, but it is less clear how robust the assembly process would be in the face of increased centriole number. Special clustering mechanisms have been invoked by which extra centrioles might cluster together to form a single effective spindle pole (Brinkley, 2001; Quintyne et al., 2005). These clustering processes

have been observed in some tumor cell lines, but in general we do not have a clear view of how centriole number might affect spindle formation. It would seem that the normal number of two centrioles per cell is advantageous, since cells have mechanisms to prevent re-duplication (Wong and Stearns, 2003; Tsou and Stearns, 2006) as well as active error correction mechanisms to restore number following perturbation (Marshall, 2007). But since we do not yet clearly understand the role of centrioles in mitosis, it is hard to predict what effect abnormal centriole numbers will have on mitosis.

In contrast to the role of centrioles in ciliogenesis, the possible role of centrioles in cell division is much more controversial. Despite recent reports that adult flies can be generated in which most cells lack centrioles (Basto et al., 2006) a more detailed study of different developmental stages showed that centrioles are essential for early fly development, when the vast majority of cell division occurs in the fly life cycle (Rodrigues-Martins et al., 2008), suggesting that centrioles are required for cell division but not for viability in non-dividing differentiated adult cells. Centrioles appear to be necessary for formation and maintenance of centrosomes (Bobinnec et al., 1998). Because centrioles are embedded in the poles of the mitotic spindle, it has traditionally been assumed that they must play a role in mitosis. However, several experiments using laser ablation and other manipulations argue that cells can form bipolar spindles in the absence of centrioles (Khodjakov et al., 2000). Indeed it is well established that spindles are self-organizing structures (Heald et al., 1993; Burbank et al., 2007), suggesting that if centrioles contribute to spindle assembly at all, they would

most likely act to fine-tune the spindle structure or function, rather than be essential for it to form in the first place. A fine-tuning function for centrioles in mitosis would predict they may be dispensable for viability, as appears to be the case. Although in some cases ablation of centrioles leads to cell-cycle arrest, this is apparently due to an increase in stress-sensitivity (Uetake et al., 2007) rather than to a direct role for centrioles in driving cell division.

If centrioles contribute to mitosis primarily by acting as fidelity factors, we would expect alterations of centriole number or structure would have only subtle effects on mitosis, so that if only a handful of cells are experimentally manipulated and observed, few if any mitotic defects might be observed. This puts a fundamental limitation on using physical manipulation, such as laser ablation, to test centriole function, because such methods are inherently done one cell at a time, making it difficult to detect rare phenotypic alterations. An alternative approach would be to examine mitosis in mutant cell lines defective in centriole structure or number. The hypothesis that centrioles act to supplement the robustness of spindles, rather than to drive their formation, suggests such mutants might have very weak mitotic phenotypes. Indeed, many such mutants have been described, particularly in the unicellular green alga *Chlamydomonas reinhardtii* (reviewed by Dutcher, 2003; Marshall and Rosenbaum, 2000), and all are viable. One such mutant is *vfl2*, caused by a point mutation in the gene encoding the EF-hand protein centrin (Taillon et al., 1992), in which centriole number is randomized due to the fact that centrioles are detached from the spindle poles (Kuchka and Jarvik 1982; Koblentz et al., 2003). In this mutant, in

which the association between centrioles and the spindle is highly aberrant, chromosome loss rates were quantified and found to be increased roughly 100-fold over wild-type, but still occurring at a relatively low frequency (Zamora and Marshall, 2005). This result confirms that centriole function in mitosis, if any, must be rather subtle. Two other mutants with similar cell-to-cell variation in centriole number, *vfl1* and *vfl3*, have been described (Silflow et al., 2001; Adams et al., 1985) and both are apparently fully viable.

Centrioles have also been implicated in cytokinesis, either by signaling to the cytokinesis machinery itself (Gromley et a., 2003; Piel et al., 2001) or by coordinating the orientation of the spindle with the cleavage furrow (Costello 1961; Ehler et al., 1995; Hinchcliffe et al., 2001). As with mitosis, it is well established that cleavage can progress without centrioles (Schatten et a., 1985) and even without spindles at all (Hiramoto 1965), so if centrioles contribute to the process at all, they would only be expected to act in a regulatory manner. Defects in cytokinesis have been observed in some instances after centriole ablation (Khodjakov and Rieder, 2001) but the frequencies are low. Therefore, mutants with centriole abnormalities might be expected to show a statistical increase in cleavage defects even if most mutant cells undergo normal division.

Testing the effect of centriole number abnormality on mitosis or cytokinesis requires a way to generate cells with abnormal centriole numbers. Tumor cells, as well as cells with defects in cell cycle progression or cleavage, can have abnormal centriole numbers, but interpretation of centriole-specific effects on such cells is complicated by the myriad of other defects seen in such

cells, for example aneuploidy in tumor cells. In this report we analyzed mitotic spindle morphology and cytokinetic furrow formation in mutants of *Chlamydomonas reinhardtii* with specific defects in copy number distribution or in centriole ultrastructure. We employ mutants in genes encoding centriole-localized proteins to minimize side-effects. We use mutants that affect either centriole number or centriole structure, in order to mimic the two predominant types of centriole abnormalities in tumor cells (Nigg, 2006). By analyzing large numbers of mutant cells, we were able to detect a range of defects in all centriole mutant cells. We then correlated defects with centriole number on a cell by cell basis to distinguish centriole-related defects from centriole-independent side effects of the mutations. Our results indicate that centrioles exert a regulatory influence on both mitosis and cytokinesis, but that bipolar spindle assembly is highly robust and only minimally perturbed by variations in centriole number.

Materials & Methods

Cell Culture

This study employed the following *Chlamydomonas reinhardtii* strains: wild-type strain cc-124, flagella-less strain bld1 (cc-2506), basal body-deficient strains bld2 (cc-478), uni3 (cc-2508), and bld10 (cc-4076), variable centriole number strains vfl1 (cc-1388), vfl2 (cc-2530) and vfl3 (cc-1686), uniflagellar mutant strain uni1-2 (cc-4219), ts flagellar assembly mutant fla10 (fla10-1 allele, cc1919), and ts vfl2 strain vfl2-R15. All strains were obtained from the *Chlamydomonas* Genetics Center (Duke University, Durham, NC). For normal growth, cells were grown and maintained in TAP media. Growth was at 25°C with continuous aeration and constant light. For cell synchronization, cells were grown in M1 (Sager and Granick Medium I) medium in a 14:10h light/dark cycle and were analyzed after two days near the end of the light cycle.

Immunofluorescence and imaging of mitotic spindles

Cells were allowed to adhere to polylysine-coated coverslips prior to fixation in cold methanol for five minutes. Coverslips were then transferred to a solution of 50% methanol/50% TAP for an additional five minutes. After fixation, cells were blocked in 5% BSA, 1% fish gelatin and 10% normal goat serum in PBS. Cells were then incubated in primary antibodies overnight: anti-centrin (a generous gift from J. Salisbury) 1:100, anti-acetylated-tubulin (T6793, Sigma) 1:500, anti-alpha-tubulin FITC conjugated (F2168) 1:100, anti-phospho-histone

H3 (06-570, Upstate) 1:500, anti-Bld10p (a generous gift from M. Hirono) 1:100, and anti-POC1 1:200 (LCK, S. Geimer, I. Zamora, E. Romijn, J. Yates, and WFM, manuscript submitted). Coverslips were then washed six times in PBS before staining with secondary antibodies from Jackson Immunoresearch at a dilution of 1:1000. Cells were then incubated with DAPI (1 μg/ml in water) and mounted in Vectashield mounting media. It is important to note that the anti-alpha-tubulin FITC conjugated antibody was added only after the other antibodies were stained with both primary and secondary antibodies to prevent cross-reactivity.

Centrin (Salisbury et al., 1988), acetylated-tubulin (LeDizet and Piperno, 1986), Bld10p (Hiraki et al., 2007) and POC1 (Keller et al., 2005) were all used for the identification of centrioles.

Cells were imaged using a Deltavision deconvolution system with a 100x N.A. 1.4 oil immersion lens, with Z-sections taken every 0.2 mm.

Quantitative image analysis

A 3D stack through each cell was generated and used for all spindle analyses. Carefully stepping through each Z-section, we counted the number of centrioles per spindle pole (based on centrin, acetylated-tubulin, Bld10p, and/or POC1 staining) and determined whether spindles were monopolar, bipolar, tripolar or unorganized (based on alpha-tubulin staining in conjunction with centriole staining). Using Softworx software, spindle lengths were measured using the centers of alpha-tubulin staining intensity at both poles. Distances from

centrioles to nearest spindle pole were measured using the center of centriole staining intensity and the center of polar alpha-tubulin staining intensity. Half spindle length was measured from the center of tubulin staining at the pole to the center of mass of the chromatin. Shape factor and chromatin area were measured using a custom MATLAB program that thresholds the DNA staining and automatically detects the edge of the chromatin region and uses the shape of the outline to calculate the area and perimeter.

Cell Death Analysis

A 0.25% solution of Erythrosine B (E9259, Sigma) in TAP was made and mixed 1:1 with *Chlamydomonas* suspension. Dead cells stain bright pink by light microscopy (Markelove et al., 2000). Approximately 500 cells were counted during each cell death experiment. Averages were pooled from at least three separate experiments. We have obtained equivalent cell death results by staining vfl mutants with phenosaffranin. For measuring cell death rates in living embedded cells, agarose embedded cells were observed and the appearance of vacuolated cell morphology was used as an indicator of death.

Cytokinesis in individual cell divisions

To determine frequency of cytokinesis defects in live vfl cells, cells were embedded in 0.4% agarose in R/2 media (Harris, 1989) and mounted under coverslips sealed with Vaseline, as previously described (Marshall et al., 2001), and imaged with either a Zeiss Standard 16 microscope with phase contrast

optics or a Zeiss axioskop with DIC optics, in both cases using 20x objective lenses. Cells that were well separated from neighboring cells were selected and their position noted on the stage micrometer. The number of flagella was then scored and recorded. Slides were then transferred to a humid chamber and re-checked periodically for 36 hours. Cytokinesis defects and cell death were scored based on visual analysis of cell morphology after division.

Cell size determination

Cells were fixed and stained for immunofluorescence using the above methods. Cells were imaged in three dimensions using a Deltavision deconvolution microscope, and centriole number was scored in each cell using FLA10 (antibody a generous gift from Douglas Cole) and acetylated tubulin as markers. Cell outlines were then traced in three dimensions using the 3D model function of the Softworx platform. Three dimensional volumes were calculated from these hand-traced models. This approach was chosen over two-dimensional measurements of diameter or other such measurements, because it gives a reliable value of volume regardless of potential differences in cell shape or orientation. A total of 16 wild-type, 26 *vfl1*, 72 *vfl2*, and 71 *vfl3* cells were measured. For volume measurements in *uni1* mutants, where it was critical to preserve flagella in order to correlate flagellar number with volume, cells were fixed in 1% glutaraldehyde and imaged by differential interference contrast microscopy in three dimensions using the Deltavision microscope with an air condenser lens. Glutaraldehyde fixation was used instead of the standard

immunofluorescence fixation protocol because the latter tends to result in flagella being torn from the cells during adherence to the coverslip, which is not of concern when scoring centriole number, but makes scoring flagellar number difficult. A total of 45 *uni1* cells were measured.

Results

Mitotic spindle aberrations in vfl mutants

If centrioles play a role in organizing the mitotic spindle, then mutants with abnormal centriole number should show defects in spindle organization. Centriole number can in principle be altered by physical manipulation such as microdissection, cell fusion, and laser ablation, but such approaches run the risk of unintended side-effects and also suffer from difficulties in obtaining results on large numbers of cells. We therefore have taken advantage of the genetics of *Chlamydomonas reinhardtii*. One set of *Chlamydomonas* mutants has been described in which centriole ultrastructure is abnormal, these include *bld2*, in which centrioles are flat discs of singlet microtubules (Goodenough and St. Clair, 1975; Dutcher et al., 2001), *uni3* in which centrioles have doublet rather than triplet microtubules (Dutcher et al., 1998), and *bld10* in which centrioles are largely absent (Matsuura et al., 2004). Analysis of spindle organization in such mutants allows us to test whether centriole structure affects mitosis. A second set of *Chlamydomonas* centriole-related mutants consists of the VFL mutants *vfl1*, *vfl2*, and *vfl3* in which centriole number is variable from cell to cell (Adams et al., 1985; Wright et al., 1985 Kuchka and Jarvik, 1982). In these mutants, centriole ultrastructure is apparently normal, but some cells lack centrioles, or have just one, while others have supernumerary centrioles. These mutants allow us to explore the effect of centriole number on spindle morphology.

Using these two sets of mutants, we examined the three-dimensional organization of mitotic spindles. We found that centriole mutants in *Chlamydomonas* displayed a range of abnormal spindle phenotypes, as illustrated in Figure 1. Defects in spindle morphology included monopolar spindles, multipolar spindles, split or multiradial spindles, and asymmetric spindles with unequal pole focus. These defects occur rarely, if ever, in wild-type cells, but were frequently seen in all mutants examined (Figure 1K). Comparing the set of all mutants versus wild-type (Figure 1J), we found that the frequency of spindle defects was statistically highly significant. We frequently observed centrioles in these mutant cells that were not associated with any spindle pole. These detached centrioles, defined as those further than 1 mm from a pole, still appeared able to induce microtubule organizing centers (MTOCs) as judged by the appearance of small asters around each detached centriole during metaphase (e.g. See Figure 1B and 1G). We did not observe any obvious clustering of extraneous centrioles such as has been reported in some mammalian cell lines (Quintyne et al., 2005).

Comparing different types of mutants, we find that a similar spectrum of defects was seen in mutants with abnormal centriole ultrastructure and in mutants with abnormal centriole number distributions (Figure 2). Similar defects also occur in asq2 mutant cells (J.L. Feldman and W.F.M., manuscript submitted) which have defects in mother-daughter centriole cohesion (Feldman et al., 2007).

In addition to examining the arrangement of spindle microtubules, we scored the compactness of the metaphase plate by measuring the area of the phospho-

histone-specific staining (Figure 3A). This analysis indicated that many centriole mutants show a small but statistically significant increase in chromatin area. This could be consistent either with decreased efficacy of chromatin congression to the metaphase plate, or with decreased chromatin condensation. In addition to area per se, a "shape factor" was calculated by taking the ratio of the circumference to the square root of the area. This is a unit-less quantity that takes its minimum value if the chromosome-containing region has a circular cross-section, and has a larger value the more closely the arrangement approaches a perfect line. We did not observe any statistically significant differences in the shape factor for the metaphase plate for any mutants compared to wild-type (Figure 3B).

Spindle morphology versus centriole number

The results of the previous section indicate that centriole number mutants in *Chlamydomonas* show a significant increase in particular spindle defects relative to wild-type cells. These defects might reflect a direct role for centrioles in spindle assembly, but two alternative explanations exist - the defect might reflect aberrations in cellular organization caused in earlier divisions, or the defects might reflect additional, centriole-independent functions of the BLD and VFL genes.

In order to determine whether the observed spindle defects were a direct consequence of the abnormal centriole number at the time of mitosis, we scored the frequency of each spindle defect versus the number of centrioles present,

either too few, the normal number of four (in mitosis), or too many, on a cell-by-cell basis. Results of this analysis (Figure 4) indicate that several of the various spindle defects correlate directly with centriole number. Cells with fewer than the normal number of centrioles (4 at metaphase) show a large increase in the frequency of monopolar spindles compared to cells with the correct number of centrioles (39/71 versus 6/61; $P<0.0001$ $c^2=27.7$). The frequency of multipolar spindles was also increased in cells with less than four centrioles compared to the correct number (10/42 versus 5/60, $P< 0.05$ $c^2=4.7$). Neither monopolar nor multipolar spindles were increased in frequency in cells with more than four centrioles.

Within bipolar spindles that were seen, unequal tubulin intensity in the two half-spindles is greatly increased in cells with less than the correct number of centrioles (38/70 versus 11/66; $P< 0.0001$ $c^2=20.9$). Tubulin asymmetry was not increased in cells with supernumerary centrioles.

The strong correlation, on a cell by cell basis, between centriole number and spindle morphology defects, indicates that the defects are not simply due to a centriole-independent side effect of the genetic background, since all cells in the comparison carry *vfl* mutations. This result could either reflect a direct role for centrioles increasing the robustness of the bipolar spindle morphology, or else a more indirect effect on overall mitotic cellular organization. It is notable that cells with supernumerary centrioles showed no increase whatsoever in the frequency of spindle defects compared to cells with the normal centriole number.

Spindle pole morphology versus local centriole number at the pole

The data of the preceding section indicate that several spindle abnormalities correlate with the total number of centrioles in the cell. This could either reflect an effect on the whole spindle, or an effect on individual poles that have incorrect centriole numbers. If centrioles exert a local influence on individual spindle poles, then we might expect to see a correlation between the centriole number at a given pole and the morphology of the half-spindle containing that pole.

In order to ask whether any of the spindle defects documented in Figure 4 might be due to a centriole-mediated function at the spindle poles, we scored the frequency of each spindle defect versus the number of centrioles present at the pole, on a pole-by-pole basis (Figure 5). This analysis only considered spindle defects that involve a single pole, namely, spindle pole focus, spindle half-length, detachment of centrioles from the pole, and multiradial/split poles. As shown in Figure 5, the frequency of abnormalities in spindle pole focus, spindle length, and multiradiality did not correlate with the number of centrioles at the pole, whereas detachment did correlate, occurring with a significantly higher frequency when the number of centrioles at a pole was different from two. The positive correlation between detachment and number may suggest that a given pole has a limited capacity for centriole recruitment.

Because the primary proposed function for centrioles at the poles is to recruit PCM and thus contribute microtubules for spindle assembly, we specifically tested whether there was any correlation between the number of centrioles at the pole and either the width of the pole or the length of the half-spindle. If centrioles

help recruit active PCM at the poles, one would expect that more centrioles would lead to more microtubules and thus a wider or thicker half-spindle. However, as plotted in Figure 6, we do not see any apparent correlation between centriole number and either pole width (Figure 6A) or half-spindle length (Figure 6B). This result argues against models for spindle size-control based on centrosome size.

Cytokinesis defects in vfl mutants

In addition to a putative role in mitosis, centrioles have also been implicated in regulating cytokinesis. To test for such a function we apply the same strategy as above, using mutants with variable centriole number to ask whether cytokinesis defects occur at a significantly increased rate when centriole number is abnormal. Observations of populations of *vfl* mutant cells show frequent failures of cytokinesis, especially incomplete cleavage furrows (Figure 7A). To quantify cytokinesis failure in *vfl* mutants, we embedded single *vfl* mutant cells and observed them before and after cell division. As tabulated in Figure 7B, we see a dramatic increase in the frequency of cleavage failure in vfl mutants as compared with wild-type cells. The increase in frequency is statistically significant (for vfl2, $P<0.005$ and for vfl3, $P<0.02$ compared to wild-type using Fishers exact test).

These results indicate that variable centriole number mutants in *Chlamydomonas* show a significant increase in cytokinesis defects. These defects might reflect a direct role for centrioles in cytokinesis, but as with the mitotic analysis described above, two alternative explanations exist - the defect

might reflect aberrations in cellular organization caused in earlier divisions, or the defects might reflect additional, centriole-independent functions of the *VFL* genes.

Cytokinesis defects in vfl2 correlate with centriole abnormality, not gene function

One approach for distinguishing direct effects of centriole number from centriole-independent side-effects of the mutations is to use a conditional *vfl2* allele (Taillon et al., 1992). We grew *vfl2*^{ts} mutants for 1 week at the nonpermissive temperature, shifted them back to the permissive temperature for 2 days, and then embedded and tracked individual cells in agarose pads. We have previously demonstrated (Marshall, 2007) that under this growth regime the *vfl2*^{ts} mutant strain shows a complete restoration of centrin fiber assembly and centriole segregation within 1 day of growth after returning the strains to the permissive temperature, suggesting that by the time we started observing cells, the molecular function of centrin was restored. However, we have also found the number of centrioles per cell takes additional generations to become fully corrected (Marshall, 2007). If such cells showed normal cleavage despite having variable numbers of centrioles, it would indicate that the cleavage failures observed in constitute *vfl2* mutants must have been caused by a centriole-independent effect of the *vfl2* mutation. However, as shown in Figure 8A, we found that in *vfl2*^{ts} mutants shifted back to the permissive temperature and grown for over 1 day, the defects in cytokinesis continue to occur.

A second approach to testing whether the cytokinesis defects are centriole-dependent is to ask whether cytokinesis defects correlate with centriole number. We tested this correlation by embedding single *vfl2* cells in agarose pads and observing them before and after division, making note of the number of flagella in the parent cell prior to division. Since in *vfl2*, all centrioles are active as basal bodies, the number of flagella can be taken as a reliable indicator of the number of centrioles as previously demonstrated using multiple protein markers as well as electron microscopy (Marshall et al., 2001). We then asked if cytokinesis defect rates correlate with flagellar number, and hence centriole number. If the cytokinesis failure was caused by a centriole-independent effect of the vfl2 mutation, the failure should occur in all cells at a rate independent of the number of centrioles that happen to be present. As seen in Figure 8A, the rate of cleavage failure correlates weakly with the number of centrioles. There is a weak but statistically significant tendency for ells with an increased number of centrioles to show an elevated rate of cleavage failure ($P<0.02$ by Fishers exact test). Cells with reduced centriole number appear to show a slightly elevated rate of cleavage failure but this is not statistically significant based on the available data.

These results suggest that the cleavage failures are unlikely to be due entirely to a centriole-independent effect of the *vfl2* mutation, and support the idea that the abnormal centriole number itself contributes to the cytokinesis defects measured in Figure 7.

Cell death in centriole mutants

Consistent with the increased frequency of abnormalities in mitosis and cytokinesis described above, we have observed a significantly increased proportion of dead cells in cultures of all centriole mutants relative to wild-type cells (Figure 9A), although from these data alone it is not possible to determine the proximal cause of death. Presence of increased cell debris has previously been noted for *vfl3* mutants (Wright et al., 1983). An accumulation of dead cells could be due to a decreased rate of cell degradation or clearance from the culture, rather than an increase in death rate. To distinguish these possibilities we observed individual mutant cells embedded in agarose and measured the frequency with which a normal-looking (in terms of cytokinesis) cell division gives rise to dead progeny cells. This analysis (Figure 9B) showed a significant increase in the rate of cell death in mutants with abnormal centriole numbers.

As with the spindle and cytokinesis defects discussed above, the increase in cell death could either be due to the centriole abnormalities or to a centriole-independent side effect of the mutations. We therefore correlated the frequency of cell death with the number of centrioles present in *vfl2* cells, using the number of flagella as an indicator of centriole number, as was done above for cytokinesis defects. The results of this analysis (Figure 9C) indicate that the frequency with which a normal cleavage division produces one or more dead progeny is a function of centriole number, with the frequency of cell death much higher for cells with one or four centrioles compared to cells with two ($P<0.02$, $P<0.01$, respectively according to Fishers exact test).

Cell size versus centriole number in vfl mutants

It has been noted that cell size is much more variable in populations of *vfl* mutant cells than wild-type (Wright et al., 1983; Adams et al., 1985). We confirmed this quantitatively by measuring cell volumes in three-dimensional deconvolution microscopy images (see Materials and Methods). We found that compared to wild-type, vfl mutants have an increased standard deviation in volume (24.0 versus 38.8), a difference that is statistically significant ($P<0.04$ by F-test).

One possible explanation for this variability might be that spindles with unbalanced numbers of centrioles might result in an asymmetric division such that a daughter that inherits more centrioles might at the same time capture more cytoplasm and therefore be larger. This possibility is based on early suggestions that the centrosome or centriole acts as a "sphere of attraction" that draws cytoplasmic components to itself (Weismann, 1893; Foe et al., 2000), but would also be consistent with a proposed role for centrioles in mediating asymmetric cell division (Yamashita et al., 2007). We tested this possibility by comparing cell size versus centriole number using three-dimensional measurements of cell volume in cells fixed and stained to detect centrioles by immunofluorescence. As shown in Figure 10A, we find that for all *vfl* mutants examined, the only correlation between size and number is that cells lacking centrioles tend to be significantly larger than other cells ($P<0.002$ based on Student's t-test n=30 for

zero centrioles and n=129 for greater than zero). Cells having one, two, three, or four centrioles all have the same size as each other on average.

Since *vfl* cells with variable numbers of centrioles also have variable numbers of flagella, we asked whether the increased size in cells lacking centrioles was due to the lack of centrioles or to the lack of flagella, by analyzing cell size in uni1 mutants, in which all cells contain exactly two centrioles, but the number of flagella can vary between 0 and 2 (Huang et al., 1982). The result shown in Figure 10B indicates that cell volume does not depend on the presence or absence of flagella.

.

Discussion

Robustness of spindle bipolarity

The most striking result of these analyses is that, although a range of spindle defects were observed in mutant cells with different numbers of centrioles, in the majority of cases the spindles were still bipolar. This was true for cells with too many centrioles as well as for cells with too few. It has been known for some time that bipolar spindles can self-organize in the absence of centrosomes, and our results are, to our knowledge, the first to show that this bipolar organization is equally robust to quantitative perturbations in centriole number, as well as to alterations in centriole ultrastructure.

Since we see a significant increase in both monopolar and multipolar spindles when the number of centrioles is less than four, we propose that centrioles may help bias spindle self-assembly towards the bipolar state by destabilizing the monopolar state.

Comparison to other studies

Numerous studies have confirmed over and over that cells without centrioles can still form bipolar spindles (Debec, 1995; LaTerra et al., 2005; Hinchcliffe et al., 2001; De Saint Phalle and Sullivan, 1998; Bobinnec et al., 1998; Basto et al., 2006) and our results also confirm this well-established conclusion. In some cases it has been reported that the poles of acentriolar spindles tend to be less well-focused than centriole-containing spindles (Debec, 1995), however we did

not observe an increase in pole width (Figure 6) suggesting that centrioles are not necessarily required for optimal pole focusing, at least in *Chlamydomonas*.

In contrast to the clear consensus that cells lacking centrioles can form bipolar spindles, the fate of cells with too many centrioles is less clear. Some studies have found that cells with supernumerary centrioles often form multipolar spindles (Lingle et al., 1999; Duensing et al., 2000; Basto et al., 2008). On the other hand, studies of a neuroblastoma cell line having a large number of centrosomes (Ring et al., 1982) showed that bipolar spindles still formed even when 10-20 centrosomes were present, with centrosomes clustered into ring-like groups at each pole. Clustering of supernumerary centrioles at poles of tumor cells have also been reported in a variety of other cells types (Quintyne et al., 2005; Basto et al., 2008). Because we do not see a similar organized clustering of centrosomes in *Chlamydomonas* VFL mutant spindles, and yet bipolar spindles are still the dominant outcome, we conclude that clustering of centrioles and centrosomes is not a necessary condition for spindle bipolarity in the presence of abnormal numbers of centrioles.

Centrioles and cytokinesis in Chlamydomonas

Cytokinesis in Chlamydomonas combines some of the features of both plant and animal cell division. In wild-type cells, the position and orientation of cleavage furrow initiation is predicted by a pair of rootlet microtubule bundles which emerge from the vicinity of the centrioles. As cytokinesis begins, an array of microtubules called the metaphase band forms along the rootlets, and these

are thought to direct the formation of the furrow (Doonan and Grief, 1987; Gaffal, 1988). This is similar to the situation in plants where a preprophase band of microtubules on the cortex determines the cleavage plane. Unlike plants, the microtubule array in Chlamydomonas then gives way to a contractile actin ring (Ehler et al., 1995) when then cleaves the cell.

The rootlets that apparently mark the site of furrow ingression are likely to be nucleated by the centrioles. Mutants in which centrioles are displaced in the cell form rootlets in corresponding displaced positions (Feldman et al., 2007). We therefore propose that many of the cytokinesis defects observed in this report may be due to misplaced or disorganized rootlets as previously suggested for the *bld2* mutant (Ehler et al., 1995). A cell with an abnormal number of centrioles cannot form the usual pair of cleavage-predicting rootlets, and would end up with abnormal numbers or positions of furrow initiating events.

Centrioles, Cilia, and Cell Size

We have shown that cells lacking centrioles tend to be larger than cells that have centrioles. As long as a cell has at least one centriole, it appears that cell size does not correlate with centriole number. These results imply that cells lacking centrioles must either grow to a larger size before initiating division, or else divide fewer times. In either case, the data may implicate centrioles or cilia/flagella in the control of cell size or cell cycle progression

There is an almost universal tendency for cells of all species to resorb their cilia or flagella prior to cell division and this might indicate a role for cilia and

flagella in regulating cell cycle progression (Quarmby and Parker, 2005; Pan and Snell, 2007). Flagella contain kinases of the NIMA family that in addition to regulating flagellar processes also affect cell cycle progression and cell size control (Mahjoub et al., 2002; Bradley and Quarmby, 2005). Another direct link between cilia/flagella and cell division has recently been provided by the finding that IFT27, a protein involved in building flagella and cilia, also appears to function in control of cell cycle progression and cytokinesis (Qin et al., 2007). One might therefore speculate that the centriole-less vfl mutant cells are larger because they lack flagella. However, the fact that flagella-less uni1 cells have the same average volume as biflagellate uni1 cells (Figure 10D) argues against this notion and suggests that it is the lack of centrioles, rather than the lack of flagella, that causes the increased cell volume. This may be consistent with reports that mammalian cells lacking centrosomes are more susceptible to stress-induced G1 arrest (Uetake et al., 2007) - since G1 is the period of cell growth in *Chlamydomonas,* a delay in G1 would lead to larger cell size for acentriolar cells.

Umen and co-workers have made substantial progress in understanding cell size control and cell cycle progression in *Chlamydomonas* through a series of elegant experimental approaches (Umen and Goodenough, 2001; Fang et al., 2006) and it is to be hoped that similar strategies may be applied to dissect the influence of centrioles on cell size or cell cycle progression.

Possibility of indirect effects of mutations

A genetic approach to testing centriole function has the danger that centriole mutations may have other, centriole-independent effects on the cell. For instance, the vfl2 mutation causes abnormal centriole numbers, but the affected protein, centrin, has also been reported to be involved in nuclear RNA transport (Resendes et al., 2008; Fischer et al., 2004), protein degradation (Chen and Madura, 2008), and cell integrity based on interaction mapping studies (Sullivan et al., 1998). Most genes analyzed in this report encode proteins that localize strictly to centrioles (Silflow et al., 2001; Matsuura 2004; Dutcher et al., 2002) and are thus less likely to produce side effects than overexpression of upstream cell-cycle regulatory signals of unclear specificity, such as Plk4/SAK (Basto et al., 2008) or viral oncogenes (Munger et a., 2006), all of which may target multiple downstream molecules with unpredictable side effects.

Most of the experiments described above were designed to test for a correlation between the types of defects with the number of centrioles present on a cell-by-cell basis. The idea behind this type of analysis is that a nonspecific effect due to the mutation would be seen in all cells, since all cells would share the same mutated gene, and would not be expected to correlate with the number of centrioles. We found correlations between spindle defects and cell size variation and centriole number, suggesting that centrioles exert a functional influence on the process of spindle assembly and cell cycle progression.

Acknowledgments

The authors thank members of the Marshall Lab for careful reading of the manuscript. Antibodies were generously provided by Jeff Salisbury and Masafumi Hirono. LCK was supported by an American Heart Association graduate fellowship. WFM was supported by a Searle Scholars Award and a WM Keck Foundation Distinguished Young Scholars in Medical Research Award. This work was funded by NIH grant R01 GM077004 and by a grant from the Concern Foundation.

References

Adams GM, Wright RL, and Jarvik JW. (1985). Defective temporal and spatial control of flagellar assembly in a mutant of *Chlamydomonas reinhardtii* with variable flagellar number. *Journal of Cell Biology* **100**: 955-964.

Basto R, Lau J, Vinogradova T, Gardiol A, Woods CG, Khodjakov A, Raff JW. 2006. Flies without centrioles. *Cell* **125**: 1375-1386.

Boveri T. Zur Frage der Entstehung Maligner Tumoren (Jena: Fischer Verlag, 1914) (English translation by M. Boveri reprinted as The Origin of Malignant Tumors, The Williams and Wilkins Co., Baltimore), 1929.

Bradley BA, and Quarmby LM. 2005. A NIMA-related kinase, Cnk2p, regulates both flagellar length and cell size in Chlamydomonas. *Journal of Cell Science* **118:** 3317-3326.

Brazelton WJ, Amundsen CD, Silflow CD, and Lefebvre PA. 2001. The bld1 mutation identifies the Chlamydomonas osm-6 homolog as a gene required for flagellar assembly. *Current Biology* **11**: 1591-1594.

Brinkley BR. 2001. Managing the centrosome numbers game: from chaos to stability in cancer cell division. *Trends in Cell Biology* **11**(1):18-21.

Burbank KS, Mitchison TJ, and Fisher DS. 2007. Slide-and-cluster models for spindle assembly. *Current Biology* **17:** 1373-1383.

Chen L and Madura K. 2008. Centrin/Cdc31 is a novel regulator of protein degradation. *Molecular Cell Biology* **28**(5): 1829-1840.

Compton DA. 2000. Spindle Assembly in Animal Cells. *Annu. Rev. Biochem.* **69**: 95-114.

Costello DP. 1961. On the orientation of centrioles in dividing cells, and its significance: a new contribution to spindle mechanics. *Biology Bulletin* **120:** 285-312.

Debec A, Detraves C, Montmory C, Geraud G, and Wright M. 1995. Polar organization of gamma-tubulin in acentriolar mitotic spindles of *Drosophila melanogaster* cells. *Journal of Cell Science* **108**: 2645-2653.

Doonan JH and Grief C. 1987. Microtubule cycle in Chlamydomonas reinhardtii: an immunofluorescence study. *Cell Motility and the Cytoskeleton* **7**: 381-392.

Duensing S, Lee LY, Duensing A, Basile J, Piboonniyom S, Gonzales S, Crum CP, and Munger K. 2000. The human papillomavirus type 16 E6 and E7 oncoproteins cooperate to induce mitotic defects and genomic instability by uncoupling centrosome duplication from the cell division cycle. *PNAS* **97**(18): 10002-10007.

Dutcher SK, Morrissette NS, Preble AM, Rackley C, and Stanga J. 2002. Epsilon-tubulin is an essential component of the centriole. *Molecular Biology of the Cell* **13**: 3859-3869.

Dutcher SK. 2001. Elucidation of basal body and centriole functions in *Chlamydomonas reinhardtii*. *Traffic* **4**: 443-451.

Fang SC, de los Reyes C, Umen JG. 2006. Cell size checkpoint control by the retinoblastoma tumor suppressor pathway. *PLoS Genet*ics **2**: e167.

Foe VE, Field CM, Odell GM. 2000. Microtubules and mitotic cycle phase modulate spatiotemporal distributions of F-actin and myosin II in *Drosophila* syncytial blastoderm embryos. *Development* **127**(9): 1767-1787.

Ghadimi BM, Sackett DL, Difilippantonio MJ, Schrock E, Neumann T, Jauho A, Auer G, and Ried T. 2000. Centrosome Amplification and Instability Occurs Exclusively in Aneuploid, but not diploid Colorectal cancer cell lines, and correlates with numerical chromosomal aberrations. *Genes, Chromosomes, and Cancer* **27**:183-190.

Goodenough UW and St. Clair HS. 1975. BALD-2: a mutation affecting the formation of doublet and triplet sets of microtubules in *Chlamydomonas reinhardtii*. *Journal of Cell Biology* **66**: 480-491.

Hinchcliffe EH, Miller FJ, Cham M, Khodjakov A, and Sluder G. 2001. Requirement of a centrosomal activity for cell cycle progression through G1 into S phase. *Science*. **291**(5508): 1547-1550.

Hiramoto Y. 1965. Further studies on cell division without mitotic apparatus in sea urchin eggs. *Journal of Cell Biol*ogy **25**: 161-167.

Huang B, Ramanis Z, Dutcher SK, and Luck DJ. 1982. Uniflagellar mutants of Chlamydomonas: evidence for the role of basal bodies in transmission of positional information. *Cell* **29**: 745-53.

Khodjakov A, Cole RW, Oakley BR, and Rieder CL. 2000. Centrosome independent mitotic spindle formation in vertebrates. *Current Biology* **10**(2): 59-67.

Khodjakov A, and Rieder CL. 2001. Centrosomes enhance the fidelity of cytokinesis in vertebrates and are required for cell cycle progression. *Journal of Cell Biology* **153**, 237-42.

Koblenz B, Schoppmeier J, Grunow A, and Lechtreck KF. 2003. Centrin deficiency in Chlamydomonas causes defects in basal body replication, segregation and maturation. *Journal of Cell Science* **116**: 2635-2646

Kramer A, Neben K, and Ho AD. 2002. Centrosome Replication, genomic instability and Cancer. *Leukemia* **16**, 767-775.

Kuchka MR and Jarvik JW. 1982. Analysis of flagellar size control using a mutant of Chlamydomonas reinhardtii with a variable number of flagella. *Journal of Cell Biology* **92**: 170-175.

Lingle WL and Salisbury JL. 1999. Altered Centrosome Structure Is Associated with Abnormal Mitoses in Human Breast Tumors. *American Journal of Pathology* **155**, *No.6*.

Mahjoub MR, Montpetit B, Zhao L, Finst RJ, Goh B, Kim AC, and Quarmby LM. 2002. The FA2 gene of Chlamydomonas encodes a NIMA family kinase with roles in cell cycle progression and microtubule severing during deflagellation. *Journal of Cell Science* **115**: 1759-1768.

Marshall WF and Rosenbaum JL. 2000. How centrioles work: lessons from green yeast. *Current Opinions in Cell Biology* **12**: 119-125.

Marshall WF, Vucica Y, and Rosenbaum JL. 2001. Kinetics and regulation of de novo centriole assembly. Implications for the mechanism of centriole duplication. *Current Biology* **11**: 308-317.

Marshall WF. 2007. Stability and robustness of an organelle number control system: modeling and measuring homeostatic regulation of centriole abundance. *Biophysics Journal* **93**: 1818-1833.

Matsuura K, Lefebvre PA, Kamiya R, and Hirono M. 2004) Bld10p, a novel protein essential for basal body assembly in Chlamydomonas: localization to the cartwheel, the first ninefold symmetrical structure appearing during assembly. *Journal of Cell Biology* **165**: 663-671.

Miller MS, Esparza JM, Lippa AM, Lux FG, Cole DG, and Dutcher SK. 2005. Mutant kinesin-2 motor subunits increase chromosome loss. *Molecular Biology of the Cell* **16**: 3810-2380.

Munger K, Hayakawa H, Nguyen CL, Melquiot NV, Duensing A, and Duensing S. 2006. Viral carcinogenesis and genomic instability. *EXS* **96**: 179-199.

Nigg, EA. 2006. Origins and Consequences of Centrosome Aberrations in Human cancers. *Int. J. Cancer*. **119**: 2717-2723.

Nigg, EA. 2007. Centrosome Duplication: of rules and licenses. *Trends in Cell Biology* **17**(5): 215-221.

Pan J, Snell W. 2007. The primary cilium: keeper of the key to cell division. *Cell* **129**: 1255-1257.

Piel M, Nordberg J, Euteneur U, and Bornens M. 2001. Centrosome dependent exit of cytokinesis in animal cells. Science 291, 1550-3.

Pihan GA, Purohit A, Wallace J, Knecht H, Woda B, Quesenberry P, and Doxsey SJ. 1998. *Cancer Research* **58**: 3974-3985.

Qin H, Wang Z, Diener D, and Rosenbaum JL. 2007. Intraflagellar

transport protein 27 is a small G protein involved in cell-cycle control. *Current Biology* **17**: 193-202.

Quarmby LM, and Parker JD. 2005. Cilia and the cell cycle? *Journal of Cell Biology* **169**: 707-710.

Quintyne NJ, Reing JE, Hoffelder DR, Gollin SM, and Saunders WS. 2005. Spindle Multipolarity is Prevented by Centrosomal Clustering. *Science* **30**:127-129.

Ring D, Hubble R. and Kirschner M. 1982. Mitosis in a cell with multiple centrioles. *Journal of Cell Biol*ogy **94**: 549-56.

Rodrigues-Martins A, Riparbelli M, Callaini G, Glover DM, and Bettencourt Dias M. 2008. From centriole biogenesis to cellular function: centrioles are essential for cell division at critical developmental stages. *Cell Cycle* **7**: 11-16.

Sankaran S and Parvin JD. 2006. Centrosome Function in Normal and Tumor Cells. *J. of Cellular Biochemistry* **99**:1240-1250.

Silflow CD, LaVoie M, Tam LW, Tousey S, Sanders M, Wu M, Borodovsky M, and Lefebvre PA. 2001. The Vfl1 protein in *Chlamydomonas* localizes in a rotationally asymmetric pattern at the distal ends of the basal bodies. *Journal of Cell Biology* **153**(1): 63-74.

Sullivan DS, Biggins S, and Rose MD. 1998. Yeast centrin, Cdc31p, and the interaction protein kinase, Kic1pm are required for cell integrity. *Journal of Cell Biology* **143**(3): 751-765.

Taillon BE . 1993. Proteins associated with the basal body apparatus in

Chlamydomonas reinhardtii: a molecular genetic and cell biological analysis. Ph.D. Thesis, Carnegie Mellon University, Pittsburgh, PA.

Taillon BE, Adler SA, Suhan JP, and Jarvik JW. 1992. Mutational analysis of centrin: an EF-hand protein associated with three distinct contractile fibers in the basal body apparatus of *Chlamydomonas*. *Journal of Cell Biology* **119**(6): 1613-1624.

Tsou MF and Stearns T. 2006. Mechanism limiting centrosome duplication to once per cell cycle. *Nature* **442**: 947-951.

Uetake Y, Loncarek J, Nordberg JJ, English CN, LaTerra S, Khodjakov A, and Sluder G. 2007. Cell cycle progression and de novo centriole assembly after centrosomal removal in untransformed human cells. *Journal of Cell Biology* **176**: 173-182.

Umen JG and Goodenough UW. 2001. Control of cell division by a retinoblastoma protein homolog in Chlamydomonas. *Genes and Development* **15**: 1652-1661.

Wong C, and Stearns T. 2003. Centrosome number is controlled by a centrosome-intrinsic block to reduplication. *Nature Cell Bio*logy **5**: 539-544.

Weismann, A. 1893. The Germ-Plasm: a theory of heredity. Charles Scribner's Sons, New York.

Wright RL, Chojnacki B, and Jarvik JW. 1983. Abnormal basal-body number, location, and orientation in a striated fiber-defective mutant of *Chlamydomonas reinhardtii*. *Journal of Cell Biol*ogy **96**: 1697-1707.

Wright RL, Adler SA, Spanier JG, and Jarvik JW. 1989. Nucleus-basal body connector in Chlamydomonas: evidence for a role in basal body segregation and against essential roles in mitosis or in determining cell polarity. *Cell Motility and the Cytoskeleton* **14**: 516-526.

Yamashita YM, Mahowald AP, Perlin JR, and Fuller MT. 2007. Asymmetric inheritance of mother versus daughter centrosome in stem cell division. *Science* **315**: 518-521.

Zamora I and Marshall WF. 2005. A mutation in the centriole-associated protein centrin causes genomic instability via increased chromosome loss in *Chlamydomonas reinhardtii*. *BMC Biol*ogy **3**: 15.

Figure Legends

Figure 1. Spindle phenotypes seen in mutants with abnormal centriole number or ultrastructure. (A-I) Example images of wildtype and abnormal spindles identified within populations of cells with varying centriole numbers and sizes. (J) Quantification of percent of wildtype and centriole mutant spindles with the indicated spindle abnormalities. (K) Actual numbers and statistical significance of *Chlamydomonas* spindles in each of the indicated categories.

Figure 1. Centriole mutants in Chlamydomonas display a range of abnormal spindle phenotypes

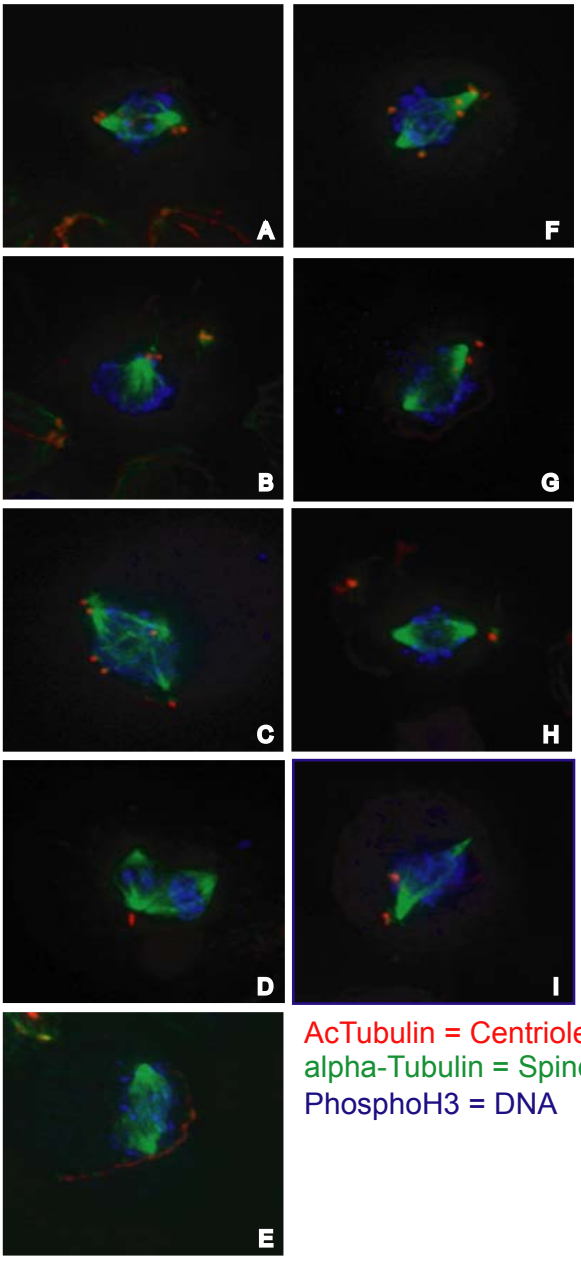

A- Wildtype Spindle
B- Monopolar Spindle
C- Multipolar Spindle
D- Split Spindle
E- Low Centriole Number
F- High Centriole Number
G- Unequal Centriole Number at Poles
H- Detached Centrioles
I- Unequal Half Pole

AcTubulin = Centrioles
alpha-Tubulin = Spindle
PhosphoH3 = DNA

J

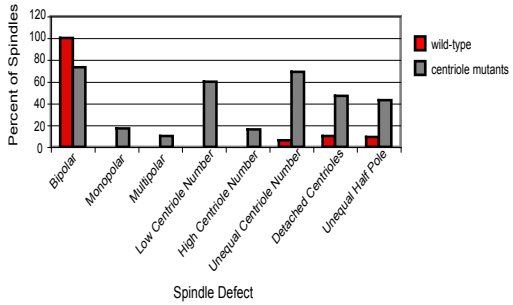

K

	Control	Mutant	Significance
Bipolar	67	199	<0.001
Monopolar	0	48	<0.001
Multipolar	0	26	0.05<p<0.02
Low Number	0	164	< 0.001
High Number	0	44	<0.001
Unequal Num	4	188	<0.001
Detached	7	127	<0.001
Unequal Poles	6	118	0.01<p<0.001
Cell Death	247	3182	<0.001

Figure 2. Percent of cells with the following spindle defects. (A) Percent of spindles with wildtype bipolar spindles, bipolar spindles, monopolar spindles and multipolar spindles. (B) Percent of spindles with the correct number of centrioles, low numbers of centrioles, high numbers of centrioles, unequal numbers of centrioles at each pole, detached centrioles on at least one pole, unequal tubulin amount at each pole, and unequal pole focus.

Figure 2. Percent of cells with the following spindle defects

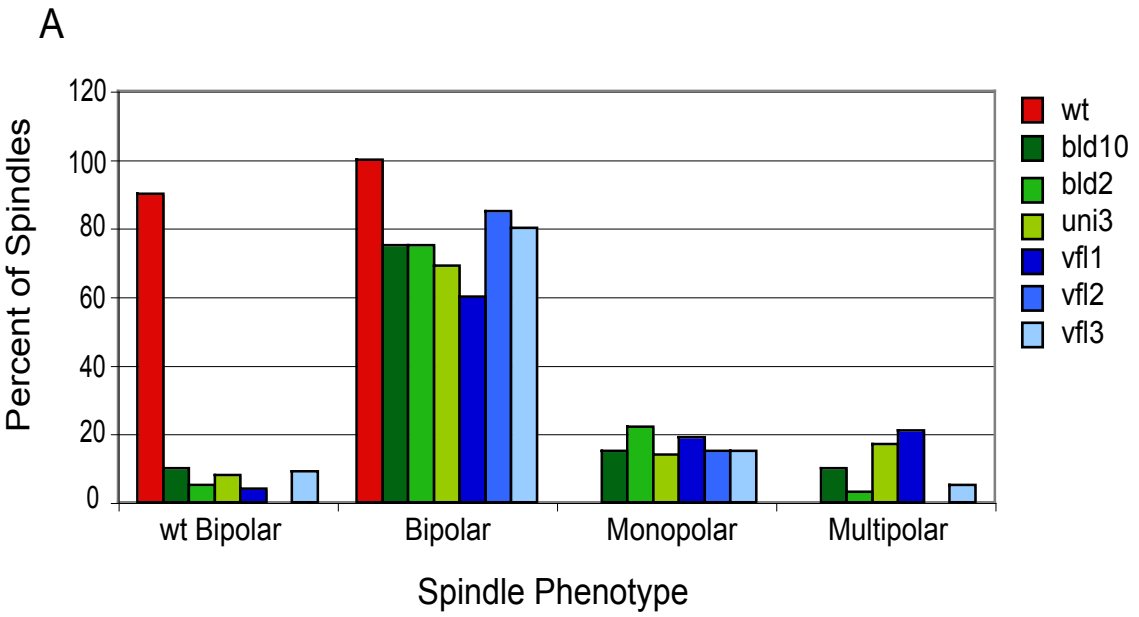

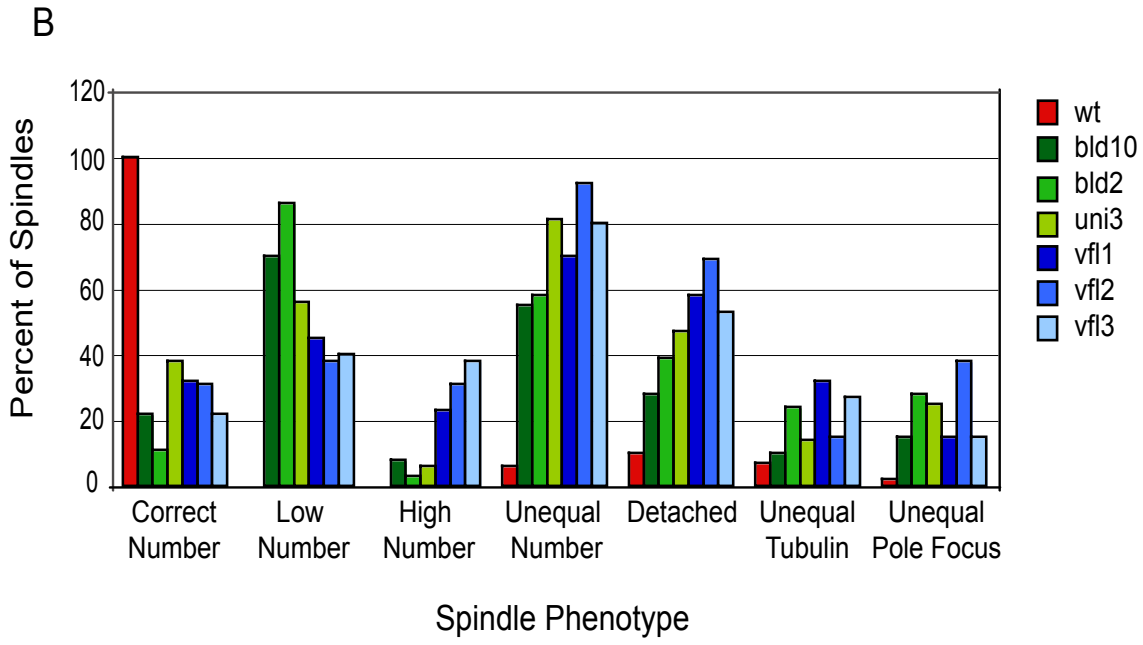

Figure 3. Analysis of chromatin in centriole mutant spindles. (A) The total amount of area covered by the DNA in a variety of *Chlamydomonas* centriole mutant spindles. (B) The DNA “shape factor” of a variety of *Chlamydomonas* centriole mutant spindles.

Figure 3. Analysis of chromatin in centriole mutant spindles

A

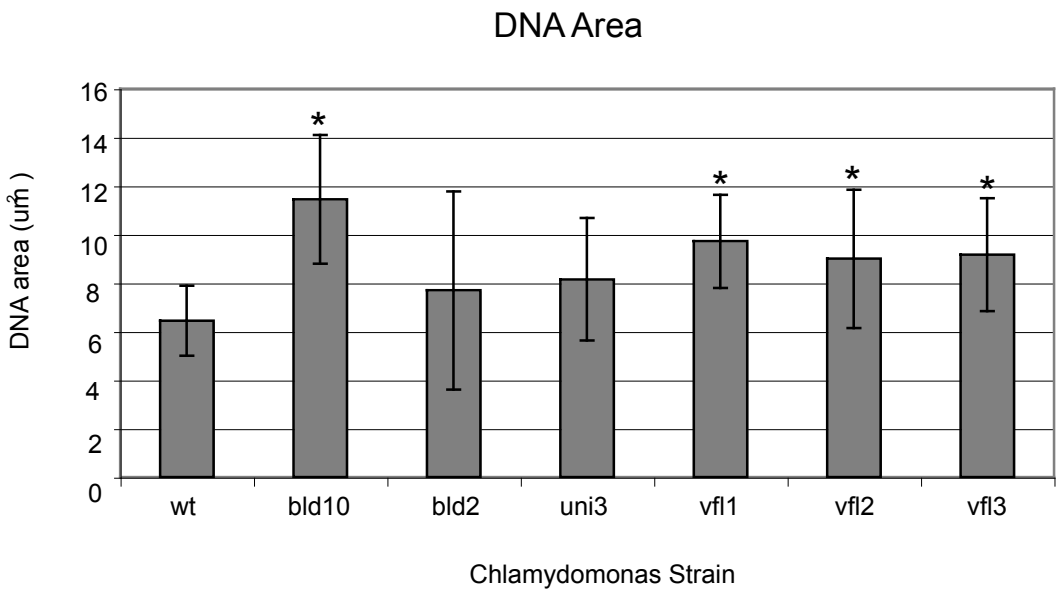

B

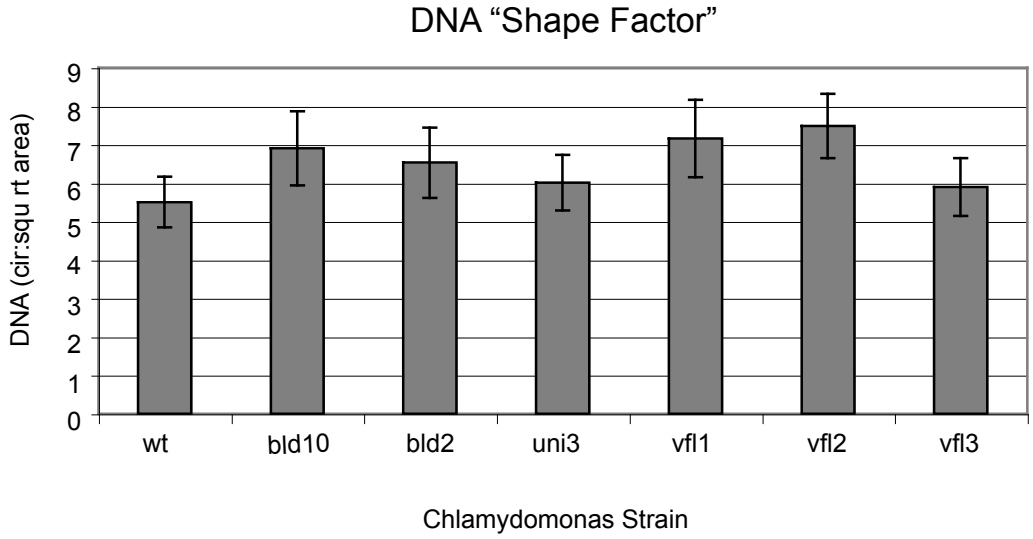

Figure 4. Percent of abnormal spindles as a function of centriole number. (A) The percent of wildtype and mutant spindles was further dissected into groups of spindles that had either the correct number of centrioles, less centrioles, or more centrioles.

Figure 4. Percent of abnormal spindles as a function of centriole number

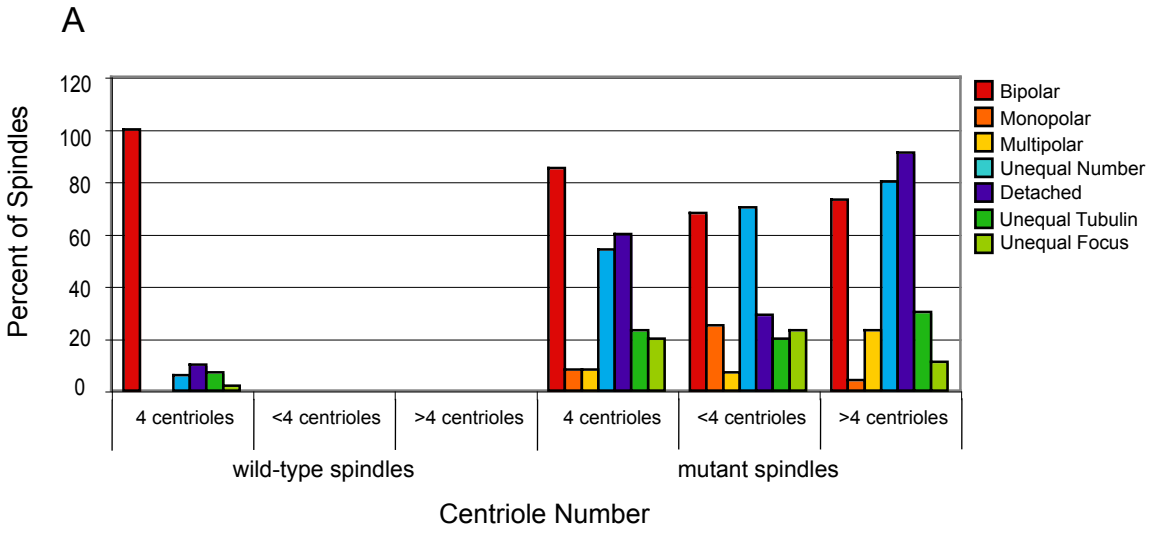

Figure 5. The number of centrioles at a pole effects the degree of centriole detachment. Spindle focus, spindle half-length, centriole detachment, and multiradialtiy were examined to determine if these phenotypes were dependent upon having the correct number of centrioles at a spindle pole.

Figure 5. The number of centrioles at a pole effects the degree of centriole detachment

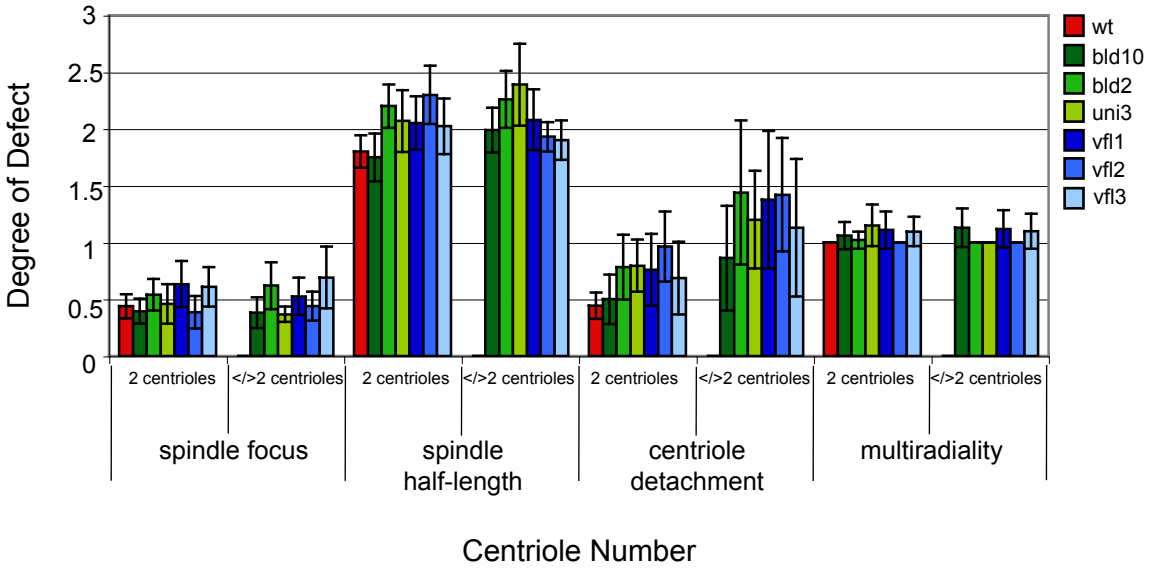

Figure 6. There is no apparent correlation between centriole number and either pole width of spindle half-length. (A) The number of centrioles at a spindle pole did not appear to affect the spindle pole focus. (B) The number of centrioles at a spindle pole did not appear to affect the spindle half-length.

Figure 6. There is no apparent correlation between centriole number and either pole width or spindle half-length

A

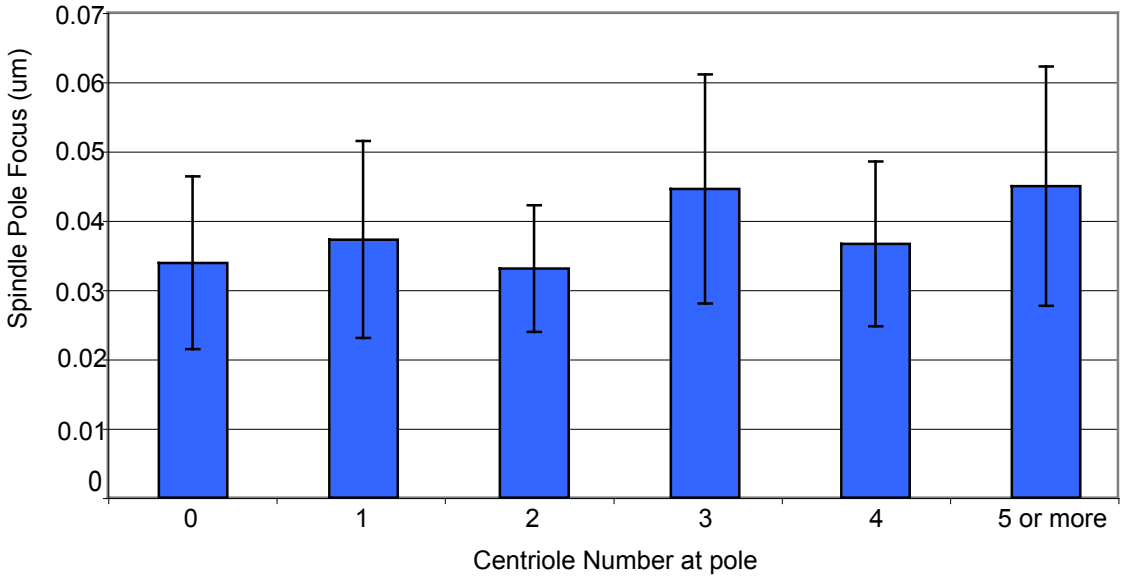

B

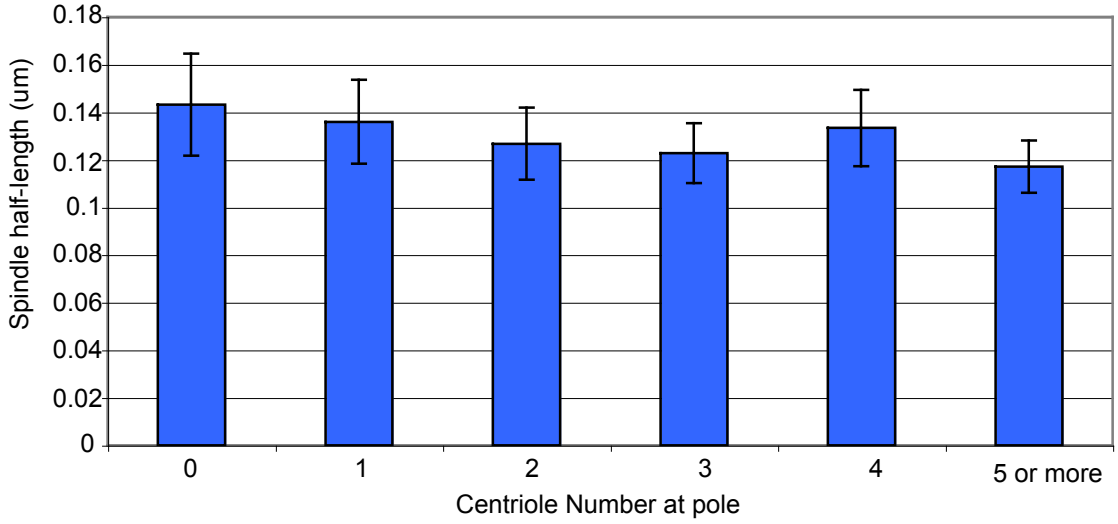

Figure 7. Defects in cytokinesis in mutants with abnormal centriole number. (A) images of normal and defective cleavage. (B) Frequency of cytokinesis defects in mutants (wt n=103; vfl1 n=129; vfl2 n=401; vfl3 n=60).

Figure 7. Centriole Number Mutants have Cytokinesis Defects

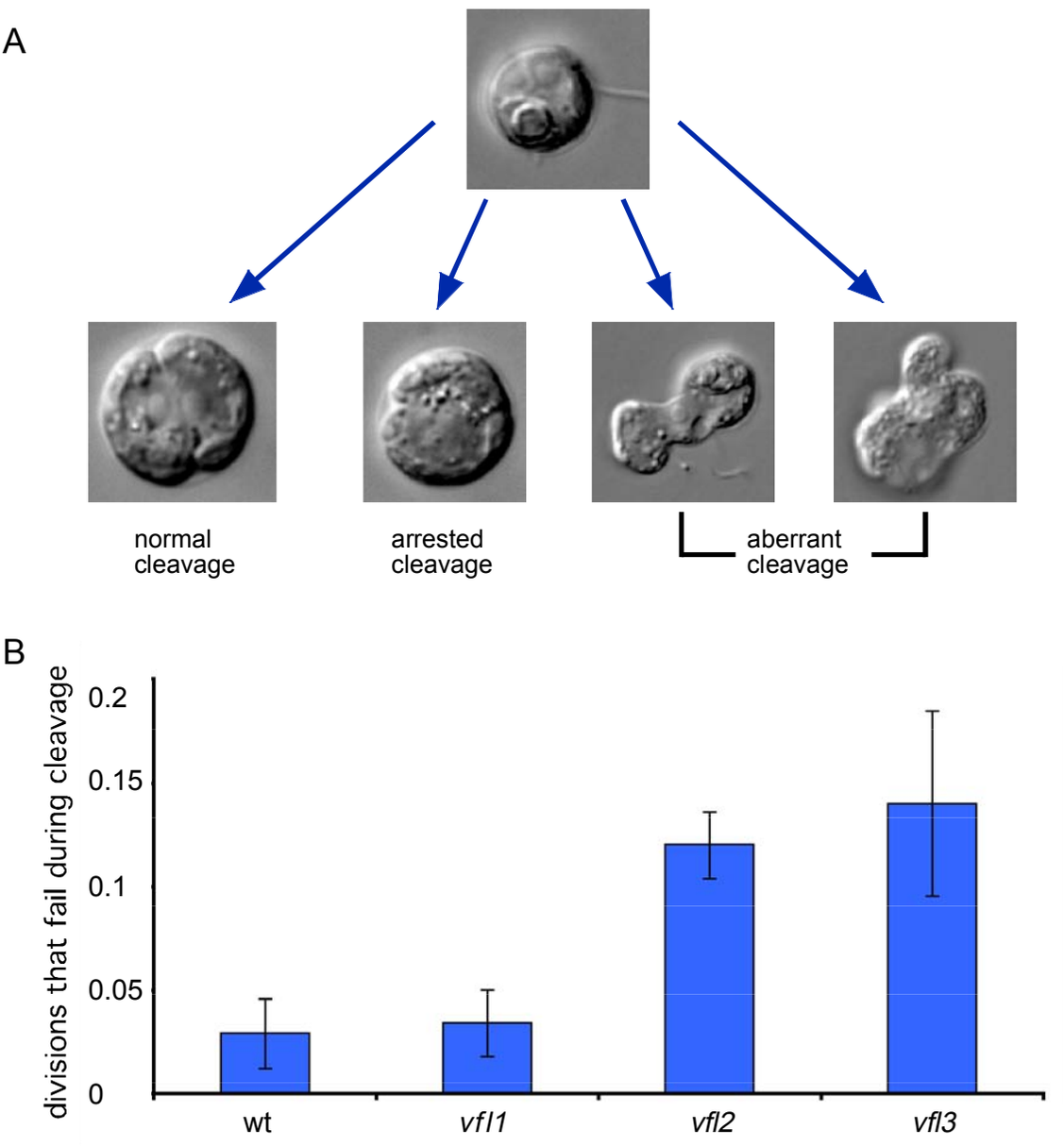

Figure 8. Correlating cytokinesis defects with centriole number abnormality. (A) defect frequency versus centriole number (n=69, 60,160, 93, and 17, respectively, for cells with 0,1,2,3, and 4 centrioles). (B) Defects following restoration of normal VFL2 gene function following down-shift of a conditional mutant (vfl2ts n=12).

Figure 8. Correlating Cytokinesis Defects with Centriole Number Abnormality

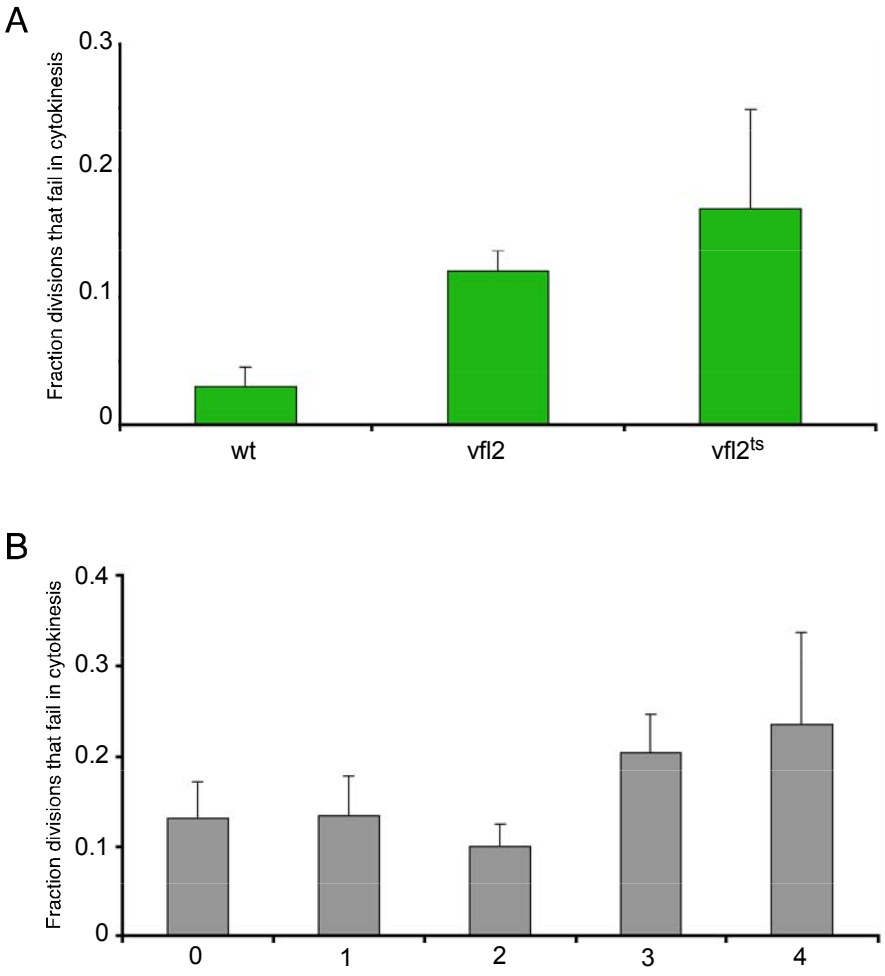

Figure 9. Cell death in centriole mutants. (A) Percent of dead cells in centriole mutant populations. (B) frequency with which a normal-looking cleavage yields one or more dead progeny cells. (C) frequency of dead progeny versus centriole number in parent cell.

Figure 9. Cell Death in Centriole Mutants

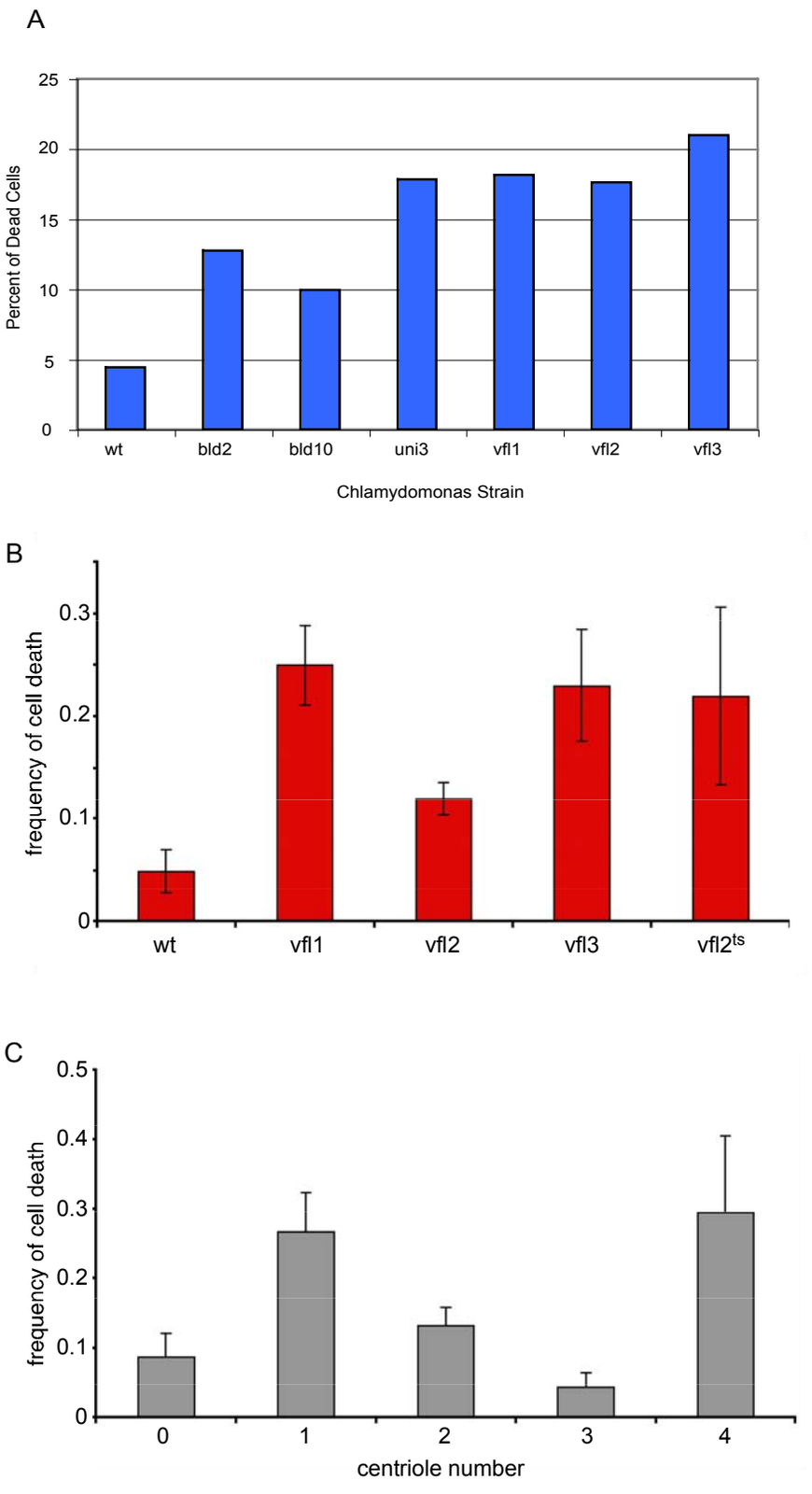

Figure 10. Cell volume versus centriole number. (A) *vfl* mutant cells lacking centrioles are larger on average than cells that contain centrioles. (B) Cell volume versus flagellar number in *uni1* mutant cells which have two centrioles in all cells but variable number of flagella.

Figure 10. Cell Volume versus Centriole Number

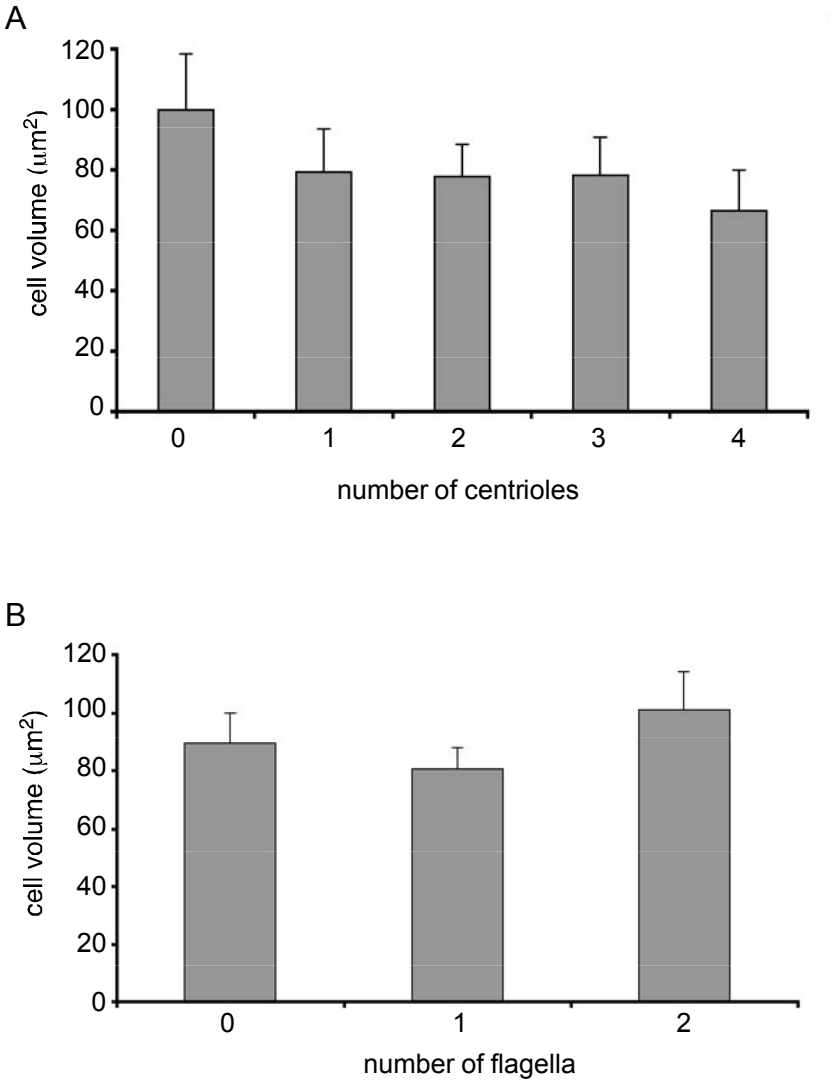

Chapter 6

Summary and Perspectives

The Future of the Centriole

During my graduate career, centrioles have gone from enigmatic, confusing, and unreachable to clinically relevant and approachable. Centrioles have emerged as sexy organelles among both cell biologists and clinicians. Their unique link to human health, through cancer and ciliopathies, are reflected through the nearly quadrupling number of papers published on centrioles in the last seven years. Scientists have made great strides in determining the precise function of centrioles along with the mechanism of their complex duplication. However, the field is still expanding. We have uncovered the protein composition of centrioles and are beginning to understand how these protein-puzzle-pieces fit together. We have an awareness of the importance of centrioles during human development and physiological function, which will continue to lead to the discovery of additional human disease genes. We have begun to appreciate the complexity of the centriole duplication cycle and can now start to investigate the smaller protein complexes necessary at each step during the assembly and maturation processes. Someone once asked me during a seminar if they thought that we would get full *in vitro* reconstitution of centrioles within my lifetime. It is a far off call but I would love for someone to prove me wrong. The centriole awaits it's future.

Publishing Agreement

It is the policy of the University to encourage the distribution of all theses, dissertations, and manuscripts. Copies of all UCSF theses, dissertations, and manuscripts will be routed to the library via the Graduate Division. The library will make all theses, dissertations, and manuscripts accessible to the public and will preserve these to the best of their abilities, in perpetuity.

Please sign the following statement:

I hereby grant permission to the Graduate Division of the University of California, San Francisco to release copies of my thesis, dissertation, or manuscript to the Campus Library to provide access and preservation, in whole or in part, in perpetuity.

Lani C Keller
Author Signature

12 June 09
Date